COLLAGEN MIMETIC PEPTIDES FOR WOUND ASSESSMENT AND HEALING

by

Sayani Chattopadhyay

A dissertation submitted in partial fulfillment

of the requirements for the degree of

Doctor of Philosophy

(Chemistry)

at the

UNIVERSITY OF WISCONSIN–MADISON

2012

COLLAGEN MIMETIC PEPTIDES FOR WOUND ASSESSMENT AND HEALING

submitted to the Graduate School of the
University of Wisconsin-Madison
in partial fulfillment of the requirements for the
degree of Doctor of Philosophy

By

Sayani Chattopadhyay

Date of final oral examination: March 16, 2012

Month and year degree to be awarded: May 2012

The dissertation is approved by the following members of the Final Oral Committee:

Ronald T. Raines, Professor, Chemistry
Nicholas L. Abbott, Professor, Chemical and Biological Engineering
Sandro Mecozzi, Associate Professor, Pharmacy
Douglas B. Weibel, Assistant Professor, Biochemistry
Eric R. Strieter, Assistant Professor, Chemistry

Dedicated to my parents, my sisters,

my grandparents, and Rishi

ABSTRACT

COLLAGEN MIMETIC PEPTIDES FOR

WOUND ASSESSEMENT AND HEALING

Sayani Chattopadhyay

Under the supervision of Professor Ronald T. Raines

at the University of Wisconsin–Madison

Collagen is one of the most abundant proteins found in nature, accounting for ¼ of the dry weight of vertebrate tissue and ¾ of the dry weight of human skin. Collagen triple helices self-assemble to form cross-linked fibers of high tensile strength and stability, and provide a highly organized, three-dimensional matrix surrounding cells. An in-depth understanding of the collagen structure and bioactivity over the last few decades has led to its development as a biomaterial for tissue repair and tissue engineering, as I describe in CHAPTER 1

Chronic wounds in skin have major impacts on the physical and mental health of affected individuals. Current clinical approaches to promote wound healing include protection of the wound bed from mechanical trauma (e.g., splinting or bandaging), meticulous control of surface microbial burden combined with topical application of soluble cytoactive factors (e.g., growth factors or exogenous extracellular matrix components), and surgical excision of the wound margin or the entire bed. These approaches often fall short, and the heterogeneity and complexity of wound beds confound any single treatment approach. Hence, there is an urgent need for new and unconventional treatment methods that will compensate for the lack of significant progress based on current therapies. This thesis reports a novel treatment strategy based on developing

collagen mimetic peptides that can enter wounded tissue and deliver cytoactive factors. My research approach relies on: (A) treating pathologic wounds by engineering the wound bed itself; and (B) modulating the key cellular elements differentially, so as to customize the treatment to specific wound types and their locations in the body.

In CHAPTER 2, I implement recent discoveries about the structure and stability of the collagen triple helix to design new chemical modalities that can anchor to natural collagen. These collagen mimetic peptides are incapable of self-assembly into homotrimeric triple helices, but are able to anneal spontaneously to endogenous collagen type I. I show that such collagen mimetic peptides containing 4-fluoroproline residues, in particular, bind tightly to bovine type I collagen *in vitro* and to a mouse wound *ex vivo*. These synthetic peptides, covalently attached to fluorophores, can aid in assessing the most damaged regions in a wound.

CHAPTERS 3 and 4 report studies in which I link the collagen mimetic peptide to compounds that are capable of modulating the various complex steps of wound healing, so as to expedite the process. These polypeptide complexes are noncovalently immobilized on cutaneous wounds in a diabetic mouse model to investigate their clinical efficacy. In CHAPTER 3, I report the use of Substance P attached to the collagen mimetic peptide for treatment of splinted-wounds in diabetic mice. A one-time topical application of the peptide conjugate led to its sustained bioactivity in the wound tissue, and we observed significantly enhanced rates of wound closure and re-epithelialization, along with lowered collagen deposition compared to commercial Substance P and vehicular controls. We also validated the synergism of insulin with Substance P activity, and showed that polyethylene glycol in the vehicle is beneficial.

CHAPTER 4 reports results in which we use a similar approach to anchor a ligand for transforming growth factor-β receptors to wound beds, and observe enhanced collagen deposition and inflammatory influx in the damaged tissue. The reported results provide a proof-of-principle for using collagen mimetic peptides as an effective bio-compatible delivery system, and show promise to treat wounds differentially, based on their nature, position in the body, and cosmetic requirements.

This therapeutic approach can be now expanded for the topical application of growth factors like VEGF and PDGF, as indicated as a future direction for the project in CHAPTER 5. My approach will enable others to anchor modulating factors in the wound bed, where they can be released over time, eliminating the need for repeated application. Thus, the strategies and results reported in this dissertation establish synthetic collagen mimetic peptides as a new modality for assessing and repairing wounds.

Acknowledgements

I would like to take this opportunity to express my deep and sincere gratitude to everyone who has provided me with assistance throughout my graduate career. First and foremost, I am grateful to Professor Ronald Raines, who gave me the opportunity to work with his group on this project. The first day I had met him in his office, he had asked me what kind of projects I saw myself working on for the next five years. I remember telling him "something that is application-based". And when I did get the opportunity to join his group, he suggested that I work on the 'wound-healing' project. This was an indication of things to come. I found the most unique balance of independence and guided research under Prof. Raines' supervision. Thereafter the last 5.5 years on this project has been an exciting journey that gave me the chance to work in widely diverse fields like animal surgery and basic histopathology. And I thank Prof. Raines' for his enthusiasm, insight, and guidance through the whole process.

I am grateful to my thesis committee: Professors Nicholas Abbott, Sandro Mecozzi, Douglas Weibel, and Eric Strieter for being available to help me through this final chapter of graduate school. I am particular grateful to Prof. Abbott for his constructive guidance and insight during the WID/ GO group meetings over the last few years. I am thankful to my collaborators at the UW School of Veterinary Medicine; in particular Prof. Jonathan McAnulty and Prof. Richard Dubielzig for not only letting me work with their groups, but also making me feel at home there. I have enjoyed working with Kathy Guthrie, Patty Kierski, Dana Tackes, Diego Calderon, and Kevin Johnson who actually made animal surgery fun! And I am grateful to Leandro Teixeira for having the patience to answer questions on histopathology from a chemist, and agreeing to go through hundreds of slides for the purpose.

I also thank Dr. Gary Case at the Peptide Synthesis Facility, for all his assistance and insightful discussion sessions, Dr. Darrell McCaslin in the Biophysics Instrumentation Facility, and Dr. Martha Vestling at the Mass Spectrometry Facility at Chemistry for their assistance.

I am grateful to the Raines group members for their assistance, incredible brain-storming sessions, and invaluable friendship. I am indebted to those who helped me at the very beginning of my graduate career, including Matt Shoulders, Frank Kotch, Annie Tam, Daniel Gottlieb, Luke Lavis, and Jeet Kalia. Joe Binder, Christine Bradford, and Greg Ellis have been great bay-mates, who gave me the opportunity to discuss matters outside science; namely running, cooking, and football. I am grateful to Langdon Martin, Ben Caes, and Mike Palte for letting me approach them with myriad questions over the last two years. I also had the privilege to work alongside: Chelcie Eller, Joelle Lomax, Sean Johnston, Mike Levine, Nadia Sundlass, Greg Jakubczak, Trish Hoang, Jim Vasta, Kristen Anderson, Rob Presler, Nick McGrath, Amit Choudhary, John Lukesh, Ho-Hsuan Chou, Kevin Desai, Caglar Tanrikulu, Raso Biswas, Brett VanVeller, Cindy Chao, Kelly Gorres, Rebecca Turcotte, Katrina Jensen, Eddie Myers, Nicole McElfresh, Ian Windsor, Thom Smith, Robert Newberry, and Matt Aronoff.

I am grateful to my friends outside of work, who have been a constant source of support and laughter. These include Jayashree Nagesh, Anushree Bopardikar, Ashok Sekhar, Piramanayagam Nainar, Neethi Ajay, Mary Beth Anzovino, and all past and present friends in the Indian Graduate Students' Association. Thanks for making my stay in Madison a happy one.

I will always be grateful to my parents, Mita and Somnath Chattopadhyay, for all the love and support they give me. Their inspiration and unfailing faith in my abilities helped me get through some of the more difficult times in the last few years. Growing up watching my father as

a chemist definitely had an important role in my decision to pursue higher studies. My two sisters Suhana and Soumi have been incredible sources of support, and have inspired me to try and be a 'good' older sibling.

Finally, I am eternally grateful to my husband and the love of my life, Rishi Amrit. His love, encouragement, patience, and unfailing support have seen me through every single day in the last three and half years. He has been my best friend and strongest critic, and his ability to see through my smiles and tears, and offer constructive advice was invaluable. I look forward to my life ahead with him.

Table of Contents

CHAPTER 2

CHAPTER 3

CHAPTER 5

List of Tables

List of Figures

List of Abbreviations

3D	three dimensional
5-FAM	5-carboxyfluorescein
Ac	acetyl
Ala, A	alanine
A°	angstrom
Arg, R	arginine
Asn, N	asparagine
Asp, D	aspartic acid
BMP	bone morphogenetic proteins
Bn	benzyl
Boc	*t*-butoxycarbonyl
Bu	*n*-butyl
Calcein-AM	acetomethoxy calcein
CD	circular dichroism
CH_2Cl_2	dichloromethane
CH_3CN	acetonitrile
CMP	collagen mimetic peptide
CO_2	carbon dioxide
CST	corticospinal tract
C-terminal	carboxy-terminal
Cys, C	cysteine

DCC	dicyclohexylcarbodiimide
dH_2O	distilled water
DHT	dehydrothermal
DIEA	diisopropylethyl amine
DMF	dimethylformamide
DMSO	dimethyl sulfoxide
DNA	deoxyribonucleic acid
ECM	extracellular matrix
EDTA	ethylenediaminetetraacetic acid
EGF	epidermal growth factor
ESI	electrospray ionization
EthD-1	ethidium homodimer-1
FDA	Food and Drug Administration (United States of America)
FGF	fibroblast growth factor
flp	(2*S*,4*S*)-fluoroproline
Flp	(2*S*,4*R*)-fluoroproline
Fmoc	9*H*-fluoren-9-ylmethoxycarbonyl
GAG	glycosaminoglycans
GH	growth hormone
Gln, Q	glutamine
Gly, G	glycine
GS	glycine–serine
GTA	glutaraldehyde

h	hour/s
HA	hyaluronic acid
HBGF	heparin binding growth factor
HBTU	*O*-benzotriazole-*N*,*N*,*N*',*N*'-tetramethyl-uronium-hexafluorophosphate
HCl	hydrochloric acid
hGF	human growth hormone
His, H	histidine
HOBt	1-hydroxybenzotriazole
HPLC	high-performance liquid chromatography
Hyp, O	(2*S*,4*R*)-hydroxyproline
i.d.	inner diameter
IACUC	Institutional Animal Care and Use Committee
IGF-1	insulin-like growth factor-1
IL	interleukin
IR	infra-red
K_d	dissociation constant
kDa	kilo Dalton
KGF	keratinocyte growth factor
Leu, L	leucine
Lys, K	lysine
MALDI–TOF	matrix-assisted laser desorption/ionization–time of flight
MeOH	methanol
Met, M	methionine

mmol	millimoles
mmol	micromoles
MMP	matrix metalloproteinase
Mmt	monomethoxytrityl
NaCl	sodium chloride
NaOH	sodium hydroxide
NH_4OAc	ammonium acetate
NHDF	normal human dermal fibroblast
NHS	*N*-hydroxysuccinimide
NK	neurokinin
Nleu	*N*-isobutylglycine
NNM	*N*-methylmorpholine
N-terminal	nitrogen-terminal
o.d.	outer diameter
°C	degree Celsius
PAA	poly(acrylic acid)
Pbf	2,2,4,6,7-pentamethyldihydrobenzofuran-5-sulfonyl
PBS	phosphate-buffered saline
PDGF	platelet-derived growth factor
PEG	poly(ethylene glycol)
Phe, F	phenylalanine
PHEMA	polyhydroxyethyl methacrylate
pM	picomolar

PMNL	polymorphonuclear leucocytes
PNA	peptide nucleic acid
PPII	polyproline II
Pro, P	proline
PVA	poly(vinyl alcohol)
PyBOP	benzotriazol-1-yl-oxy-tris-pyrrolidino-phosphonium hexafluorophosphate
PyBrOP	bromo-tris-pyrrolidino-phosphonium hexafluorophosphate
Sar	sarcosine
SARA	Smad anchor for receptor activation
Ser, S	serine
SPPS	solid-phase peptide synthesis
Sub P	Substance P
*t*Bu	*tertiary*-butyl
TEA	triethyl amine
TFA	trifluoroacetic acid
TGF-β	transforming growth factor-β
THF	tetrahydrofuran
T_m	melting temperature
TNF	tumor necrosis factor
Trt	trityl
Tyr, T	tyrosine
TβRI	transforming growth factor-β receptor I
TβRI-ED	transforming growth factor-β receptor I-extracellular domain

TβRII	transforming growth factor-β receptor II
TβRII-ED	transforming growth factor-β receptor II-extracellular domain
Tβrl	transforming growth factor-β receptor ligand
UV	ultraviolet
v/v	volume per volume
VEGF	vascular endothelial growth factor
vWA	van Willebrand factor type A
VWF	van Willebrand factor
w/v	weight per volume
β-Ala	β-alanine
μL	microliter
μM	micromolar

CHAPTER 1*

Development and applications of collagen-based biomaterials for wound healing

* This chapter is in preparation for publication as a review:

Sayani Chattopadhyay and Ronald T. Raines; (2012) Development and applications of collagen-based biomaterials for wound healing

1.1 Introduction

Over the past two decades, numerous innovations have occurred in the area of collagen-based biomaterials, and these have had a major impact in advancing our approach towards soft-tissue repair and tissue engineering. Since the turn of the 20th century, collagen-based materials were used in the form of gut sutures, human cadaver and porcine skin, amnion, and placenta. These early efforts led the way to development of injectable collagen matrices and bone-regeneration scaffolds, along with evolution and improvement of production techniques and cross-linking methods. For most soft and hard connective tissues, collagen fibrils and their networks comprises the majority of the extracellular matrix (ECM) and forms a highly organized, three-dimensional scaffold surrounding the cells. It plays a dominant role in maintaining the biological and structural integrity of the ECM and is a highly dynamic and flexible material that undergoes constant re-modeling to define cellular behavior and tissue function (Aszódi *et al.*, 2006).

Collagen is found in abundance in nature and can be easily purified from living organisms, as it constitutes more than 30% of vertebrate tissue. It is surface-active and is capable of penetrating a lipid-free interface (Fonseca *et al.*, 1996). It shows biodegradability and higher biocompatibility compared to other natural polymers like albumin and gelatin, and is non-toxic and very weakly antigenic towards biological systems (Maeda *et al.*, 1999). One of the major reasons for the use of collagen as a biomaterial is its capability to form fibers with high tensile strength and stability via cross-linking and self-aggregation. It can be modified and formulated in a large number of forms that are now commercially available (Table 1.1). An in-depth understanding of the collagen structure and bioactivity achieved over many years has helped to harness these diverse properties of collagen and applying them for biomedical purposes.

1.2 The Collagen Molecule

Collagen is the most abundant protein in animals and its presence in all connective tissue makes it one of the most studied biomolecules of the ECM. It accounts for about 25% of the dry weight of mammals and in humans, comprises ~75% of the dry weight of skin. To date, 29 different types of collagen, based on their polymeric structures have been characterized (collagen type XXIX belongs to the class of collagens containing von Willebrand factor (VWF) type A (vWA) domains (Söderhäll *et al.*, 2007)), and all of them display a triple-helical primary structure. Of these, collagen I, II, III, V, and XI have fibrillar structures. Collagen helices are comprised of three α-chains that assemble together based on their molecular sequences. The three parallel polypeptide strands in a left-handed polyproline II-type (PPII) helical conformation coil around one another to form a right-handed triple helix (Figure 1.1). In animals the individual collagen triple helices (tropocollagen) come together in a complex manner to form macroscopic fibers and networks that are observed in tissue, bone, and basement membrane. Each α chain in the collagen helix is composed of thousands of amino acids, and each third residue is glycine (Gly) resulting in the Xaa-Yaa-Gly repeat unit, where Xaa and Yaa can be any amino acid (Table 1.2). The presence of Gly is essential at every third residue in order to ensure a tight packing of the three α chains in the tropocollagen molecule. The Xaa position is often occupied by (2*S*)-proline (Pro) and the Yaa position by (2*S*,4*R*)-4-hydroxyproline (Hyp), making Pro-Hyp-Gly the most common repeat triplet in collagen (Ramshaw *et al.*, 1998). The 29 different types of collagen are composed of approximately twenty five different α-chain conformations, a combination of which assembles to form the different types. Although these three chains can be identical, heterotrimeric triple helices are more prevalent than the homotrimeric forms.

Of the various types of collagen characterized, only a few are used in the production of collagen-based biomaterials. Tropocollagen assembles into 10–300 nm sized fibrils and then the fibrils agglomerate to form collagen fibers that range between 0.5 to 3.0 μm in diameter. Fibril forming collagens (type I, II, III, and V) have large sections of homologous sequences independent of the organism (Timpl, 1984), and constitute the most commonly used formsof collagen-based biomaterials for wound healing and tissue engineering purposes. In type IV collagen (basement membrane), the regions with triple-helical conformations are interrupted with large non-helical domains as well with short non-helical peptide interruptions. Fibril associated collagens (type IX, XI, XII, and XIV) have small chains, type VI is microfibrilla collagen and type VII is anchoring-fibril collagen (Samuel *et al.*, 1998). Type I collagen is at present the "gold-standard" in the field of tissue-engineering.

1.2.1 Origin and *in vivo* interactions

Collagen can be extracted from different sources, including almost all living animals. Common sources for biomedical applications include bovine skin and tendons, porcine skin, and rat-tail. The properties of the protein differ from one animal to the other: typically human or porcine dermis, or collagen from swine intestine or bladder mucosa are used (Badylak, 2004). It is sometimes used as a de-cellularized ECM that can act as a scaffolding material for tissue regeneration. However care has to be taken to account for the immunological, physical scaffold size, and availability of such acellular collagen.

The interaction between the cells with collagen, directly or indirectly, gives rise to the cell-matrix interactions. Direct cell–collagen interactions involve four different kinds of receptors: (i) receptors (like glycoprotein VI) that recognize peptide sequences containing the

Pro-Hyp-Gly unit (Smethurst *et al.*, 2007),(ii) receptors of the integrin family and discoidin domain receptor 1 and 2, that bind to Phe-Hyp-Gly sequence, (iii) receptors of integrin-type that recognize cryptic motifs in the collagen structure, and (iv) receptors with affinity for the non-collagenous domains of the molecule. Many proteins (like decorin and laminin) that contain RGD or similar sequences recognized by integrin, can bind to both collagen and integrin, promoting cell adhesion and proliferation (Fiedler *et al.*, 2008).

1.2.2 Biodegradability of collagen

As a primary structural protein in the body, collagen is particularly resistant to enzymatic attack by neutral proteases. At neutral pH the triple helix is, however, cleaved at certain positions by matrix metalloproteinases (MMPs). Collagen types I–III are hydrolyzed by MMP-1, MMP-2, MMP-8, MMP-13, and MMP-14 (Aimes *et al.*, 1995; Fields, 1991; Ohuchi *et al.*, 1997). Some others, like MMP-3 and MMP-9, bind to type I collagen but do not participate in its degradation (Allan *et al.*, 1991; Allan *et al.*, 1995).

The ability of the MMPs to hydrolyze collagen depends on three criteria: successful binding to collagen molecules, unwinding of the three polypeptide strands, and cleaving each strand of the triple helix. The collagen fibrils are degraded starting from the exterior. After the triple helix is unwound, further degradation of the collagen molecule is facilitated by gelatinases and non-specific proteases that act on these fragments and break them down to small peptides and amino-acid residues.

Application or introduction of exogenous collagen elucidates a complex cellular response that depends on the type of collagen. High biocompatibility and biodegradability of collagen by human collagenases makes exogenous collagen ideal for use in biomedical applications, and the

rate of degradation can be modulated by cross-linking techniques (Weadock *et al.*, 1996). Some of the degradation products of collagen types I–III has been shown to induce chemotaxis of human fibroblasts (Postlethwaite *et al.*, 1978), and such degradation is thought to promote restoration of tissue structure and functionality (Yannas *et al.*, 1982).

1.2.3 Collagen-based biomaterials

Collagen-based biomaterials can be classified into two categories based on the extent of their purification from natural sources: de-cellularized collagen matrices that maintain the original tissue properties and ECM structure; and functional scaffolds prepared via extraction, purification, and collagen polymerization.

The first technique of de-cellularizing collagen entails physical (snap freezing and high pressure), chemical (acidic and alkaline treatment, chelation with EDTA, and using detergents and solutions of high osmolarity), and enzymatic (trypsin treatment) methods to produce the biomaterial (Gilbert *et al.*, 2006). Collagen in this form is typically used as sutures, cardiac valves, and ligamentary prostheses. In the second technique, collagen-based scaffolds have been synthesized by processing collagen solutions with other biomolecules, such as elastin (Buijtenhuijs *et al.*, 2004), glycosaminoglycans (GAG) (Ellis *et al.*, 1996), and chitosan (Wu *et al.*, 2007). Based on their application, the products are gels, sponges, tubes, spheres, and membranes (Table 1.3). Production of such biomaterials requires the extraction and purification of collagen from natural tissues. The dissolution of collagen is, however, impeded by the low solubility of natural collagen due to the presence of covalent cross-linking. Natural collagen is insoluble in organic solvents but can dissolve in aqueous solutions, depending on the nature of the cross-linking present. The most common solvent systems in use include neutral salt solution

(0.15–0.20 M NaCl) (Fielding, 1976), dilute acidic solutions (0.5 M acetic acid, citrate buffer), and proteolytic enzymes, as collagen triple helix is moderately resistant to proteases like pepsin, chymotrypsin, or ficin below ~20 °C (Piez, 1984). The telopeptide ends of polymeric chains are affected, but under controlled conditions the helices remain intact. Pepsin at 1:10 ratio of enzyme to dry tissue weight in dilute acetic acid provides a medium in which collagen can be swollen and dissolved (Piez, 1985).

1.2.4 Cross-linking in collagen

The high tensile strength and proteolytic resistance of natural collagen can be attributed to cross-linking. But due to dissociation of such linkages over time and the extraction processes, the reconstituted forms of collagen (sponges, films) become weak and can disintegrate on handling or under the pressure of surrounding tissues *in vivo*. Hence efforts have been made to use cross-linking agents to control the *in vivo* absorption as well as rate of biodegradation. Cross-linking in collagen takes advantage of chemical modifications of the amino and carboxyl groups within the molecules in order to form covalent bonds. These polymerization techniques are grouped into three types:

(i) Chemical cross-linking using formaldehyde (Ruderman *et al.*, 1973), glutaraldehyde (Harriger *et al.*, 1997; Wu *et al.*, 2007), carbodiimides (Powell *et al.*, 2006; Powell *et al.*, 2007), polyepoxy compounds (Tu *et al.*, 1993), acyl azides (Petite *et al.*, 1990), and hexamethylenediisocyanate (Zeugolis *et al.*, 2009). A major drawback of the chemical cross-linking approach is the toxic effects of residual molecules and compounds formed during *in vivo* degradation (Speer *et al.*, 1980; van Luyn *et al.*, 1992). In an alternative approach, the biomaterials are stabilized by forming ionic bonds between the amino groups of polycationic

molecules like chitosan and the carboxyl groups of collagen. Non-toxic chitosan is mixed with collagen just before lyophilization, making the process simple.

(ii) Physical cross-linking circumvents the problems posed by chemical methods and involves the use of ultraviolet (UV) light or thermal sources to induce collagen-scaffold polymerization. Both dehydrothermal treatment (DHT) and exposure to UV light at 254 nm increase the temperature for collagen shrinkage, tensile strength of the fibers, and resistance to proteolytic degradation (Weadock *et al.*, 1995). UV irradiation takes only 15 min (in contrast to DHT treatment, which takes 3–5 days. DHT treatment increases the sensitivity of collagen to trypsin and lowers the propensity for degradation by pepsin and lysosomal cathepsins (Gorham *et al.*, 1992). Similarly, UV-irradiation increases enzymatic resistance, thereby increasing load-bearing capacity (Weadock *et al.*, 1996).

(iii) Enzymatic cross-linking agents such as transglutaminase have also been used to enhance tensile strength and hydrolytic resistance in collagen-based biomaterials (Khew *et al.*, 2008). This method is the least cytotoxic as no residues or by-products are left behind in the scaffold structure.

1.3 Collagen in Wound Healing

Collagen fibers, sponges, and fleeces have long been used in medicine as hemostatic agents. Collagen sponges are particularly useful in this regard, as their wet strength allows the suturing of the material to soft tissue, thereby providing a template for new tissue growth. Collagen-based implants have been used as vehicles for delivery of cultured keratinocytes and

drugs for skin replacement and burn wounds (Boyce, 1998; Leipziger *et al.*, 1985; McPherson *et al.*, 1986b). Implanted collagen sponges are infiltrated by amorphous connective tissue containing GAG, fibronectin, and new collagen, followed by various cells—primarily fibroblasts and macrophages. Reports have shown that when cells are bound to an extracellular matrix, like implanted collagen sponge, there is an increase in the production of new collagen (Postlethwaite *et al.*, 1978). Depending on the degree of cross-linking, the collagen sponge is degraded into peptide fragments and amino acids in 3–6 weeks by collagenases, and the implant is then replaced by native collagen type I produced by the fibroblasts. Chemical composites with other biomaterials, and acetylated, succinylated, or methylated collagen have also been used for the purpose of immobilizing therapeutic enzymes or controlled drug delivery. One such modification that shows promise for future applications is biotinylation of collagen (Boyce *et al.*, 1992). After covalent attachment of biotin, a model substance (horseradish peroxidase) was bound either with an avidin bridge or via avidinylation of the protease. Biotinylation of collagen was also used to attach peptide growth factors like heparin binding growth factor (HBGF) and epidermal growth factor (EGF), and thereby modulate healing in full-thickness wounds (Stompro *et al.*, 1989).

1.3.1 Skin Replacement

A full-thickness excision wound in porcine model was used to study the effects of a collagen matrix implant on granulation tissue formation, wound contraction, and re-epithelialization (Leipziger *et al.*, 1985). The wounds with the implants showed enhanced granulation tissue formation and re-epithelialization, and contraction was reduced significantly, showing a bias towards wound regeneration and cosmetic utility. In subsequent works, artificial skin was developed as a form of sponge and cultured skin substitutes developed on collagen lattices were used for skin wounds. Reconstituted collagen type I is useful for this purpose by

virtue of its mechanical strength and biocompatibility (Rao, 1996). Cultured skin substitutes preserved from cryo-preserved skin cells have been used to cure chronic diabetic wounds (Boyce, 1998). In lieu of pathological skin, the contracted collagen lattice served as a support for epithelial growth and differentiation (Yannas *et al.*, 1989). Collagen implants have also been used in corneal healing, and corneal cells appeared normal when cultured individually on synthetic collagen matrix (Orwin *et al.*, 2000). Corneal scaffolds have also been constructed with recombinant human collagen (Griffith *et al.*, 2009) and can induce collagen secretion by fibroblasts (Carrier *et al.*, 2008). Microbial baggage control has been attempted by the addition of antimicrobial drugs like amikacin to bovine skin collagen (Boyce *et al.*, 1993). Cutaneous models with melanocytes (Régnier *et al.*, 1997), dendritic cells (Bechetoille *et al.*, 2007), and adipose tissue (Trottier *et al.*, 2008) have been developed.

Cultured skin substitutes exhibited delayed keratinization after grafting in comparison to native skin autografts (Supp *et al.*, 1999). To address this issue, collagen-based systems were modified with other proteins like glycosaminoglycan (GAG), and fibrin. Human epidermal keratinocytes were cultured on membranes composed of GAGs and collagen (Boyce *et al.*, 1988). Keratinocytes and fibroblasts were attached to those membranes, which were then cross-linked, reducing their rate of bio-degradation (Boyce *et al.*, 1995; Harriger *et al.*, 1997). When the collagen-substitutes were incubated in reduced humidity *in vitro*, they stimulated restoration of a functional epidermis (Supp *et al.*, 1999). Similarly, cultured cells were best grafted in combination with either a thin layer of collagen or fibrin, but not both (Lam *et al.*, 1999). Attachment and delivery of peptide growth factors via an avidin bridge has been attempted by covalent biotinylation of bovine collagen. The activity of the growth factor was not

compromised, and the strategy demonstrated potential for modulating wound healing (Boyce *et al.*, 1992; Stompro *et al.*, 1989).

More recently, acellular bilayer artificial skin with an outer later composed of silicone and an inner layer composed of collagen matrix was developed as a split-thickness skin graft, and proven to be biocompatible with the long-term post-operative tissue (Suzuki *et al.*, 2000). Bilayered-collagen gel seeded with human fibroblasts in the lower part and human keratinocytes in the upper layer have been used as the 'dermal' matrix of an artificial skin. This product was commercialized by Organogenesis (U.S.A) under the brand name Apligraf®, and was the first bio-engineered skin to receive FDA approval, in 1998. Organogenesis has other collagen-based products currently under development, including Revitix™ (a topical cosmetic product), VCTO1™ (a bilayered bio-engineered skin), or Forta-Derm™ Antimicrobial (an anti-microbial wound dressing).

1.3.2 Aqueous Injectables and Hydrogels

Dermatological defects have been treated with subcutaneous injections of collagen solutions for the last few decades. This application is of high commercial success, particularly in the area of plastic and reconstructive surgery. Injectable autologous dermal collagen has been developed for this purpose. An extensive study (McPherson *et al.*, 1986a) showed that treating reconstituted pepsin-solubilized bovine corium collagen dispersions with glutaraldehyde (GTA) had a significant impact on their physiochemical stability and that the biological response was a function of the degree of cross-linking (McPherson *et al.*, 1986b). At low GTA concentrations, the response was characterized primarily by influx of fibroblasts, neovascularization, and little inflammation. Treatment of the collagen dispersions with higher concentrations of GTA caused a

foreign body/giant cell reaction, and calcification. The neutral solubility of such treated fibrils decreased at elevated temperatures, but there was a significant increase in proteolytic stability compared to the non–cross-linked fibers. The cross-linked solutions were more viscous than their un-treated counterparts (McPherson *et al.*, 1986a; Wallace *et al.*, 1989). The increased viscosity made it difficult to inject the cross-linked formulations into the affected tissue, where the distribution of the injected material was not uniform and formed palpable masses, as seen in histological sections. A blend containing hyaluronic acid (HA) (0.3–0.5%) resulted in a significant ease in the injection process. A patent filed by the same group indicated that low molecular weight compounds such as maltose and neutral polymers such as dextran can be used as lubricants to facilitate injection into the tissue.

The effectiveness of local anesthetics and central analgesics, when formulated as collagen-based injections was improved by 30 to 5-fold compared to control injections of the drugs alone. The question posed was whether this prolonged delivery was due to a slow-down in the rate of diffusion of the drug due to the viscosity of collagen, or due to interactions between the drug molecule and collagen. Subsequent work (Rosenblatt *et al.*, 1989) showed that fibrillar collagen was capable of moderating the release-rate of only very large protein drugs such as fibrinogen, and significant amounts of non-fibrillar content was necessary to regulate the diffusion of smaller proteins like chymotrypsinogen. In reality, the apparent slow diffusion of drugs when delivered via collagen matrices was a combined result of both electrostatic and hydrophobic interactions.

The scope for using injectable collagen formulations for the delivery of growth factors and consequent cellular regeneration and tissue repair is vast. In a porcine model, intestinal wound repair was attempted by treatment with collagen suspensions carrying transforming

growth factor-β (TGF-β) or fibroblast growth factor (FGF). Wounds treated with the collagen dispersion of the growth factors were stronger than were control wounds. These formulations were also successful in partially reversing the steroid-induced impairment of breaking-load in intestinal-wound models (Slavin *et al.*, 1992). Investigations of cellular function, migration, proliferation, and differentiation in collagen gels led to further understanding of the mechanism and kinetics of transport, as well as the influence of growth factors, laminin, and fibronectin (Parkhurst *et al.*, 1992; Parkhurst *et al.*, 1994; Saltzman *et al.*, 1992).

Collagen gels positioned between the stumps of transected spinal cord resulted in axons emerging from the interface with the spinal tissue and then growing into the implanted collagen gel within a month (Marchand *et al.*, 1993). The tensile strength and durability of the collagen implant was strengthened by co-precipitation with chondroitin-6-sulfate or cross-linking by carbodiimide, which also regulated the normal scarring process, promoted axon growth (Marchand *et al.*, 1993), and fibroblast proliferation (Docherty *et al.*, 1989). The efficacy of injectable fluid collagen solution into the lesion that self-assembles *in situ* was also compared to implanted solid collagen gel (Joosten *et al.*, 1995). Corticospinal Tract (CST) axons were visualized in the matrix, along with an influx of astroglial and microglial cells into the collagen. The solid collagen gel in the form of a sponge on the other hand, which was implanted pre-assembled,did not show any axon growth or the influx of astroglial and microglial cells.

Collagen hydrogels have been used as a drug delivery system due to its capacity to present a large and constant surface area. A common practice has been to combine natural and synthetic polymers with synergistic properties. This imparts higher mechanical strength to the natural polymers and biological acceptability to their synthetic counterparts. Synthetic polymers such as poly(vinyl alcohol) (PVA) and poly(acrylic acid) were blended with natural polymers

such as collagen and hyaluronic acid (HA), formulated into hydrogels, films, and sponges that were then loaded with growth hormone (GH) (Cascone *et al.*, 1995). These formulations provided a controlled-release of GH from the collagen hydrogel, based on the collagen content of the system. Due to their low antigenicity, bovine and equine collagen matrices are used routinely in clinical applications. Gels have been formulated with atelocollagen, produced by the removal of telopeptide ends using pepsin, and were used for the delivery of chondrocytes in order to repair cartilage defects (Uchio *et al.*, 2000).

A recent development in the field has been the development of a drug-delivery system using liposomes sequestered in collagen gel that can release insulin and GH into circulation in a controlled manner (Weiner *et al.*, 1985). Collagen interacted with these vesicles, decreasing lipid peroxidation as well as the permeability of neutral or negatively charged liposomes suspended in the collagen gel (Pajean *et al.*, 1993; Weiner *et al.*, 1985) in the results was a slow diffusion of the encapsulated compound over a period of 3–5 days. Collagen can also be used as an additive in oil-based suspensions, to sustain the release of proteins lyophilized, ground, and suspended in a lipophilic liquid. This technology appears to have good potential for a topical treatment of surgical and non-surgical wounds, and burns.

1.3.3 Sponges

Commercially available collagen sponges are insoluble forms of the protein derived from animals like cows, horses, and pigs. It is prepared by lyophilizing aqueous acid- or alkali-swollen collagen solutions containing 0.1–5% of dry matter. The porosity of such sponges is controlled by varying the collagen content and freezing-rate. These sponges are capable of absorbing large amounts of tissue exudate, adhere smoothly to the wet wound bed and maintain a moist

environment, while shielding against mechanical trauma and bacterial infection (Yannas, 1990). They are used routinely as a wound dressing for severe burns, pressure sores, donor site, leg ulcers, and in *in vitro* systems (Geesin *et al.*, 1996). Collagen sponges have been combined with elastin, fibronectins, and GAGs to impart resilience and fluid-binding capacity (Doillon *et al.*, 1986; Lefebvre *et al.*, 1992). These materials can be cross-linked further with GTA and conjugated to polymers such as polyhydroxyethyl methacrylate (PHEMA), to produce hydrophilic matrices with increased mechanical strength. Three-dimensional collagen lattices loaded physiologically with fibroblasts have been developed as an *in vitro* model for wound healing (Carlson *et al.*, 2004). Collagen promotes cellular motility, and inflammatory cells actively invade the porous scaffold (Chvapil *et al.*, 1986). A highly vascularized granulation tissue forms, that in turn stimulates the formation of new granulation tissue and epithelial layers. Sponge implantation in burn wounds caused a rapid recovery of the skin due to an intense infiltration of neutrophils in the sponge (Boyce *et al.*, 1988).

Collagen-based sponges by virtue of the above properties, act as an effective scaffold for the activity of exogenously applied growth factors in wounds. Type I collagen sponge expedites wound healing by promoting the deposition of newly synthesized large-diameter collagen fibers parallel to the fibers in the sponge; thereby reversing the decreased tensile strength in large open dermal wounds. When these sponges are further seeded with fibroblasts or coated with basic fibroblast growth factor (FGF) prior to implantation in a guinea-pig dermal wound model, they promote both early dermal and epidermal wound healing (Marks *et al.*, 1991). Recombinant platelet-derived growth factor (PDGF), on introduction into the wound matrix via a collagen sponge scaffold facilitated increased fibroblast influx into the wounds and enhanced capillary formation in comparison to control treatments (Lepistö *et al.*, 1994).

Collagen sponges were also found to be suitable for short-term delivery of antibiotics to the wounds bed, and sponges soaked with solutions of gentamicin, cefotaxim, fusidic acid, clindamycin, and vancomycin released 99.9% of the antibiotics under sink conditions after two days *in vitro* (Wachol-Drewek *et al.*, 1996). Local infection was contained when gentamicin containing collagen matrix was placed on a septic focus in rat abdomen (Vaneerdeweg *et al.*, 1998). These sponges did not exhibit any unwanted side-effects and were absorbed into the tissue after a few days (Stemberger *et al.*, 1997).

Apart from acting as a scaffold for growth factors and antibiotics, porous collagen sponges have also found use for cell culture, either for tissue engineering purposes *ex vivo* or as a direct implant. They have been used to create cartilage via chondrocytes (with or without FGF) (Fujisato *et al.*, 1996; Toolan *et al.*, 1996), abdominal walls via myoblasts (van Wachem *et al.*, 1996), and develop axons in spinal cord from Schwann cells (Paíno *et al.*, 1994). Dense collagen type I matrices can also act as a scaffold for *in vitro* fibroblast cell culture (Sung *et al.*, 2009) and studies into angiogenesis (Cross *et al.*, 2010).A combination of collagen biomaterials and mesenchymal stem cells could provide a useful strategy to treat wounds and a current topic involves delivery of such stem cells using collagen scaffolds (Altman *et al.*, 2008; Trottier *et al.*, 2008). A modified sponge that can act as an artificial skin graft was developed by combining fibrillar collagen with gelatin (Koide *et al.*, 1993), that was then stabilized via dehydrothermal cross-linking. A similar sponge incorporating gelatin has since been used as a carrier matrix for mesenchymal stem cells targeting cartilage stem cell therapy (Ponticiello *et al.*, 2000).

1.3.4 Recombinant collagen sponges

Recombinant collagen sponges self-assemble into ordered biological structures and fibrils. Upon formulation via in-mold cross-linking, a homogeneous three-dimensional sponge with porous microstructures interconnected by thin sheets of collagen fibrils was produced (Olsen *et al.*, 2003). This assembly was in contrast to the commercial natural collagen sponge, which has thicker sheets and fibers. Recombinant collagen type I in the form of sponges exhibited a lower inflammatory reaction compared to its natural counterpart, whereas recombinant collagen type II is a good choice as a carrier for chondrogenic growth factors. Due to its superior hemostatic properties, recombinant collagen type III is well suited for wound-management applications.

1.3.5 Films and membranes

Collagen films have been used in wound healing and tissue engineering primarily as a barrier membrane. Films of approximately 0.1–0.5 mm thickness were cast from collagen solutions and air-dried in a manner similar to ophthalmological shields. As an added advantage, films made from bio-degradable materials like telopeptide-free reconstituted collagen demonstrated a slow release of encapsulated drugs (Rubin *et al.*, 1973). Drugs were loaded into the collagen membranes via hydrogen bonding, covalent bonding, or encapsulation. They afford easy sterilization and become pliable after hydration, without compromise to their mechanical strength.

Collagen membranes have been used for wound dressings, dural closures, reinforcement of compromised tissues, and guided tissue regeneration. Wound healing in diabetic *db/db* mice was moderated by a sustained release of human growth hormone (hGF) encapsulated in collagen

films (Maeda *et al.*, 2001). In another study, films made with collagen–polyvinyl alcohol (PVA) mixtures cross-linked with GTA vapors have been tested as a depot formulation for recombinant hGF (Cascone *et al.*, 1995). A patent (Song *et al.*, 1992) gives details of single and multilayer collagen films as vehicles for the sustained release of pharmaceuticals, especially growth factors. The individual collagen films were attached together by applying gentle pressure to form multilayer membranes, and PDGF was released from these films at a constant rate up to 100 h and improved wound healing *in vivo*.

These bio-degradable collagen membranes can serve as scaffolds for the survival of transfected fibroblasts (Rosenthal *et al.*, 1997). A blend of collagen and another polymer, such as an atelocollagen matrix, added on the surface of polyurethane films promoted the attachment and proliferation of fibroblasts, and supported their growth (Park *et al.*, 2000). Collagen-based films and membranes contain extra matrices that improve the conditions for long-term cell survival. Olsen and co-workers have also demonstrated the feasibility of using recombinant collagen type I from *P. Pastoris* yeast to formulate films that can be used for tissue engineering and guided tissue regeneration post dental surgery.

1.3.6 Wound dressings

Collagen plays a pivotal role in pre- and post-operative surgical applications. Due to their low antigenicity and inherent biocompatibility with most endogenous tissue, natural collagen has been used historically for surgical repair and abdominal wall repair (Van der Laan *et al.*, 1991). Wound dressings based on collagen are practical and easily remodeled due to their simple membrane structure, relative uniformity, and abundant availability. These factors were taken into account for the development of novel surgical adhesives synthesized from porcine collagen and

polyglutamic acid. The adhesives were used to prevent air from leaking out of damaged lungs during the long process of recovery. The absorption of such collagen-based adhesives can be regulated by altering the collagen content of the system.

Collagen-based wound dressings have been in use for a long time for the purpose of burn wound coverage and ulcer treatments (Doillon *et al.*, 1986; Peters, 1980; Yannas *et al.*, 1982). They have a distinctive practical and economic advantage compared to growth factor and cell-based treatment of full-thickness wounds. They have been formulated in a number of different forms (Table 1). An unconventional form of these treatments consisting of powdered avian collagen was effective in expediting chronic wound healing (Whitaker *et al.*, 1992). The powder promoted cellular recruitment, activation of the inflammation phase of wound healing, and support for new tissue growth—very similar in function to collagen sponges.

Some common and commercially viable skin, dermal substitutes, and dressings like Alloderm™ (human dermis), Amniograph™ (amniotic membrane), Integra® (acellular collagen-GAG scaffold), and Oasis™ (porcine skin), are used for medical applications. A combination of collagen with alginate was also successful in promoting the inflammatory phase of the wound healing, while imparting mechanical strength—a characteristic of collagen fibrils.

Collagen dressings were also synthesized with a semi-occlusive polymer film attached to its outer surface (Zitelli, 1987). Such occlusive films are resistant to bacterial attack as well as further mechanical trauma, and provides proper air and vapor permeability. They are also successful in reducing contraction and scarring, and increasing the rate of epithelialization. A commercially successfully example of such a dressing used extensively in burn care is Biobrane®, which consists of a silicone membrane knitted with a nylon membrane—both of

which are incorporated with porcine collagen peptides (Figure 1.2). Used as a temporary dressing, this composite promotes granulation and acts as an adjunct therapy for full-thickness wounds (Lal *et al.*, 2000; Smith, 1995).

1.4 Synthetic collagen and collagen mimetic peptides

The efficacy of collagen as a biomaterial in wound healing and engineering collagen type I in skin and tendons is well established, but the use of such collagen derived from animal sources is sometimes complicated by allergic reactions and pathogen transmissions (Koide, 2007). Recombinant triple-helical collagen produced in *Escherichia coli* has much promise (Pinkas *et al.*, 2011).

A potential alternative to conventional biomaterials are synthetic peptides that can be constructed easily in laboratory settings from natural amino acids, be processed easily, and have a controlled degradation pattern. They are susceptible to modifications with non-natural amino acids and other small molecules. Peptide-based biomaterials were developed to mimic the intricate fibrillar structure of native collagen-based ECM and function as a scaffold for cells. A promising candidate in this regard is peptide-amphiphile nanofibers (Hartgerink *et al.*, 2001; Hartgerink *et al.*, 2002). An undecapeptide was shown to self-assemble into cylindrical nanofibers, ~7 nm in diameter and several micrometers in length due to the presence of N-terminal alkyl chains. The peptide fragment, when exposed to the aqueous environment displayed repeated chemistry on the fiber surface—a phosphoserine residue stimulated formation of calcium phosphate minerals, while Arg-Gly-Asp segment promoted cell adhesion and growth on the surface of the fiber.

Nanofibrillar gels cross-linked by the self-assembly of self-complementary amphiphilic peptides in a physiological medium were developed by Zhang and co-workers (Zhang, 2003). These gels have more than 90% water content and the matrix is composed of interwoven nanofibers ~10 nm in diameter and 200 nm pores (Marini *et al.*, 2002). The tailor-made self-assembling peptides were shown to provide *de novo*-designed scaffolds for three-dimensionalcell cultures. These nanofibrillar gels maintained the morphology of differentiated chondrocytes and developed a cartilage-like ECM rich in proteoglycans and collagen type II, thereby showing potential for an active role in cartilage repair (Kisiday *et al.*, 2002).

The development of artificial collagen-like materials from collagen mimetic peptides has much potential. Native chemical ligation have been used to polymerize CMPs in aqueous solutions (Paramonov *et al.*, 2005). The resulting 1000-kDa peptides exhibited fiber-like structures that were micrometers in length. The presence of cysteine and lysine residues on these peptides can be exploited for further cross-linking and modification by functional moieties.

Other groups have developed novel peptide-based systems for synthesizing collagen-like supramolecules via the spontaneous assembly of preorganized collagen mimetic peptides (Koide *et al.*, 2005; Kotch *et al.*, 2006). The repeat unit in these peptides is Pro-Hyp-Gly, which is also the most common repeat unit in natural type I collagen, and the peptide strands are linked to each other via disulfide bridges in a staggered arrangement. This design promotes the formation of elongated triple-helical supramolecules (Kotch *et al.*, 2006).

Peptoid-containing collagen mimetic peptides developed by Goodman and co-workers (Johnson *et al.*, 2000) were shown to interact with epithelial cells and fibroblasts when immobilized on a synthetic surface. The cell-binding peptides required a minimum of nine Gly-

Pro-Nleu units and were not cytotoxic. Amine-functionalized latex nanoparticles functionalized with $(Gly\text{-}Pro\text{-}Hyp)_{10}$ units were shown to be capable of inducing human platelet-aggregation, with a potency close to that of type I (Cejas *et al.*, 2007), and these Gly-Pro-Hyp segments represent functional platelet-collagen receptor recognition motifs within collagen (Smethurst *et al.*, 2007). These peptides can thus play active roles in the wound-healing process. A short peptide $(Pro\text{-}Pro\text{-}Gly)_5$ was also established to be a potent chemo-attractant for alveolar macrophages that induces the migration of polymorphonuclear leucocytes (PMNL) into lungs (Inoue *et al.*, 2009; Laskin *et al.*, 1990; Laskin *et al.*, 1994). Coating with peptides mimicking segments of type I collagen promoted mesenchymal cell adhesion to hydroxyapatite surface and improved bone formation (Hennessy *et al.*, 2009).

Triple-helical stability and cellular responses of collagen segments can be affected by even a single-site replacement of Hyp with (4*R*)-Flp or (4*S*)-flp, as shown by Fields and co-workers (Malkar *et al.*, 2002). (4*R*)-Flp-containing peptide has a greater T_m than does its (4*S*)-flp or Hyp analogue, and also promoted greater cell adhesion and spreading on its surface. This rational use of fluoroproline residues in the mimetic strands could form the basis for new collagen ligands and biomaterials.

To advance the use of collagen mimetic peptides in the engineering of wounds, a key requisite is the ability of such peptides to anneal or adhere to endogenous collagen. Single strands of collagen mimetic peptides containing $(Pro\text{-}Hyp\text{-}Gly)_n$ as well as polyethylene glycol conjugated with these peptides have been shown to bind to collagen films (Wang *et al.*, 2005) and show promise for imaging and wound-healing studies (Wang *et al.*, 2008a). Gold-nanoparticles functionalized with $(Pro\text{-}Hyp\text{-}Gly)_n$-based peptides were visualized to bind to the 'gap' regions of native collagen (Mo *et al.*, 2006). These peptides have a bias to be in their

homodimeric triple-helical form at room temperature. This bias mandates pre-heating to temperatures as high as 80 °C to unfold the peptides before they can be used for binding with native collagen, and restricts work to synthetic surfaces and conditions that are not clinically relevant. Accordingly, there is an imperative need for the development of collagen mimetic peptides that can interact with natural collagen at room temperature and physiological conditions. In this thesis, I address this need and further the use of synthetic collagen as an effective biomaterial.

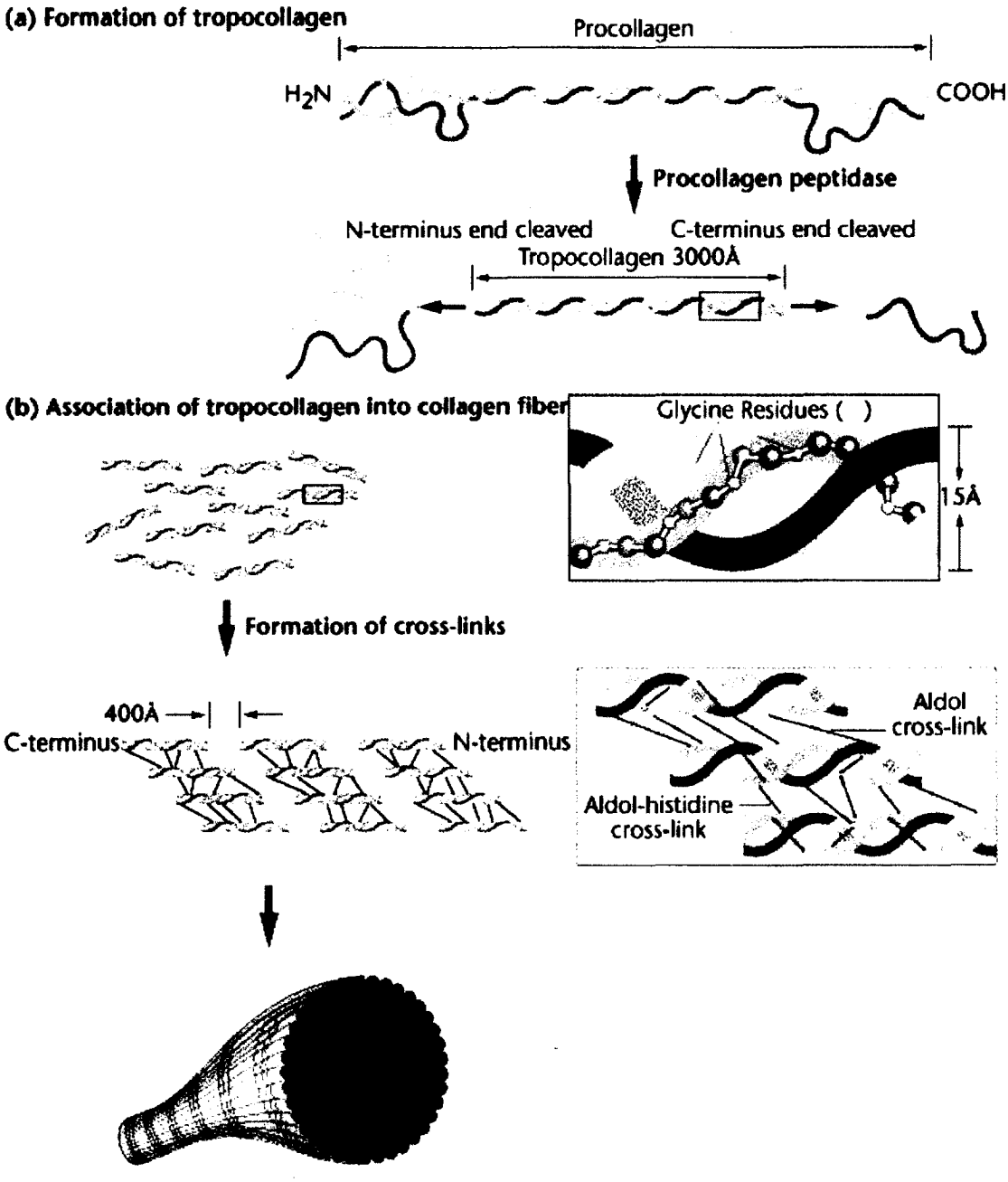

Figure 1.1. Higher order assembly of collagen triple helix. [Adapted from (Klug *et al.*, 1997)]

Table 1.1. Commercial forms of reconstituted collagen

Collagen Form	Name (Company)
Partially Purified Skin	Life Cell
Collagen Sponge	Helistat (Integra LifeSciences) Instat (Johnson & Johnson) ActiFoam (MedChem) SkinTemp (BioCor)
Collagen Fiber	Helitene (Integra LifeScience) InstatFibrillar (Johnson & Johnson) Avitene (Medichem)
Collagen Powder	BioCore (Medifil)
Collagen Composite Dressing	Fibracol (Johnson & Johnson) Biobrane (UDL Laboratories)
Hydrolyzed Collagen	Chronicure (Derma Sciences)

Table 1.2. Amino-acid composition of human type I collagen [Adapted from (Piez, 1985)]

Amino Acid	α1(I)-chain	α2(II)-chain
Alanine	124	111
Arginine	53	56
Asparagine	13	23
Aspartic Acid	33	24
Glutamic Acid	52	46
Glutamine	27	24
Glycine	345	346
Histidine	3	8
Hydroxylysine	4	9
Hydroxyproline	114	99
Isoleucine	9	18
Leucine	22	33
Lysine	34	21
Methionine	7	4
Phenylalanine	13	15
Proline	127	108
Serine	37	35
Threonine	17	20
Tyrosine	5	4
Valine	17	34

Table 1.3. Biomedical Applications of Collagen

Composition	Biomaterial Form	Applications
Collagen	Gel	Cosmetic Skin Defects Drug Delivery Vitreous Replacement Surgery Coating of Bioprostheses
	Sponge	3D Cell Culture Wound Dressing Hemostatic Agent Skin Replacement Drug Delivery
	Hollow Fiber Tubing	Cell Culture Nerve Regeneration
	Sphere	Micro-carrier for Cell Culture Drug Delivery
	Membrane	Wound Dressing Dialysis Tissue Regeneration Corneal Shields Skin Patches
	Rigid Form	Bone Repair
	Sponge	3D Cell Culture Wound Dressing Skin Replacement
Collagen + GAG	Membrane	Tissue Regeneration Skin Patches
Collagen + Hydroxyapatite	Powder Sponge	Bond-Filling and Repair Drug Delivery (BMP)

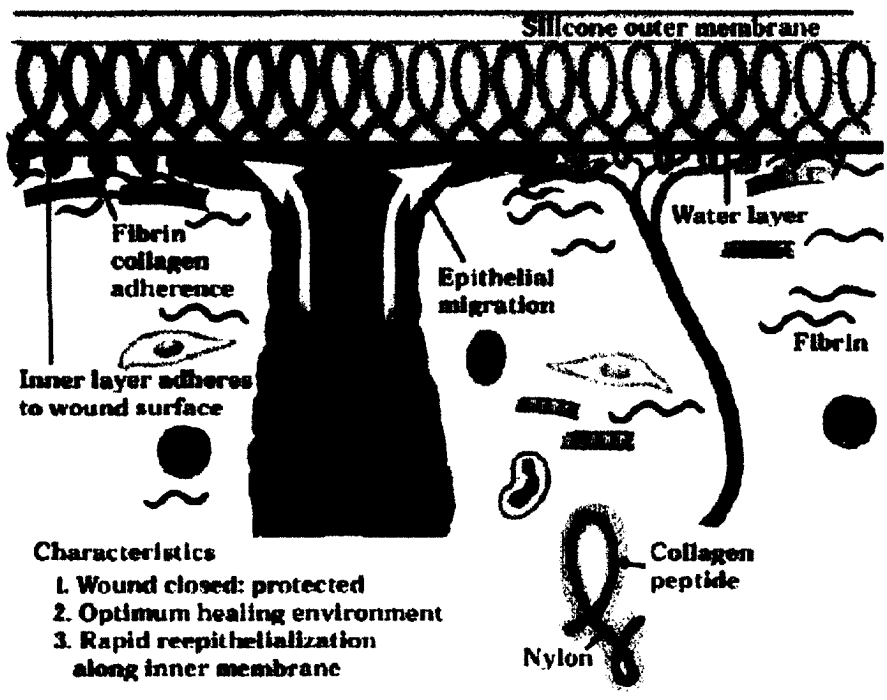

Figure 1.2. Bilayer structure of Biobrane® and its adherence to wound surface to promote healing [Adapted from www.burnsurgery.org (Demling *et al.*)]

CHAPTER 2*

Peptides that anneal to natural collagen *in vitro* and *ex vivo*

* This chapter has been submitted for publication as:

Sayani Chattopadhyay, Christopher J. Murphy, Jonathan F. McAnulty, and Ronald T. Raines; (2012) Peptides that anneal to natural collagen *in vitro* and *ex vivo*

2.1 Abstract

Collagen comprises ¼ of the protein in humans and ¾ of the dry weight of human skin. Here, we implement recent discoveries about the structure and stability of the collagen triple helix to design new chemical modalities that anchor to natural collagen. The key components are collagen mimetic peptides (CMPs) that are incapable of self-assembly into homotrimeric triple helices, but are able to anneal spontaneously to natural collagen. We show that such CMPs containing 4-fluoroproline residues, in particular, bind tightly to mammalian collagen *in vitro* and to a mouse wound *ex vivo*. These synthetic peptides, coupled to dyes or growth factors, could herald a new era in assessing or treating wounds.

2.2 Introduction

Collagen is a helix of three polypeptide strands. Each of these strands consists of ~300 Xaa-Yaa-Gly units, where Xaa is often (2*S*)-proline (Pro) and Yaa is (2*S*, 4*R*)-4-hydroxyproline (Hyp). Studies with collagen mimetic peptides (CMPs) show that replacing Pro with Hyp in the Yaa position stabilizes the collagen triple helix (Inouye *et al.*, 1976). Initially, this stability was attributed to water molecules forming bridging hydrogen bonds between the 4-hydroxyl groups and main-chain oxygen (Bella *et al.*, 1995). We showed, however, that collagen stability was enhanced dramatically by replacing Hyp in the Yaa position with (2*S*, 4*R*)-4-fluoroproline (Flp; Table 1), which has a side chain that is compromised severely in its ability to form hydrogen bonds (Engel *et al.*, 1998; Holmgren *et al.*, 1998; Holmgren *et al.*, 1999). We concluded that stereoelectronic effects were responsible for the extra stability conferred by Hyp (Bretscher *et al.*, 2001; Holmgren *et al.*, 1998; Holmgren *et al.*, 1999; Kotch *et al.*, 2008). Briefly, the 4*R*-electronegative substituents enforce a C^{γ}-*exo* ring pucker that preorganizes the main-chain dihedral angles of the residue in the Yaa position to be those required in a collagen triple (Shoulders *et al.*, 2009b; Shoulders *et al.*, 2010).

In contrast to Hyp in the Yaa position, Pro in the Xaa position of a collagen triple helix adopts a C^{γ}-*endo* ring pucker (DeRider *et al.*, 2002; Vitagliano *et al.*, 2001). Accordingly, we found that replacing Pro in the Xaa position with (2*S*, 4*S*)-4-fluoroproline (flp), which prefers an *endo* ring pucker, enhances triple-helical stability (Doi *et al.*, 2003; Hodges *et al.*, 2003; Renner *et al.*, 2001). Even though introducing flp into the Xaa position or Flp into the Yaa position is highly stabilizing, introducing *both* is highly destabilizing due to steric interactions between proximal fluoro-groups within the same cross section of a triple helix (Doi *et al.*, 2005; Hodges *et al.*, 2005; Shoulders *et al.*, 2008; Shoulders *et al.*, 2009a). Nevertheless, reagents that can have

adverse consequences for the structure and heterotrimeric triple helices in which $(flp\text{-}Flp\text{-}Gly)_7$ and $(Pro\text{-}Pro\text{-}Gly)_7$ are in a ratio 1:2 or 2:1 are more stable than the homotrimeric triple helices attainable from either of these strands alone (Hodges *et al.*, 2005).

Natural collagen is not effective in retaining passively absorbed materials. Efforts have been made to deliver and immobilize materials on natural collagen by chemical coupling. (Tiller *et al.*, 2001) Such covalent modification requires the use of electrophilic reagents that can alter the attributes of endogenous collagen, as well as damage other biopolymers. Hence, we sought to develop a non-covalent means to anchor a material to natural collagen.

Strand invasion plays a key role in molecular biology. A common example is the invasion of a single DNA or PNA strand into a DNA duplex to form base pairs with one of the parental DNA strands within a displacement loop (or "D-loop") (Kasamatsu *et al.*, 1971; Nielsen, 1999). Natural collagen contains loops or interruptions in its triple helix, (Long *et al.*, 1995; Paterlini *et al.*, 1995) and these domains are accessible to CMPs (Leikina *et al.*, 2002; Miles *et al.*, 2001; Mo *et al.*, 2006). We sought to take advantage of this phenomenon in wound tissue, which abounds in frayed and broken collagen (Figure 2.1). We suspected that fluoroproline-based CMPs might anneal to collagen under physiological conditions, unlike $(Pro\text{-}Hyp\text{-}Gly)_n$- based peptides, which require a high-temperature pre-treatment to dissociate triple helices into single strands (Wang *et al.*, 2005; Wang *et al.*, 2008a). Such heating could damage the peptide or a pendant molecule, and is not attractive in a clinical setting. Here, we report on the annealing of CMPs to natural collagen *in vitro* and *ex vivo*.

2.3 Experimental procedures

2.3.1 General materials and methods

Commercial chemicals were of reagent grade or better, and were used without further purification. Anhydrous THF, DMF, and CH_2Cl_2 were dispensed from CYCLE-TAINER® solvent delivery systems from J. T. Baker (Phillipsburg, NJ). Other anhydrous solvents, including DMSO, were obtained in septum-sealed bottles. In all reactions involving anhydrous solvents, glassware was either oven- or flame-dried.

Flash chromatography was performed with columns of silica gel 60, 230–400 mesh from Silicycle (Québec City, Canada). Semi-preparative HPLC was performed with a Varian Dynamax C-18 reversed phase column. Analytical HPLC was performed with a Vydac C-18 reversed phase column.

IRDye® 800CW NHS ester was from LI-COR (Lincoln, NE). Rhodamine Red™-X NHS ester and 5-carboxyfluorescein NHS ester were from Life Technologies (Grand Island, NY). Insoluble calf-skin collagen from ICN Biomedicals (Irvine, CA) and rat-tail type I collagen (5 mg/ mL) from Life Technologies were used for the *in vitro* annealing and retention studies, respectively. Cryopreserved PrimaPure™ normal human (adult) dermal fibroblasts (NHDF) were from Genlantis (San Diego, CA), and a LIVE/DEAD®Viability / Cytotoxicity Kit for mammalian cells was from Life Technologies.

Mass spectrometry was performed with either a Micromass LCT (electrospray ionization, ESI) mass spectrometer from Waters (Milford, MA) in the Mass Spectrometry Facility in the Department of Chemistry or an Applied Biosystems Voyager DE-Pro (matrix-assisted laser

desorption/ionization) mass spectrometer from Life Technologies in the Biophysics Instrumentation Facility at the University of Wisconsin–Madison.

2.3.2 Peptide synthesis

Peptides were synthesized by SPPS using an Applied Biosystems Synergy 432A Peptide Synthesizer from Life Technologies at the University of Wisconsin–Madison Biotechnology Center. The first seven coupling were of a normal duration (30 min), subsequent couplings were extended (120–200 min). Fmoc-deprotection was achieved by treatment with piperidine (20% v/v) in DMF. CMPs **1–4** were synthesized on FmocLys(Boc)-Wang resin (100–200 mesh). CMPs **1–3** were synthesized by segment condensation of their corresponding Fmoc-tripeptides (3 equiv).

. For CMP **1**, Fmocflp-Flp-GlyOH was synthesized from commercial BocflpOH and BocFlpOH, (Chorghade *et al.*, 2008) as described previously (Hodges *et al.*, 2005). Briefly, PyBOP-mediated coupling of BocFlpOH to the tosylate salt of glycine benzyl ester yielded a dipeptide, which was converted to its HCl salt, coupled to FmocflpOH, and subjected to hydrogenation to yield the tripeptide. Fmocflp-Flp-GlyOH, FmocGlyOH, and FmocSer(*t*Bu)OH were used in SPPS, resulting in CMP **1**.

For CMPs **2** and **3**, FmocPro-Pro-GlyOH was synthesized by using *N,N'*-dicyclohexylcarbodiimide-mediated coupling as reported previously (Jenkins *et al.*, 2005). FmocPro-Pro-GlyOH, FmocProOH, FmocSarOH, FmocGlyOH, and FmocSer(*t*Bu)OH were used in SPSS, resulting in CMPs **2** and **3**.

CMP **4** was synthesized by the sequential coupling of FmocProOH, FmocGlyOH, and FmocSer(*t*Bu)OH by SPPS.

Peptides were cleaved from the Wang resin by using 95:2.5:2.5 TFA / triisopropylsilane / H_2O (total volume: 2 mL), precipitated from *t*-butylmethylether at 0 °C, and isolated by centrifugation. Peptides were purified by semi-preparative HPLC using the following linear gradients: CMP **1**, 5–45% B over 60 min, CMP **2**, 10–90% B over 50 min, and CMP **3**, 5–85% B over 45 min, where solvent A was H_2O containing TFA (0.1% v/v) and solvent B was CH_3CN containing TFA (0.1% v/v). All peptides were judged to be >90% pure by analytical HPLC and MALDI–TOF mass spectrometry: *m/z* $[M + H]^+$ calculated for CMP **1** 2531, found 2635; *m/z* $[M + Na]^+$ calculated for CMP **2** 2403, found 2402; *m/z* $[M + Na]^+$calculated for CMP **3** 2417, found 2416; *m/z* $[M + H]^+$ calculated for CMP **4** 2658, found 2657; *m/z* $[M + H]^+$ calculated for $(Pro\text{-}Hyp\text{-}Gly)_7$ 1889, found 1889.

2.3.3 CMP–Fluorophore conjugates synthesis

The general method optimized for the mg-scale synthesis of peptide–dye conjugates was as follows. A CMP (1 equiv) was mixed with a fluorescent dye (1.13 equiv) in a sufficient volume of DMSO containing triethylamine (20 equiv). The resulting solution was allowed to stir at room temperature in the dark for 48 h, and then subjected to purification by reversed phase HPLC using a linear gradient 10mM triethylammonium acetate (pH 7.0) and MeOH. The purified products were characterized by HRMS–ESI or MALDI mass spectrometry. The highly anionic products of conjugation to IRDye® 800CW NHS were stored in glass vials with the ammonium form of a cation-exchange resin. This resin was prepared by stirring Dowex™

50WX4-50 resin overnight in 1 M NH_4OAc. Before use, the resin was washed in 1 M NH_4OAc, water, acetone, and hexane, and air-dried.

2.3.4 *In vitro* annealing

A 660 μM solution (50 μL) of ^{R}CMPs **1–4** or Rhodamine Red™-X NHS ester (Figure 2.2) that had been reacted with ethylamine (2 equiv) was added to calf-skin type I collagen (~10 mg) in a Falcon™ tube. The tubes were incubated in a water bath at 37 °C. After 2 h, each tube was agitated with a vortexing mixer and washed vigorously with phosphate-buffered saline (PBS; 4×), DMSO (4×), and MeOH (4×). These washings were discarded, and the samples were incubated in MeOH at room temperature for 12 days.

2.3.5 Retention on a collagen gel

Rat-tail type I collagen (5 mg/mL), sterile 10× PBS, sterile 1 N NaOH, and sterile H_2O were cooled on ice. The amount of each reagent was calculated to make a collagen solution with a final concentration of 3.8 mg/mL in 1× PBS as follows:

Total volume of collagen gel: $\mathbf{V}$

Volume of collagen ($\mathbf{V_1}$) = $\mathbf{V} \times [\text{collagen}]_{\text{final}} / [\text{collagen}]_{\text{initial}}$

Volume of 10× PBS ($\mathbf{V_2}$) = $\mathbf{V} / 10$

Volume of 1 N NaOH ($\mathbf{V_3}$) = $\mathbf{V_1} \times 0.025$

Volume of H_2O ($\mathbf{V_4}$) = $\mathbf{V} - (\mathbf{V_1} + \mathbf{V_2} + \mathbf{V_3})$

The 10× PBS, 1 N NaOH, and H_2O were mixed in a sterile tube. The collagen suspension was added slowly to the mixture, which was then mixed thoroughly. This suspension was added to the wells of a 48-well plate (200 μL/plate), which was incubated at 37 °C in a 93% humidity incubator for 1 h. The resulting gel was rinsed with 1× PBS. Solutions (0.5 mM) of ^{F}CMP **1**, ^{F}CMP **2**, and neutralized 5-FAM were prepared in PBS containing DMSO (5% v/v). An aliquot (20 μL) of each solution was added to the wells. The plates were incubated at 37 °C and 93% humidity, and the gel was washed with 4-°C PBS until no more fluorescence was detected in the wash solution. The total amount of wash volume was 300 μL per well. The wells were the re-filled with PBS buffer (500 μL), and the culture plate was incubated at 37 °C, 90% humidity and 5% v/v CO_2. The PBS was exchanged as above every 48 h. The concentrations of labeled peptide released during incubation were determined at 2-day intervals by measuring the absorbance of the wash solutions at 494 nm using a Cary 50Bio spectrophotometer from Varian (Palo Alto, CA).

2.3.6 *Ex vivo* annealing

Pelts were harvested from euthanized mice and stored at –80 °C. Immediately prior to an annealing experiment, pelts were thawed and shaved with an electric clipper. The treatment area was cleaned in a circular motion with cotton swabs wetted with sterile PBS, and all residual hair was removed. Two identical cutaneous defects were created in each pelt by using a 6-mm biopsy punch, and the top layer of skin was removed by using a forceps and scissors. The wounds were washed with sterile PBS and air-dried. One wound on each pelt was treated with a 50-μM solution (25 μL) of fluorescently labeled ^{IR}CMPs **1** or ^{IR}CMP **2**, and the other wound was treated with the same amount of the free dye (IRDye® 800CW NHS ester) that had been reacted with ethylamine (2 equiv). The treated wounds were incubated for 1 h at room temperature in a moist

environment, and then washed with PBS and DMSO successively for 10 min each. Similar comparisons between CMP **2** and CMP **4** were made by creating identical wounds on mice pelts, and treating one of them with ^{R}CMP **2** and the other with ^{R}CMP **4**. (For the pelts treated with free and conjugated RhodamineRed™-X dye, it was necessary to rub the wounds with DMSO during the wash due to the highly hydrophobic nature of the dye.) The pelts were then imaged using an Odyssey Imager from LI-COR (for the IRDye® 800CW) and a dissecting fluorescent microscope (for the Rhodamine Red™-X Dye).

2.3.7 Multiplex cytotoxicity assay

Solutions of CMPs **1** and **2**, and $(Pro\text{-}Hyp\text{-}Gly)_7$ (20 mM) were diluted in anhydrous DMSO to a final concentration of 100×. Serial dilutions were made in DMSO in 96-well polypropylene microtiter plates using the Precision XS liquid handler from BioTek (Winooski, VT). Compounds were divided equally into the wells of a 384-well microtiter plate in all 4 quadrants using a Biomek FX liquid handler with 96-channel pipetting head from Beckman Coulter (Brea, CA). Compounds were stored at –20 °C in DMSO until the day of the assay. Freeze-thaw cycles were limited to a maximum of ten per plate.

NHDF cells were maintained as reported previously. (Langenhan *et al.*, 2005) Cells were harvested by trypsinization using trypsin (0.25% w/v) and EDTA (0.1% w/v), and then counted with a Cellometer Auto T4 cell counter from Nexcelom (Lawrence, MA), before dilution for plating. Cell plating, compound handling, and assay set-up were performed as reported previously, (Langenhan *et al.*, 2005) except that the cells were plated in 50-μL volumes in 384-well clear-bottom tissue-culture plates from Corning (Lowell, MA). Compounds were added from 384-well stock plates at a 1:100 dilution using a Biomek FX liquid handler. Loaded plates

were incubated for 72 h at 37 °C and 5% v/v CO_2. Calcein AM (to 10 μM) and ethidium homodimer-1 (to 100 μM) were added (total volume: 30 μL), and the plates were incubated for 30 min at 37 °C. The emission in each well was determined by using a Safire-2 microplate reader from Tecan (Männedorf, Switzerland) to monitor emission at 530 and 615 nm for calcein AM and ethidium homodimer-1, respectively. CellTiter-Glo reagent (15 μL) from Promega (Madison, WI) was added, and the resulting solution was incubated for 10min at room temperature with gentle agitation to lyse the cells. The luminescence in each well was determined to confirm the data from the absorbance measurements.

2.4 Results and discussion

2.4.1 Design and synthesis of collagen mimetic peptides

CMPs containing seven Xaa-Yaa-Gly units can be synthesized readily by solid-phase peptide synthesis (SPPS). These peptides can form stable triple helices (Table 1) that resemble those in natural collagen, as is apparent from circular dichroism spectroscopy, analytical ultracentrifugation, X-ray crystallography, fiber diffraction analysis, and electron microscopy (Fallas *et al.*, 2010; Fields, 2010; Jenkins *et al.*, 2002; Koide, 2007; Przybyla *et al.*, 2010; Shoulders *et al.*, 2009c; Woolfson, 2010). This synthetic strategy facilitates the introduction of nonnatural residues, like flp and Flp (Chorghade *et al.*, 2008), into a CMP.

As our preferred CMP, we chose Ac-(flp-Flp-Gly)$_7$-(Gly-Ser)$_3$-LysOH (**1**). The N-terminal acetyl group precludes any unfavorable Coulombic interactions with natural collagen, and the C-terminal lysine residue provides an amino group for conjugation by *N*-acylation. The (Gly-Ser)$_3$ unit serves as a flexible, soluble spacer.

As control CMPs, we chose Ac-(Pro-Pro-Gly)$_7$-(Gly-Ser)$_3$-LysOH (**2**), Ac-(Pro-Pro-Gly)$_3$-(Pro-Pro-Sar)-(Pro-Pro-Gly)$_3$-(Gly-Ser)$_3$-LysOH (**3**), and Ac-Pro$_{21}$-(Gly-Ser)$_3$-LysOH (**4**). We anticipated that CMP **2** should be effective in annealing, though less so than CMP **1** because of its lesser preorganization (Bretscher *et al.*, 2001; DeRider *et al.*, 2002; Kotch *et al.*, 2008). The methyl group of the central sarcosine (Sar) in CMP **3** provides a subtle but strong impediment to triple-helix formation by obviating the interstrand GlyNH···O=CPro hydrogen bond (Chen *et al.*, 2011), but allows CMP **3** to retain the other physicochemical characteristics of CMP **2**. Finally, the linear polyproline strand of CMP **4** is not capable of annealing to natural collagen by triple-helix formation.

CMPs **1**–**3** were synthesized by a convergent route relying on the condensation of Xaa-Yaa-Gly units. CMP **4** was synthesized the sequential coupling of amino-acid monomers. For annealing experiments, biocompatible dyes were conjugated to the CMPs by *O*- to *N*-acyl transfer using an NHS ester of the dyes (Figure 2.2).

2.4.2 Annealing of collagen-mimetic peptides to collagen *in vitro*

In initial wound assessment studies, we treated insoluble calf-skin collagen (type I) with fluorescently labeled CMPs **1**–**4**, as well as with the unconjugated fluorophore. We monitored the changes in color and binding by visual inspection over several days. CMPs **1** and **2**, which have flp-Flp-Gly and Pro-Pro-Gly units, respectively, annealed to collagen firmly as seen by the persistent color of the insoluble collagen after 12 days (Figure 2.3A and 2.3B). In contrast, collagen treated with CMPs **3** and **4**, and free dye lost all apparent color during the first day and retained none after 12 days (Figure 2.3C–2.3E). These initial results validated our strategy (Figure 2.1), but did not differentiate between CMPs **1** and **2**.

2.4.3 Retention of collagen-mimetic peptides on a collagen gel

Next, we assessed the time-dependent retention of CMPs **1** and **2** on a gel of rat-tail collagen (type I) under physiological conditions. Over the course of days, CMP **1** exhibited much greater retention than did CMP **2** (Figure 2.4). Nearly a third of the fluoroproline-containing CMP (**1**) was retained after two weeks, whereas virtually all of the proline-containing CMP (**2**) was lost after one week. These data are consistent with the preorganization endowed by the fluoroproline residues (Hodges *et al.*, 2005).

2.4.4 Annealing of collagen-mimetic peptides to an *ex vivo* wound

Then, we analyzed the ability of CMPs **1** and **2** to bind to cutaneous wounds on pelts harvested from mice. Identical wounds were created on mice pelts by removing the top layer of the skin, and the consequence wound beds were treated with CMP **1**, CMP **2**, or the free fluorophore, incubated, and washed. Both CMPs **1** and **2** remained annealed to the wound bed after aggressive washing, whereas the free dye did not (Figure 2.5A–C). We repeated the experiment by treating the wound on one side of the pelt with CMP **2** and the other side with CMP **4**. As expected, CMP **2** showed much greater binding than did CMP **4** (Figure 2.5D and 2.5E). The fluorescence in these experiments was limited primarily to the wound bed and its edges, where the concentration of damaged collagen is likely to be higher than in the surrounding unbroken skin.

2.4.5 Toxicity of collagen-mimetic peptides to human cells

Finally, we performed cytotoxicity assays on CMPs **1** and **2** to determine their suitability for future work *in vivo*. The CMPs were tested for toxicity towards a relevant model, normal

human dermal fibroblast cells. Doxorubicin served as the positive control and $(Pro\text{-}Hyp\text{-}Gly)_7$ as the negative control. Both peptides proved to be non-toxic to human fibroblast cells (Figure 2.6).

2.5 Conclusions

We have demonstrated the efficacy of the strategy depicted in Figure 2.1. Both the $(flp\text{-}Flp\text{-}Gly)_7$-based CMP (**1**) and the $(Pro\text{-}Pro\text{-}Gly)_7$-based CMP (**2**) bind strongly to collagen at room temperature *in vitro* and *ex vivo*. Binding does not require heating the CMP prior to its application. CMP **1** is retained longer on collagen than is CMP **2**, providing the option of a long-term attachment of an effector molecule or its sustained release over a shorter time period. Neither peptide is toxic to human fibroblast cells. We anticipate that either CMP **1** or CMP **2** could be used to affix a pendant molecule in a wound bed, obviating the need for repeated application. This methodology avails a myriad of possibilities for the delivery of therapeutic small molecules, peptides, and proteins, and could be especially useful for treating highly traumatized wounds (*e.g.*, in burn patients) or slowly healing wounds (*e.g.*, in diabetic patients) (Gurtner *et al.*, 2008; Schultz *et al.*, 2009). We foresee a CMP with a pendant dye highlighting areas of maximal tissue damage (which would have many sites for annealing), and a CMP with a pendant growth factor expediting the healing process.

Table 2.1. Thermostability of synthetic collagen triple helices

Collagen Mimetic Peptide	Xaa	Yaa	Triple Helical T_m (°C)
(Xaa-Yaa-Gly)$_7$	Pro	Hyp	36 (Bretscher *et al.*, 2001)
	Pro	Flp	45 (Bretscher *et al.*, 2001)
	flp	Pro	33 (Hodges *et al.*, 2003)
	Pro	Pro	No helix (Hodges *et al.*, 2005)
	flp	Flp	No helix (Hodges *et al.*, 2005)
(Xaa-Yaa-Gly)$_{10}$	Pro	Hyp	61–69 (Berisio *et al.*, 2004; Holmgren *et al.*, 1999)
	Pro	Flp	91 (Holmgren *et al.*, 1999)
	Flp	Pro	58 (Doi *et al.*, 2003)
	Pro	Pro	31–41 (Holmgren *et al.*, 1999; Nishi *et al.*, 2005)
	flp	Flp	30 (Doi *et al.*, 2005)

Figure 2.1. Representation of a collagen mimetic peptide (CMP) annealing to damaged collagen to anchor a molecule (X) in a wound bed

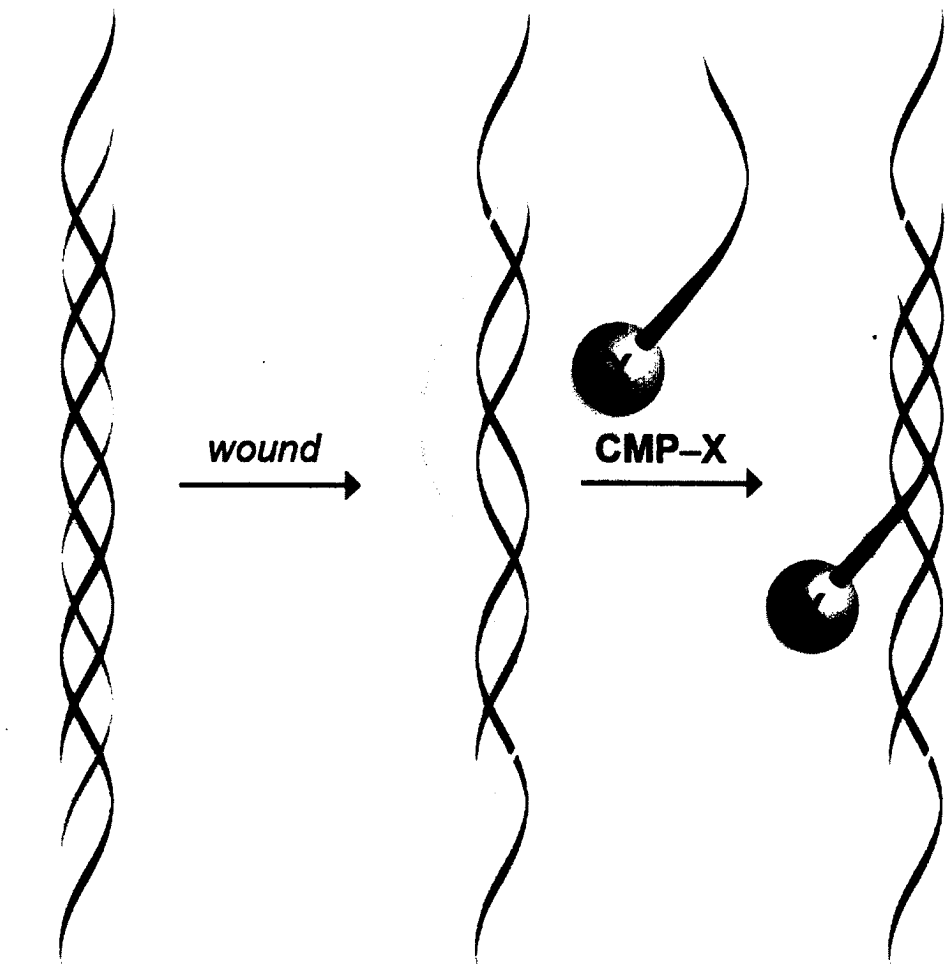

Figure 2.2. CMPs (**1–4**) and dyes used in this work. Each CMP has a C-terminal $(Gly\text{-}Ser)_3$-LysOH segment. CMP–dye conjugates are indicated in the text with a superscript: ^{IR}CMP for IRDye® 800CW, ^{R}CMP for Rhodamine Red™-X, and ^{F}CMP for 5-carboxyfluorescein.

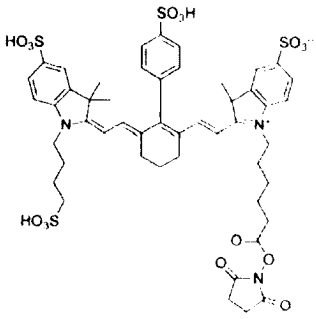

IRDye® 800CW NHS ester

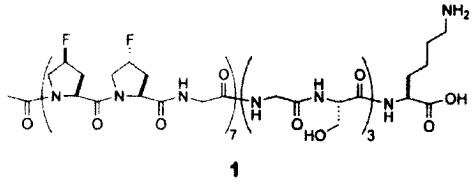

1

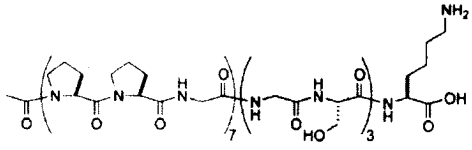

2

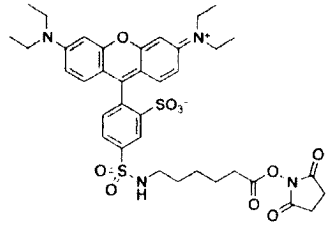

Rhodamine Red™-X NHS ester

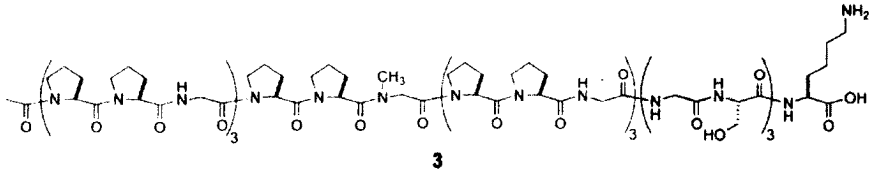

3

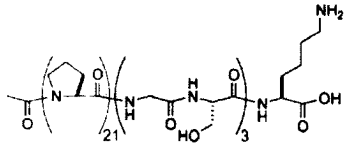

4

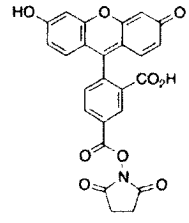

5-carboxyfluorescein NHS ester

Figure 2.3. Photographs of CMPs annealed to calf-skin type I collagen. Fluorescently labeled CMPs in MeOH were added to collagen, which was washed with PBS, DMSO, and MeOH, and photographed after 12 days. (A) ^{R}CMP **1**; (B) ^{R}CMP **2**; (C) ^{R}CMP **3**; (D) ^{R}CMP **4**; (E) Rhodamine Red™-X NHS ester that had been reacted with ethylamine.

Figure 2.4. Plot of the retention of CMPs on a gel of rat-tail type I collagen. Fluorescently labeled CMPs were applied to a gel, which was then washed at 48-h intervals and monitored for at 494 nm. ◆: ^{F}CMP **1**; ■ : ^{F}CMP **2**; ◯: 5-carboxyfluorescein NHS ester that had been reacted with ethylamine.

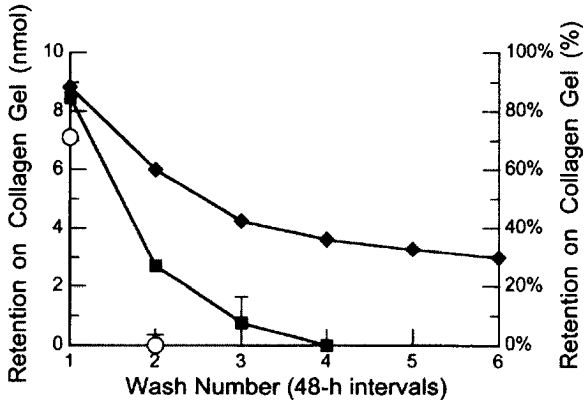

Figure 2.5. Photograph of the annealing of CMPs to mouse collagen *ex vivo*. Fluorescently labeled CMPs were applied to 6-mm cutaneous wounds on mouse pelts, washed, and imaged. (A) ^{IR}CMP **1**, photograph. (B) ^{IR}CMP **1**, fluorescence image. (C) ^{IR}CMP **2**, fluorescence image. (D) ^{R}CMP **2**, fluorescence image. (E) ^{R}CMP **4**, fluorescence image. In panels A–C, the circles (6 mm) denote wounds treated with IRDye® 800CW NHS ester that had been reacted with ethylamine. In panels (B) and (C), the mouse pelts are outlined.

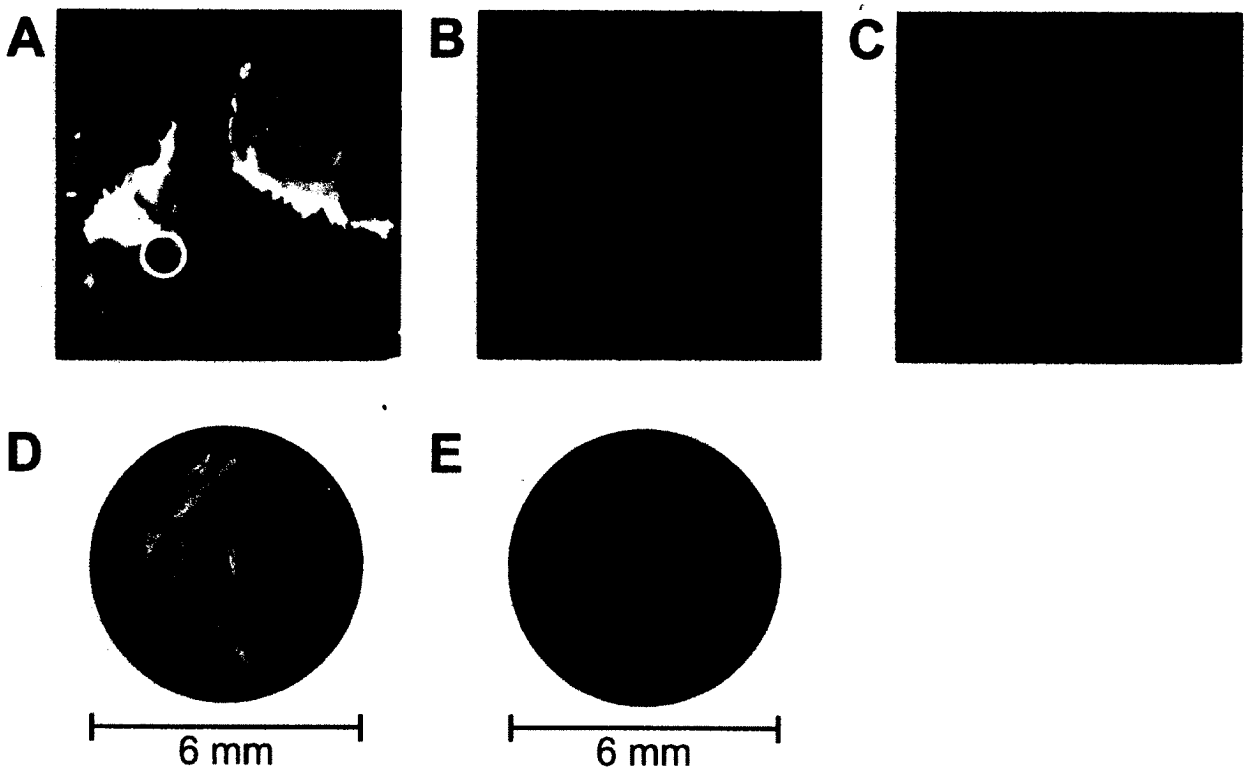

Figure 2.6. Cytotoxicity of CMPs. The proliferation of human dermal fibroblast cells was assessed by fluorescence emission using a Calcein AM / EthD-1 assay after incubation for 72 h with unlabeled CMPs [◆, CMP **1**; ■, CMP **2**; ●, $(Pro\text{-}Hyp\text{-}Gly)_7$] or doxorubicin (◯).

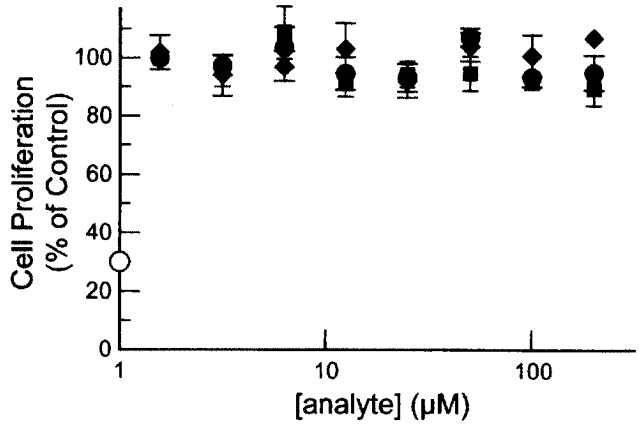

2.6 Acknowledgments

We are grateful to N. L. Abbott, M. D. Shoulders, F. W. Kotch, L. J. Martin, and G. A. Ellis for contributive discussions. This work was supported by grants R01 AR044276 and RC2 AR058971 (NIH), and a Wisconsin Institute of Discovery Seed Grant. MALDI–TOF mass spectrometry was performed at the University of Wisconsin–Madison Biophysics Instrumentation Facility, which was established with Grants BIR-9512577 (NSF) and S10 RR13790 (NIH).

CHAPTER 3*

Noncovalent immobilization of a Substance P–collagen mimetic peptide conjugate promotes wound healing in mice

* This chapter has been prepared for publication as:

Sayani Chattopadhyay, Kathleen M. Guthrie, Leandro Teixeira, Christopher J. Murphy, Richard R. Dubielzig, Jonathan F. McAnulty, and Ronald T. Raines; (2012) Noncovalent immobilization of a Substance P–collagen mimetic peptide conjugate promotes wound healing in mice

3.1 Abstract

Wound healing is a complex process involving an inflammatory reaction, deposition of fresh epithelial tissue, collagen deposition, contraction, and wound repair, all of which require the recruitment of cytoactive factors. The one-time application of such factors to wounds does not maintain a sufficient concentration to promote substantial healing. Here we report on an improved mode for the topical application of a cytoactive factor to a wound bed. This mode relies on the ability of a collagen mimetic peptide (CMP) to anneal to damaged collagen triple helices within the bed. As a model factor, we choose Substance P, a neuropeptide of the tachykinin family that is known to mediate vasodilation and inflammatory response in early wound healing. Using splinted wounds in mice, we show that the one-time application of a CMP–Substance P conjugate enhances wound closure and re-epithelialization compared to unconjugated Substance P and vehicular controls. In addition, we validate the synergism of insulin with Substance P and show that polyethylene glycol in the delivery vehicle improves healing. These data predicate a new paradigm for the efficacious localization of cytoactive factors in wound beds.

3.2 Introduction

Chronic and slow-healing pathologic wounds have a major debilitating effect on the physical and mental health of patients, as well as being a significant drain on health care resources. Commonly, slow-healing wounds manifest in victims of severe burn injuries and physical trauma, whereas chronic wounds emerge from diabetes and vascular problems. Healing of these wounds is a complex process in which humoral and neural factors, the extracellular matrix, and various cell types participate at specific times (Baum *et al.*, 2005; Gibran *et al.*, 2007; Singer *et al.*, 1999). Re-epithelialization, granulation, tissue formation, collagen deposition, and contraction are important phases of the healing process that determine the quality of healing, as well as the bias for wound repair or wound regeneration. (Gurtner *et al.*, 2008) Among the molecular factors that modulate the immunologic and inflammatory responses in wounds are the neuropeptides (Holzer, 1988), such as Substance P (**SubP**).

SubP is an undecapeptide of the tachykinin family that is produced by sensory neurons, stored in the terminal end of unmyelinated cutaneous nerve fibers, and released upon noxious stimuli (Holzer, 1988). Nerve fibers containing **SubP** have been localized in human skin and burn wounds in the vicinity of blood vessels and sweat glands (Dunnick *et al.*, 1996). After release from the sensory nerves, **SubP** binds to a specific cell-surface neurokinin receptor (NK-1) or is degraded by neural peptidases. Hence, **SubP** does not need to be internalized into the cells to stimulate proliferative activity in the wound bed. Upon release, **SubP** not only mediates vasodilation in early wound repair (Holzer, 1998; Iwamoto *et al.*, 1989), release of histamine by mast cells (Barnes *et al.*, 1986; Weidner *et al.*, 2000), and angiogenesis (Seegers *et al.*, 2003), indicating that healing is promoted by an interaction between tissue and nervous system, but also leads to interaction with immunocompetent cells, including granulocytes (Wiedermann *et al.*,

1989; Wiedermann *et al.*, 1993) and monocytes (Ruff *et al.*, 1985; Wiedermann *et al.*, 1989). These effects are not restricted to the initial point of stimulus, but are also observed in the surrounding area. **SubP** shows a proliferative activity on fibroblasts (Kähler *et al.*, 1993a; Kähler *et al.*, 1996; Nilsson *et al.*, 1985; Ziche *et al.*, 1990) and keratinocytes via the NK receptors (McGovern *et al.*, 1995; Tanaka *et al.*, 1988). This neuropeptide thus participates in vasodilation associated with inflammatory response and stimulates proliferation of epithelial, vascular, and connective tissue.

Previous efforts to study wound-healing mediated by **SubP** *in vivo* have involved its administration by subcutaneous or intraperitoneal injections (Barnes *et al.*, 1986; Buttow *et al.*, 2003; Delgado *et al.*, 2005) in small rodents, as well as topical application on dorsal wounds of diabetic mice (Scott *et al.*, 2008) and human corneal wounds (Lee *et al.*, 2002). These treatments improved healing—wound size and scab formation decreased significantly as a function of increasing **SubP** concentration in comparison to saline-treated controls (Delgado *et al.*, 2005). Moreover, the neuropeptide was shown to induce production of TNF-α, IL-1β, IL-2, and IL-6 by T-cell lymphocytes, macrophages, and neutrophils, thereby increasing the rate of wound healing (Delgado *et al.*, 2003).

To enhance the activity of **SubP**, we sought to design a delivery system for **SubP** that would provide for sustained residency of the peptide in the wound. We reasoned that a strategy based on collagen would have numerous advantages. Collagen comprises ¼ of the protein in humans and ¾ of the dry weight of human skin (Shoulders *et al.*, 2009b). The most abundant forms of collagen, type I and type II, can be isolated easily from animal tissues and have been used as shields in ophthalmology, sponges in wound care, pellets and gels for biologic delivery, and matrices for cell culture (Lee *et al.*, 2001).

Collagen fibers have a loose structural network, and are thus ineffective at retaining passively absorbed materials. Efforts have been made to immobilize molecules on endogenous collagen by covalent coupling to its amino-acid side chains (Tiller *et al.*, 2001). This strategy is, however, confounded by the heterogeneity of natural collagen and by collateral damage that necessarily ensues upon immobilization. Recently, we described a strategy that circumvents these issues. Our strategy exploits the propensity of a collagen mimetic peptide (**CMP**) to anneal to endogenous collagen under physiological conditions. We showed previously that peptides containing $(ProProGly)_7$ moieties in their sequence are capable of binding to native type I collagen *in vitro* and *ex vivo* at room temperature and neutral pH, and can anchor molecules conjugated to them in the wound tissue (Figure 3.1) (Chattopadhyay *et al.*, 2012). Here, we report on the conjugation of **SubP** to a **CMP** with the sequence $(ProProGly)_7$, and on the testing of this conjugate as an agent for healing wounds in mice.

3.3 Methods

3.3.1 Materials

Commercial chemicals were of reagent grade or better, and were used without further purification. Anhydrous solvents were obtained from CYCLE-TAINER® solvent delivery systems (J. T. Baker, Phillipsburg, NJ). HPLC-grade solvents were obtained in sealed bottles (Fisher Chemical, Fairlawn, NJ). In all reaction mixtures having anhydrous solvents, glassware was either oven- or flame-dried. Commercial **SubP** (acetate salt hydrate, Sigma–Aldrich, St. Louis, MO) and insulin (Novolin® R; rDNA origin, Novo Nordisk, Princeton, NJ) were used as controls. Polyethylene Glycol 8000 (PEG) (Fisher Bioreagents®, Fairlawn, NJ) and bacteriostatic

0.9% v/v NaCl (Hospira, Lake Forest, IL) were used to prepare 5% w/v PEG/saline solution as a vehicle.

Male mice (BKS.Cg-*Dock7*^{m}+/+ *Lepr*^{db}/J, Jackson Laboratories, Bar Harbor, ME) were used as the animal model. The mice were anesthetized with Isoflurane (Abbott Laboratories, Abbott Park, IL) and injected with Buprenex (buprenorphine hydrochloride, Reckitt Benckiser, Berkshire, UK) for pain management, and their wounds were cleaned with 4% w/v chlorhexidine gluconate (Purdue Products, Stanford, CT) and saline. O-ring splints (15 mm o.d. × 11 mm i.d., 2-mm thickness, Carr® silicone O-rings from McMaster (Chicago, IL) came in ready-to-use packages.

Semi-preparative HPLC was performed with a Varian Dynamax C-18 reversed-phase column. Analytical HPLC was performed using a Vydac C-18 reversed-phase column. Mass spectrometry was performed with an Applied Biosystems Voyager DE-Pro (matrix-assisted laser desorption/ionization) mass spectrometer from Life Technologies (Carlsbad, CA) in the Biophysics Instrumentation Facility at University of Wisconsin–Madison.

3.3.2 Peptide synthesis and purification

Peptides were synthesized by solid-phase peptide synthesis using a 12-channel Symphony® peptide synthesizer from Protein Technologies (Tucson, AZ) at the University of Wisconsin–Madison Biotechnology Center. **SubP** is an undecapeptide with the sequence ArgProLysProGlnGlnPhePheGlyLeuMetNH_2. To synthesize **CMP–SubP**, the C-terminal Met residue was coupled to the resin after a swell cycle, and the subsequent ten amino acids were added by extended (60-min) couplings. Seven FmocProProGlyOH tripeptides were added by

normal (30-min) couplings. Fmoc-deprotection was achieved by treatment with piperidine (20% v/v) in DMF.

CMP itself was synthesized by SPPS on Fmoc-Gly-Wang Resin (0.4–0.7 mmol/g, 100–200 mesh, Novabiochem®, EMD Chemicals, Gibbstown, NJ) by the sequential coupling of FmocProOH and FmocProProGlyOH. The **CMP–SubP** strand was initiated by coupling the terminal methionine residue to NovaPEG Rink Amide Resin (0.44 mmol/g, Novabiochem®, EMD Chemicals Gibbstown, NJ) and subsequent segment condensation using excess (5 equiv/coupling) FmocLeuOH, FmocGlyOH, FmocPheOH, FmocGln(Trt)OH, FmocProOH, FmocLys(Boc)OH, FmocArg(Pbf)OH, and FmocProProGlyOH trimers (which were synthesized as reported previously (Jenkins *et al.*, 2005). The residues were converted to active esters by treatment with 1-hydroxybenzotriazole (HOBt, 3 equiv), *O*-benzotriazole-*N*,*N*,*N*′,*N*′-tetramethyl-uronium-hexafluoro-phosphate (HBTU, 3 equiv) and *N*-methylmorpholine (NMM, 6 equiv). **CMP** was cleaved from the Fmoc-Gly-Wang Resin by using 95:2.5:2.5 trifluoroacetic acid/triisopropylsilane/water (total volume: 2 mL) and **CMP–SubP** was cleaved from the NovaPEG Rink Amide Resin using 92.5:5:2.5 trifluoroacetic acid/thioanisole/ethanedithiol (total volume: 3 mL). The NovaPEG Rink Amide Resin requires excess cleavage solution due to the high swelling properties of the resin and was washed multiple times with TFAat the end of the cleavage. Both the peptides were precipitated from *t*-butylmethylether at 0 °C, isolated by centrifugation and purified by semi-preparative HPLC using the following linear gradients: **CMP**, 5% B to 85% B over 45 min, and **CMP–SubP**, 10% B to 90% B over 50 min; where solvent A was H_2O containing TFA (0.1% v/v) and solvent B was CH_3CN containing TFA (0.1% v/v). **CMP** was readily soluble in dH_2O but **CMP–SubP** required addition of CH_3CN (12% v/v) to form a clear solution for HPLC analysis. All the peptides were judged to be >90%

pure by HPLC and MALDI–TOF mass spectrometry: (*m/z*) $[M + H]^+$ calculated for **CMP** 1777, found 1777; (*m/z*) $[M + H]^+$ calculated for **CMP–SubP** 3107, found 3108.

3.3.3 *In vivo* mouse model

Male mice (homozygous for *Lepr*^{db}, Jackson Laboratories, Bar Harbor, ME) were used between the ages of 8–12 weeks. The mice were housed in groups until the day of surgery. After surgery, mice were housed in separate cages and monitored for changes in behavior and weight gain or loss. The experimental protocol followed the guidelines issued by the Institutional Animal Care and Use Committee (IACUC) at the University of Wisconsin–Madison. The mice were provided food and water *ad libitum*, as well as enrichment, and housed in a temperature-controlled environment with 12-h light and dark cycles.

On the day of the surgery the mice were anaesthetized with isoflurane using an induction chamber. Buprenorphine, diluted in 0.9% w/v saline to a concentration of 0.01 mg/mL, was injected subcutaneously (0.4 mL/mouse) for pain management. Eyes were lubricated and hind nails clipped. The craniodorsal region was shaved using electric clippers, and the shaved area was scrubbed with alternating cotton swabs of chlorhexidine and sterile saline in circular strokes. Residual hair was removed. For the non-splinted wound model, identical 8-mm wounds were created on either sides of the body with a biopsy punch, and the wounding was completed using forceps and scissors to prevent the punch from lacerating the subcutaneous tissue. For the splinted-wound model, splints were bilaterally placed in a symmetric arrangement, as per Galiano et al using adhesive (Krazy Glue® Gel, Elmer's, Columbus, OH) and then secured to the skin using 8 interrupted sutures (5-0 nylon suture), encircling the splints with the knots. Wounds were created in the center of the splints using the 8-mm biopsy punch, and the skin was removed

using forceps and scissors. The wounds were then treated with the test compound, and allowed to incubate for 30 min while the mouse was still under anesthesia. The wounds were then photographed, and the mice were then allowed to recover on a warming pad.

The treated mice were monitored daily for behavioral changes, and their body weights were recorded on days 1, 3, 6, 9, 12, and 16. Splints were checked daily, and any broken or untied suture was replaced according to the experimental protocol. During a 24-h period, if only one suture were compromised, it was replaced with a new suture. If, however, two or more sutures were compromised during a 24-h period, the wound was no longer considered splinted and was removed from the study.

Digital photos were taken on the last day of the experiment and image analysis was performed by calculating the wound area (mm^2) using ImageJ Software. Wound closure was defined as the reduction in area between wound edges over the course of study and was reported as a percentage of the original wound size.

3.3.4 Harvesting the wounds

Histopathology cassettes were labeled for mouse and wound identification. Note cards (1 $inch^2$) were fitted to the bottom of the histopathology cassettes and one edge was labeled "cranial" that would be lined up with the cranial side of the wound harvested. On the final day of the experiment, mice were euthanized using Beuthanasia®-D (0.5 mL/mouse). Using a scalpel blade and scissors, a ¾ inch × ¾ inch square area of tissue is taken from the mouse, keeping the wound centered in the tissue section. Deep dissection was performed to harvest several layers of tissue deep in the wound. The square section of tissue was affixed to the note card, with the

cranial edge lined up against the labeled edge of the card. The cassettes were then closed and placed in formalin-filled jars, to be processed for histopathological processing.

3.3.5 Histopathological analyses

After euthanasia, the entire wound bed as well as the intact skin margin greater than 5 mm was excised to the retro-peritoneum. The harvested tissue was then fixed in formalin (10% v/v) for at least 24 h, and then sectioned through the center of the lesion. The center was marked with India ink prior to fixation. Routine paraffin processing was performed and the tissue samples were serially sectioned at a thickness of 5 μm, making sure that the center of the lesion was included on the slide. The slides were stained with hematoxylin, eosin, and picosirius red. A mounted digital camera (Olympus DP72, Melville, NY) was used to photograph the sections using light microscopy. Size of the wound, length of re-epithilialization, amount of fibrovascular proliferation in the dermis, and inflammatory response were measured as parameters to study wound healing on the slides containing the center of the lesion. Measurements were taken and analyzed using image-analysis software (CellScience Dimension 1.4, Olympus, Melville, NY). Size of the wound was defined as the area of the wound not covered by advancing epithelial layer and was calculated by measuring the distance between the opposite free edges of the wound. Length of re-epithelialization was defined by the length of the layer of proliferating keratinocytes covering the wounds area and was calculated by measuring the distance between the free edge of the keratinocyte layer and the base where the cells were still associated with native dermal tissue. Both sides of the lesion were measured and the final result was the sum of the two measurements. For wounds that had undergone complete re-epithelialization, a single measurement was taken from base to base.

Fibrovascular dermal proliferation was measured by examining the picosirius red-stained sections under polarized light, which highlights newly deposited dermal collagen. The wound bed was designated with the image-analysis software, and the amount of new collagen in the selected area was measured and expressed as a percentage of the total wound area. The inflammatory response was assessed using a semi-quantitative histopathological scoring system ranging from 0 to 4, where 0 indicated no inflammation, 1 indicates 0–25% of the wound area being affected, 2 indicates 25–50% of the wound area being affected, 3 indicates 50–75% of the wound area being affected, and 4 indicates >75% of the wound area being affected. The inflammatory response was also categorized as 'acute' when more than 75% of the cells were neutrophils; 'chronic active' when there was a 1:1 ratio of neutrophils and mononuclear cells; and 'chronic' when >75% of the inflammatory cells were mononuclear.

3.3.6 Statistical analyses

Data were analyzed with a Mann–Whitney rank sum test, and statistical significance was set to $p < 0.05$. Analyses were executed using the program GraphPad Prism, Version 5.0 (GraphPad Software, La Jolla, CA).

3.4 Results and discussion

Male mice (homozygous for *Lepr*^{db} strain) become obese at 3–4 weeks of age, and their blood sugar typically elevates at 4–8 weeks of age. These genetically diabetic mice were chosen for our study because they exhibit relevant characteristics similar to those of human adult-onset type II diabetes mellitus (Coleman, 1978; Kämpfer *et al.*, 2000), including an impaired wound-

healing response (Brem *et al.*, 2007). These mice also exhibit delayed and reduced expression of keratinocyte growth factor (Werner *et al.*, 1994) and peripheral neuropathy similar to diabetic adult humans (Norido *et al.*, 1984), and the course of wound healing in these mice follows closely the clinical observations of human diabetic patients (Greenhalgh, 2003).

The collagen mimetic peptide **CMP** and its **SubP** conjugate (**CMP–SubP**) were synthesized by solid-phase peptide synthesis (SPPS). Previously, we reported that $(ProProGly)_7$ moieties anneal to type I collagen *in vitro* and *ex vivo* (Chattopadhyay *et al.*, 2012). We have also shown that these peptides can be used to anchor small-molecule fluorophores in *ex vivo* wound tissue at room temperature, and that they are not toxic to dermal fibroblast cells. An earlier effort to localize a collagen mimetic peptide to collagen gel *in vitro* employed a $(ProHypGly)_n$ sequence without a pendant cytoactive factor (Wang *et al.*, 2008b). These peptides required pre-heating at 80 °C to disrupt triple-helical structure prior to application. In contrast, our strategy is effected at physiological conditions. In designing **CMP–SubP**, we chose to conjugate **SubP** to the C-terminus of **CMP**. **SubP** is capable of inducing cellular responses through unique receptors recognizing different portions of the molecule, and both the N- and C-terminus have been found to be active in this regard (Ananthanarayanan *et al.*, 1992; Bar-Shavit *et al.*, 1980; Ruff *et al.*, 1985). Studies have established that the C-terminal region of **SubP** displays biological activities that are mediated by the neurokinin receptor (Bury *et al.*, 1976; Iwamoto *et al.*, 1990; Rosell *et al.*, 1977; Yanaihara *et al.*, 1977). The C-terminal amide is also crucial to is biological activity, as the free acid is largely inactive in the chemotaxis of monocytes (Ruff *et al.*, 1985) and in its ability to bind to human T cells (Payan *et al.*, 1984). Accordingly, we decided to conjugate **CMP** to the N-terminus of **SubP** for our studies.

We chose to use an excisional wound model for our experiments. These wounds, which heal from the margins, provide the broadest assessment of the various parameters for wound healing, such as re-epithelialization, fibrovascular proliferation, contracture, and angiogenesis (Greenhalgh *et al.*, 2001). Mice models, though convenient, are dissimilar from human skin models in that the major mechanism of wound closure is contraction; in humans, re-epithelialization and granulation tissue-formation are the major phases of wound healing (Davidson, 1998; Greenhalgh *et al.*, 2001). The use of splints around excise wounds in *db/db* mice is known to allow healing by granulocyte formation and re-epithilialization, while minimizing the effects of contraction (Galiano *et al.*, 2004). A splinted wound model also facilitates the application of topical agents directly onto the wound bed, and can avail two side-by-side wounds on the same mouse.

3.4.1 CMP-SubP in wound healing

Two splinted wounds (8-mm o.d.) were created in the craniodorsal region of each *db/db* mouse (n = 8 mice/16 wounds) under anesthesia and topically treated with 25 μL of a solution of **CMP–SubP** (1 mM) in 5% w/v PEG/saline vehicle. Insulin (5 μL, 50 I.U. in saline) was added to each of the wounds, and the mice were incubated for 30 min under anesthesia. The recovered mice were monitored over a period of 16 days. **SubP** has been known to act synergistically in presence of insulin or insulin-like growth factor 1 (IGF-1) to promote wound healing (Lee *et al.*, 2002; Nakamura *et al.*, 1997; Nishida *et al.*, 1996; Reid *et al.*, 1993; Yamada *et al.*, 2004). As a control, we treated mice in a similar manner with insulin (5 μL, 50 I.U. + 25 μL of saline). Insulin, alone, has been reported to be effective in wound healing. Clinical evidence indicates that insulin increases vascularization, stimulates proliferation, enhances phagocytosis and promotes contraction in the wound (Belfield *et al.*, 1970). Re-epithelialization and collagen

deposition were also promoted in burn-wound rat models (Madibally *et al.*, 2003). When injected in diabetic mice wounds, insulin treatment caused a reduction in the mean hyperglycaemia levels (Weringer *et al.*, 1982), but it has been suggested that the increased rate of wound healing may also be attributed to zinc that is used to crystallize insulin (Greenway *et al.*, 1999). Polyethylene glycol in saline solution (PEG 8000, 5% w/v) (Brown *et al.*, 1994; Greenhalgh *et al.*, 1990) was used to dissolve **CMP–SubP** and was also tested as a control, along with saline (0.9% w/v sodium chloride). **CMP** (25 μL, 1 mM) and **SubP** in 5% w/v PEG/saline were used as controls to compare against the sustained biological activity of **CMP–SubP**.

Closure of excisional wounds in mice by contraction, when the wound margins are drawn towards the centre of the wound, is believed to occur via contractile activity of myofibroblasts (Cass *et al.*, 1997). Sensory nerves influence wound myofibroblasts, and delayed wound closure in mature rats have been associated with innervations (Liu *et al.*, 1999). Capsaicin-induced innervations of sensory nerves caused impaired wound contraction and healing (Smith *et al.*, 2002). This effect can be reversed by administration of **SubP** (Khalil *et al.*, 1996), which has been shown to enhance neuronal area and promote cellular proliferation (Buttow *et al.*, 2003). *db/db* mice have been reported to have significantly lower epidermal nerve profile count, area fraction and area density compared to *db/–* mice (Underwood *et al.*, 2001). Our results show that **CMP–SubP** treatment of the wounds exhibited full closure by Day 16 of the experiment (Figure 3.2F). In comparison wounds treated with **CMP** and commercial **SubP** individually were still open on Day 16 (Figure 3.2E and 3.2D). Insulin by itself was unable to repair the wound (Figure 3.2C), whereas saline and 5% w/v PEG/saline treated-wounds showed considerable scab formation and no discernible improvement in healing (Figure 3.2A and 3.2B). These results were supported by histopathological analysis, which indicated that all wounds treated with

CMP–SubP were closed completely (Figure 3.3A), whereas **CMP** and **SubP** showed improved contraction compared to insulin and the vehicular controls. We hypothesized that by annealing to collagen, **CMP** helps to sequester the new collagen secreted by the cells and allow a faster assimilation of their microenvironment. The proliferation and differentiation of mesenchymal stem-cell has been reported to be favored by the presence of CMPs (Lee *et al.*, 2008). Measurement of the new epithelial layer formed in the course of the treatment showed a mirroring trend, with our test peptide exhibiting a mean of ~7 mm of re-epithelialization in wounds that were originally 8 mm in diameter (Figure 3.3B). The extent of re-epithelialization of **CMP** is less than that of **SubP**, indicating that wounds treated with the former peptide closed preferably due to contraction healing rather than enhanced keratinocyte proliferation. Among other factors, wound healing is impaired in diabetic mice by significantly reduced keratinocyte growth factor expression (Werner *et al.*, 1994), whereas epithelial cell growth and DNA synthesis was reported to be stimulated by **SubP** in lens epithelial cells *in vitro* (Reid et al., 1993). Our results *in vivo* (Figure 3.5i) support this research, and show that anchoring of SubP in the wound tissue by using a **CMP** domain to anneal to endogenous collagen, improves its stimulatory activity compared to free **SubP**.

Fibrovascular influx and deposition of new collagen in the wounds was highlighted by staining with picosirius red (Figure 3.5ii) and measured as a percentage of the total area. Our results indicate that collagen deposition was down-regulated in the presence of **SubP** (Figure 3.4). In comparison to the saline control, **CMP**- and insulin-treatment showed comparable collagen formation. This finding is in accord with previous reports of **SubP** causing a decrease in collagen biosynthesis, concomitant to a down-regulation of pro-α1 (I) collagen mRNA and an

increase of collagen biodegradation, when incubated with human lung fibroblast cells (Ramos *et al.*, 2007).

SubP has been shown to stimulate DNA synthesis in human skin fibroblasts (Nilsson *et al.*, 1985), and to be a potent effector of human fibroblast migration *in vitro*, as mediated by the NK-1 receptor that binds to the C-terminus of the peptide (Kähler *et al.*, 1993b; Parenti *et al.*, 1996). The C-terminus is also responsible for the chemotaxis of human monocytes into the wound (Ruff *et al.*, 1985). This pro-inflammatory activity of **SubP** as seen in treatment with free **SubP** (Figure 3.6) is higher than that with **CMP–SubP**. The observed inflammation was largely in the acute stage and composed of polymorphonuclear leucocytes (PMNLs). Previous work indicated that phagocytic activity by the PMNLs and macrophages in this phase is stimulated by the tetrapeptide at the N-terminus of **SubP** (Bar-Shavit *et al.*, 1980). The migratory activity of the PMNLs also depends on the N-terminal sequence, and probably occurs via a non-receptor-mediated mechanism, with the participation of basic groups in the N-terminal region (Wiedermann *et al.*, 1989). In **CMP–SubP**, the N-terminus is blocked by covalent conjugation with the anchoring peptide, and hence its pro-inflammatory activity might be diminished compared to its free analogue. The unblocked C-terminus is, however, still capable of mediating fibroblast and monocyte migration into the wounds.

3.4.2 Wound Closure in presence of insulin

As discussed above, **SubP** is known to act synergistically with insulin or IGF-1 to promote epithelial cell growth and significantly increase wound closure *in vitro* and in corneal wound models. As prerequisites for our current study, we decided to test the need for insulin in our skin wound model. We created unsplinted wounds on the craniodorsal region of diabetic

mice (3 mice/group) and treated them with 15μL of **CMP–SubP** (20μmol/mL in saline). One of these groups was also treated with 5μL of insulin (50 I.U. in saline). The third group was treated with both **CMP–SubP** and insulin, but the delivery vehicle for both the compounds was 5% w/v PEG/saline instead of saline. The wounds were monitored for 12 days, and then photographed and subjected to histopathological analysis.

On inspecting the wounds visually, there was significant reduction in the size of the wounds treated with **CMP–SubP** in the presence of insulin compared to the group that was treated only with the peptide (Figure 3.7). In the absence of insulin, there was also considerable scabbing and the wound had an unhealthy appearance. This finding was consistent with histopathological scoring, which indicated an increased trend towards wound closure, as well as re-epithelialization, in the presence of insulin (Figure 3.8A). Collagen deposition in the absence of insulin was markedly higher, increasing the possibility of scar formation (Figure 3.8B). Depression of inflammatory response over time, as observed earlier, was absent upon omission of insulin. On comparing the above two groups with a similar group (5% w/v PEG/saline as the delivery vehicle), we observed greater wound closure with the change in delivery medium (Figure 3.9A and 3.9B). The wounds treated with the peptide in saline (without insulin) actually appeared to have become worse by gross measurement (Figure 3.9A), as is also apparent in Figure 3.7. The same trend was observed in the histopathological analysis, and the wounds treated with 5% w/v PEG/saline as the vehicle showed smaller epithelial gap between the edges of the wounds. The results indicate that **CMP–SubP** is more accessible to the wound tissue when it is uniformly dissolved in the PEG solution; and this vehicle provides an environment that promotes cell proliferation and migration compared to saline solution.

3.5 Conclusions

Substance P can be administered topically for wound healing studies. Its role as a mediator in wound healing mechanisms is however enhanced, even in the reported range of dosage by anchoring it to the wound bed with collagen mimetic peptides that are believed to form triple helices with native collagen type I. **CMP–SubP** conjugate was shown to be more effective when treated simultaneously with small quantities of insulin on Day 0. The application of insulin was also topical and hence does not elevate the symptoms and effects of diabetes in the mouse model. We observed complete closure of 8-mm o.d. cutaneous wounds with increased levels of epithelialization. Collagen formation was depressed in the presence of Substance P, and that finding could benefit by minimizing the occurrence of scar tissue upon wound healing. Hence, with improved epithelialization and down-regulated collagen deposition, this strategy would be useful for the treatment of smaller and surface wounds, with a bias towards wound regeneration over wound repair. The strategy also circumvents the need for repeated administration as well as conventional intrusive techniques like subcutaneous injections.

Figure 3.1. Representation of a collagen mimetic peptide–Substance P conjugate (**CMP–SubP**) annealing to a damaged collagen triple helix.

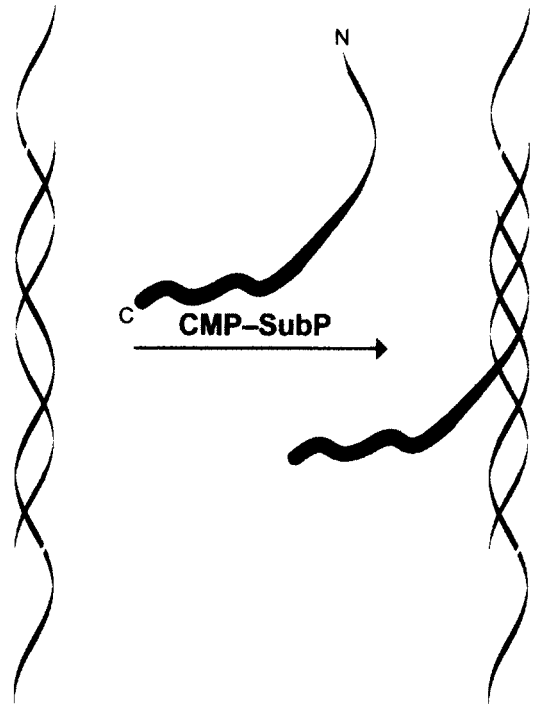

damaged collagen triple helix **immobilized Substance P**

$(ProProGly)_7$–ArgProLysProGlnGlnPhePheGlyLeuMetNH_2
CMP–SubP

Figure 3.2. Photographs depicting the effect of **SubP**-immobilization on splinted mouse wounds. Images are from Day 0 (immediately post-treatment) or Day 16 after removal of the splints but before euthanasia. Wounds were treated with (A) saline; (B) PEG (5% w/v) in saline; (C) insulin (50 I.U.) in saline; (D) **SubP** (25 nmol) in PEG/saline; (E) **CMP** (25 nmol) in PEG/saline; (F) **CMP–SubP** (25 nmol) in PEG/saline. Saline-treated wounds showed extensive scabbing (>85% of the total wound area). Wounds treated with free **SubP** had more scabs than those treated with CMP–SubP.

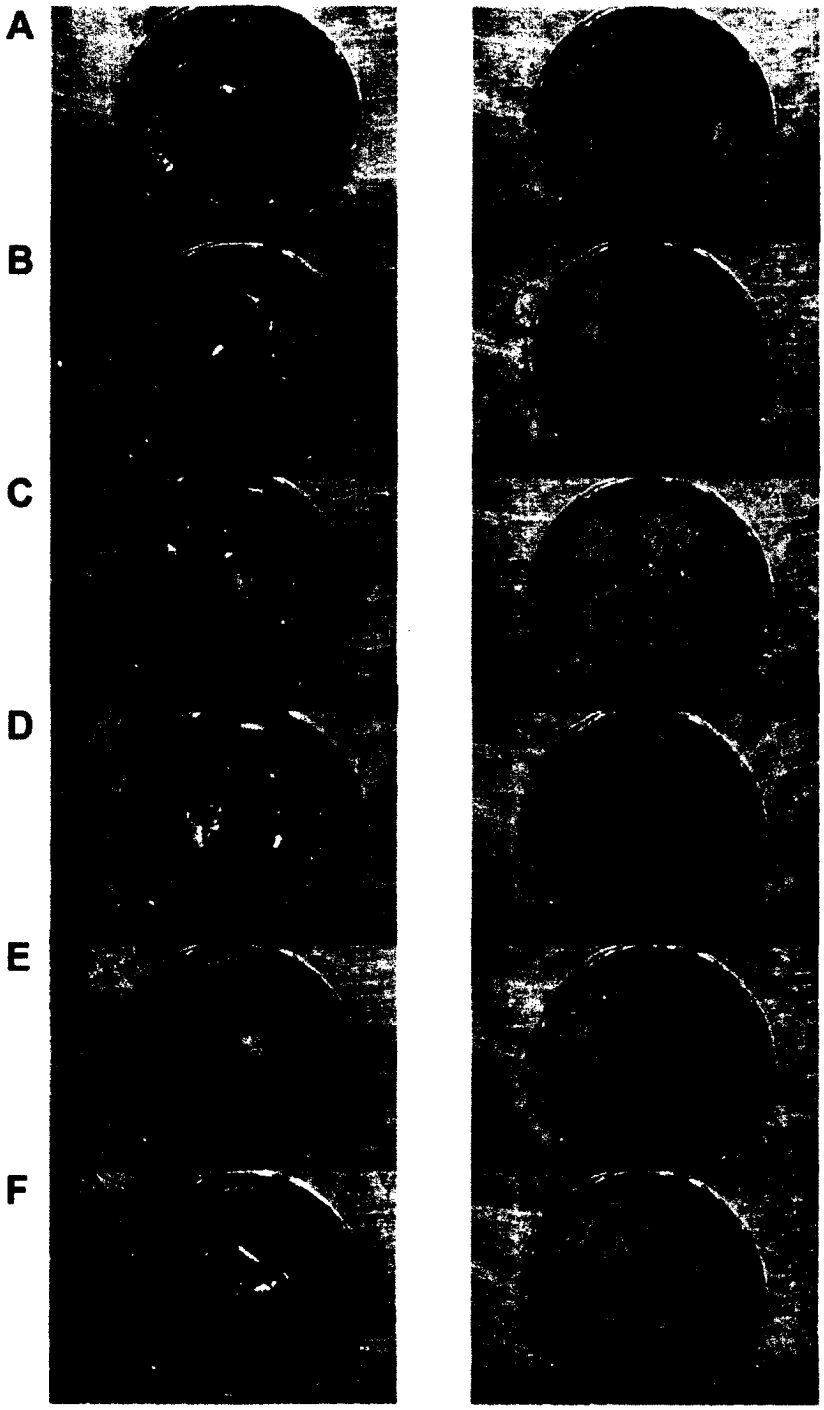

Figure 3.3. Bar graph showing the effect of **SubP**-immobilization on the size and re-epithelialization of splinted mouse wounds. Data are from Day 16 post-treatment. (A) The mean size of the **CMP–SubP** treated wounds was zero (all the wounds were closed), and the result was significantly different from that of all controls ($p< 0.05$). (B) Re-epithelialization in wounds treated with free **CMP** was less than those treated with either **SubP** or **CMP–SubP**, indicating that wound closure was primarily due to contraction in these wounds. **CMP–SubP** treatment showed significantly more extensive epithelial layer formation compared to both saline and PEG/saline controls ($p< 0.05$). Values are the mean ± SE ($n = 16$).

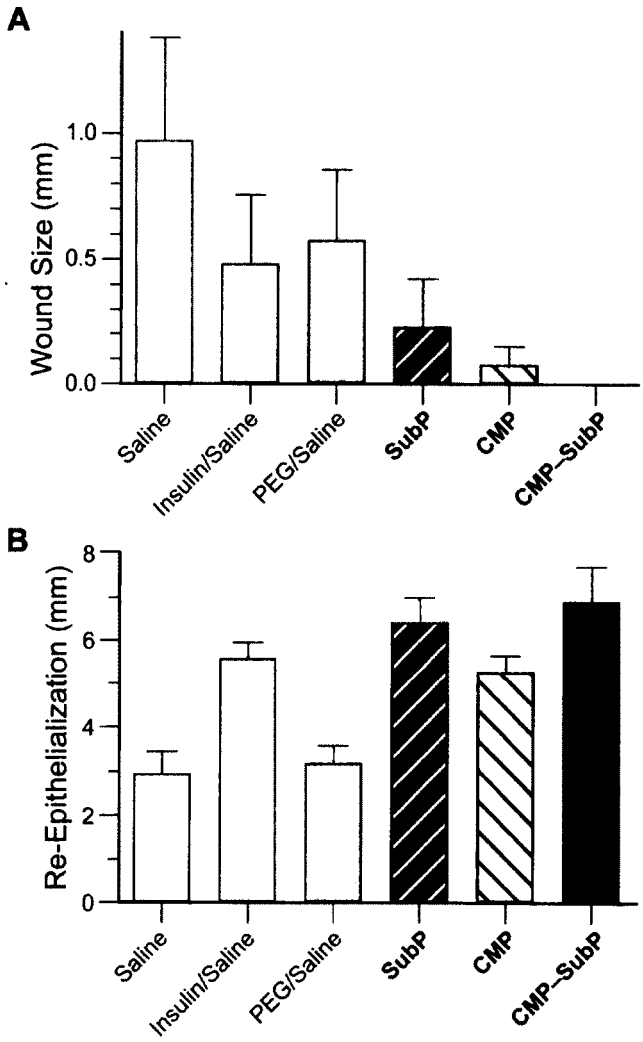

Figure 3.4. Bar graph showing the effect of **SubP**-immobilization on collagen deposition in splinted mouse wounds. Data are from Day 16 post-treatment. Collagen deposition was down-regulated in wounds treated with both free and conjugated **SubP**. Values are the mean ± SE (n = 16) and refer to collagen deposition as a percentage of the total area of the wound.

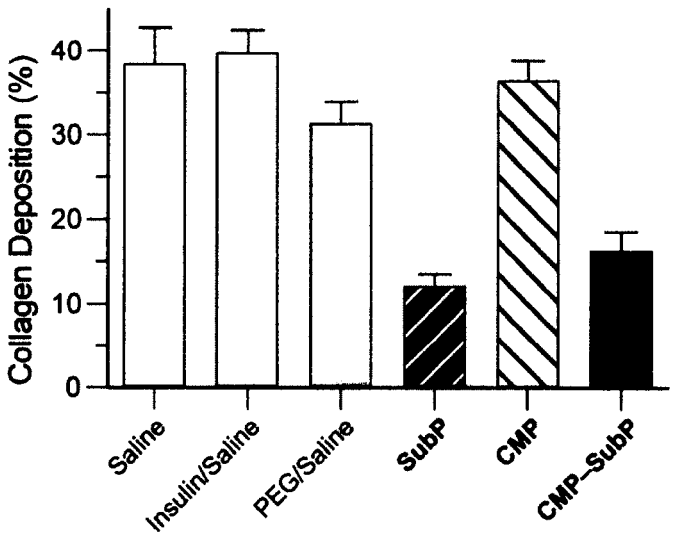

Figure 3.5. Histological images depicting the effect of **SubP**-immobilization on healing pattern of splinted mouse wounds. Data are from Day 16 post-treatment. Left: Wounds stained with hemotoxylin and eosin. Right: Wounds stained with picosirius red and imaged under polarized light. Wounds were treated with (A) saline; (B) PEG (5% w/v) in saline; (C) insulin (50 I.U.) in saline: (D) **SubP** (25 nmol) in PEG/saline; (E) **CMP** (25 nmol) in PEG/saline; (F) **CMP–SubP** (25 nmol) in PEG/saline. Lesions were present in all control wounds (edges indicated by "*" symbols), whereas treatment with **CMP–SubP** led to complete closure, minimal or no scab formation, and uniform granulation tissue formation.

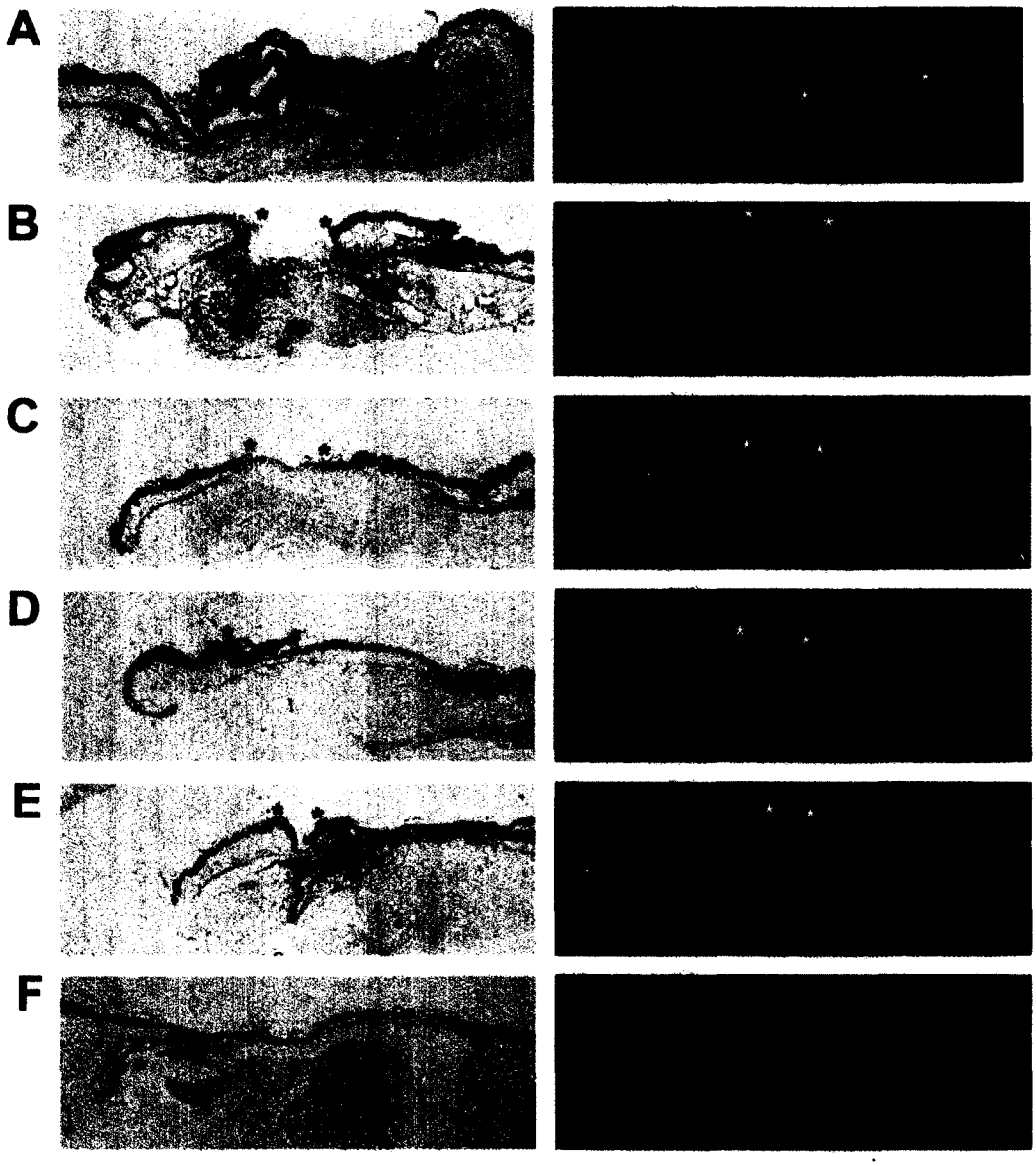

Figure 3.6. Bar graph showing the effect of **SubP**-immobilization on inflammation in splinted mouse wounds. Data are from Day 16 post-treatment. Inflammation was scored on a scale of 0–4, and was lower in wounds treated with CMP–SubP. Values are the median ± SE (n = 16).

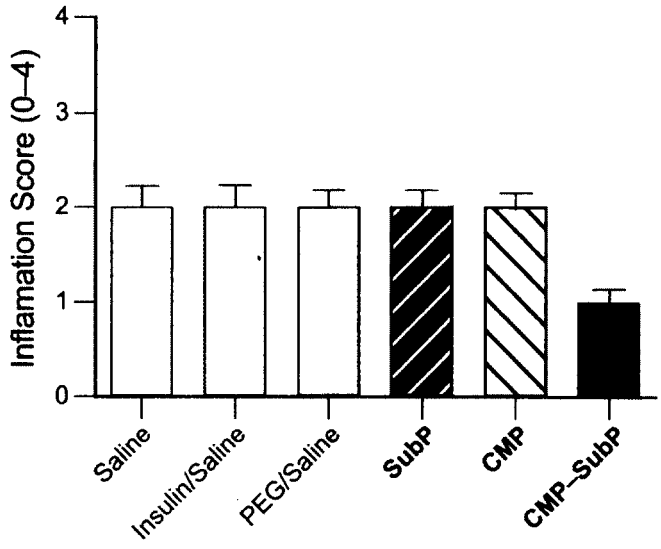

Figure 3.7. Photographs depicting the additive effect of insulin and **SubP**-immobilization on non-splinted mouse wounds. Images are from Day 0 (immediately post-treatment) or Day 12 before euthanasia. Wounds were treated with (A) CMP–**SubP** in saline; (B) CMP–SubP + insulin (50 I.U.) in saline. In the absence of insulin, wounds showed extensive scab formation and appeared to become more damaged over a period of 12 days.

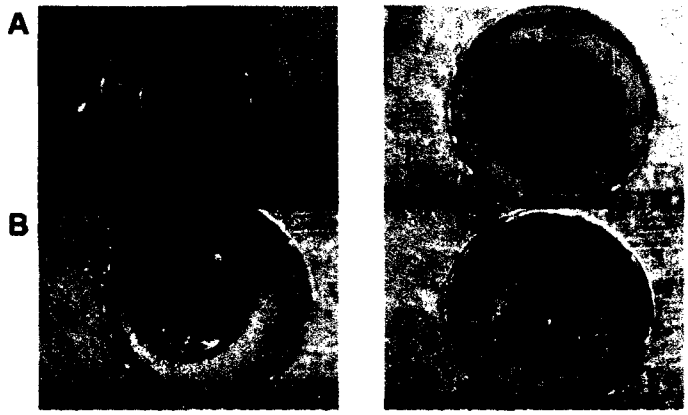

Figure 3.8. Bar graphs showing the additive effect of insulin during **SubP**-immobilization on non-splinted mouse wounds. Data are from Day 12 post-treatment. (A) Wound size and re-epithelialization. (B) Collagen deposition and inflammation (0–4 scale). Additional insulin decreased wound size, collagen deposition, and inflammation, and increased re-epithelialization. Values are the mean ± SE ($n = 6$).

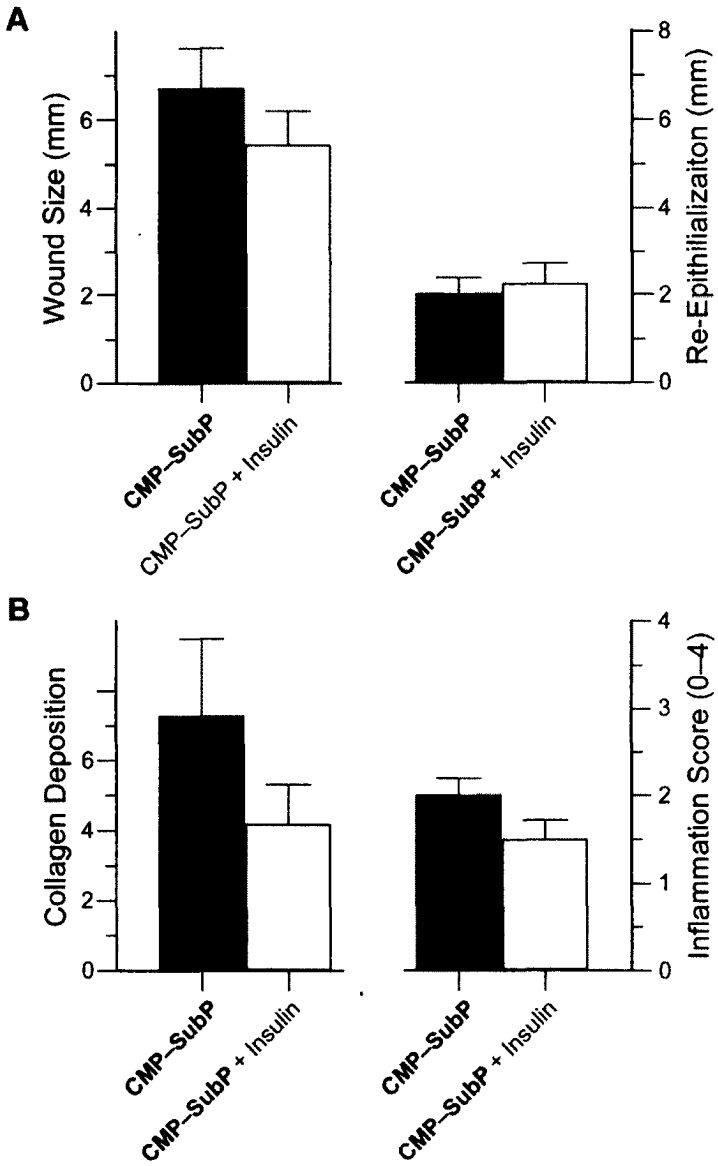

Figure 3.9. Bar graphs showing the effect of **SubP**-immobilization in saline (with and without insulin) and in 5% w/v PEG/saline (with insulin) medium on non-splinted mouse wounds. Data are from Day 12 post-treatment. (A) Wound closure, which refers to the reduction of the area between wound edges after 12 days. (B) Wound size, which refers to histopathological measurement of the largest diameter after 12 days. Values are the mean ± SE ($n = 6$).

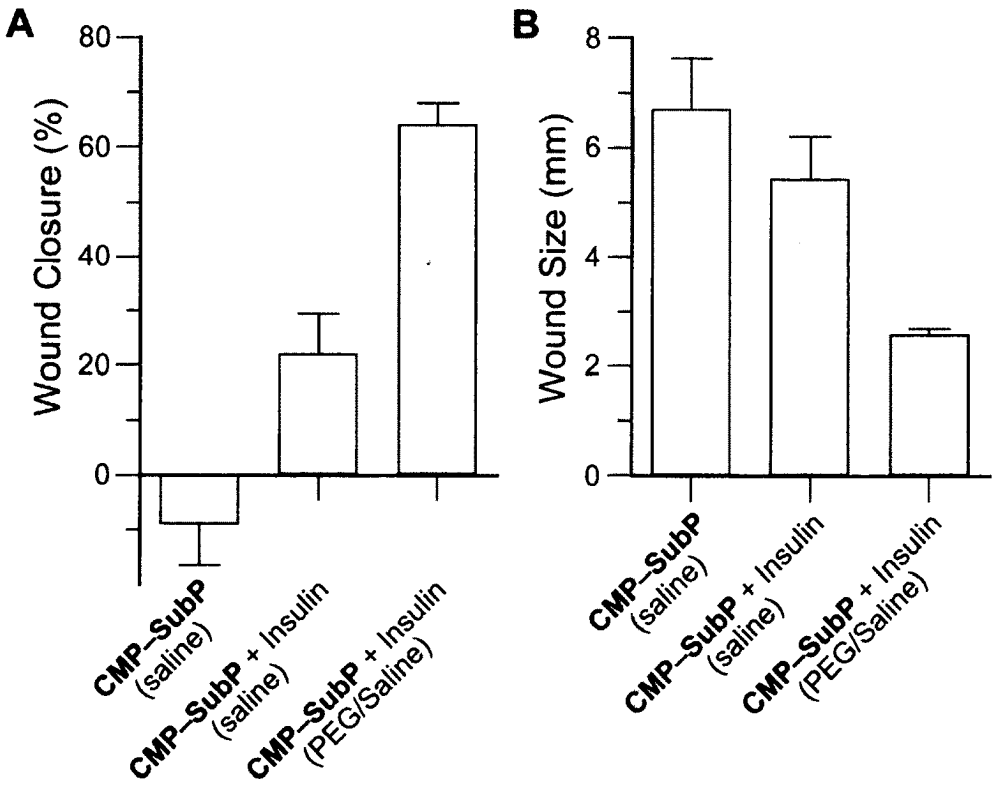

3.6 Acknowledgements

We are grateful to Patricia Kierski, Diego Calderon, Dana Tackes, Kevin Johnson, and Zachary Joseph for help with the wound surgery and animal care. We are also grateful to Prof. Nicholas Abbott and Dr. Michael Schurr for contributive discussions. This work was supported by grants R01 AR044276 and RC2 AR058971 (NIH). MALDI–TOF mass spectrometry was performed at the University of Wisconsin–Madison Biophysics Instrumentation Facility, which was established with Grants BIR-9512577 (NSF) and S10 RR13790 (NIH).

CHAPTER 4*

Immobilizing a TGF-β receptor ligand in the collagen matrix of cutaneous wounds modulates wound healing

* This chapter is in preparation for publication as:

Sayani Chattopadhyay, Kathleen M. Guthrie, Leandro Teixeira, Lingyin Li, Laura, L. Kiessling, Richard R. Dubielzig, Jonathan F. McAnulty, and Ronald T. Raines; (2012) Immobilizing a TGF–β receptor ligand in the collagen matrix of cutaneous wounds modulates wound healing

4.1 Abstract

Transforming growth factor-β (TGF-β) comprises a set of structurally related low molecular weight polypeptides, defined by their ability to regulate a large number of cellular processes including proliferation, differentiation, motility, adhesion, and apoptosis. TGF-β has been the focus of considerable research due to its important roles in almost every phase of wound healing—it stimulates chemotaxis, angiogenesis, and deposition of collagen in the extracellular matrix. TGF-β activity is initiated by the formation of a heterotetrameric complex of the growth factor with the extracellular domains of its receptors, initiating a signaling cascade. We sought to take advantage of a synthetic peptide ligand for TGF-β receptors (Tβrl) that is capable of amplifying the signaling activity by preorganizing the extracellular domains of the receptors, thereby poising them for activation by endogenous TGF-β. Such preorganization promotes avid binding of TGF-β to the receptor complex. Here, we report on an improved mode for immobilizing the synthetic peptide ligands in a wound bed and display them multivalently. This mode is based on the ability of a collagen mimetic peptide (CMP) to bind to damaged collagen triple helices in the wound bed. Using an excisional wound model in diabetic mice, we show that a one-time topical application of TGF-β receptor ligand–CMP conjugate increases local collagen deposition in the extracellular matrix along with an enhanced influx of inflammatory cells compared to the unconjugated peptide ligand and vehicular controls. We also demonstrate improved wound closure and re-epithelialization using a splinted-wound model in mice. These data affirm the utility of collagen mimetic peptides in the delivery and immobilization of growth factors in wound beds, thereby effecting a controlled modulation of the wound-healing process.

4.2 Introduction

Transforming growth factor-beta (TGF-β) and related factors play an important role in the development, homeostasis, and repair of virtually all tissues in living organisms (Massagué, 1998). It is a homodimer of relative molecular mass 25kDa (Assoian *et al.*, 1983). The monomeric form of the natural TGF-β homodimer is biosynthesized by proteolysis of a larger 391-residue precursor polypeptide (Derynck *et al.*, 1985). TGF-β is primarily produced by the degranulating platelets, monocytes, and fibroblasts. Once the mature TGF-β is released extracellularly, it participates in the stimulation of cellular activities, angiogenesis, and extra-cellular matrix (ECM) deposition via a unique receptor signaling that is initiated when the growth factor binds and mediates the assembly and activation of a cell-surface receptor complex (Hart *et al.*, 2002; Wrana *et al.*, 1992). The relatively large amounts of TGF-β found in platelets, along with platelet-derived growth factor (PDGF), led to the suggestion that TGF-β may play a role in wound healing (Sporn *et al.*, 1983). Intraperitoneal injections of TGF-β in rats led to increased fibroblast proliferation, collagen deposition and a sterile infiltrate of inflammatory cells (Sporn *et al.*, 1983).

The TGF-β receptor is made up of two separate transmembrane glycoproteins, TβRI and TβRII, which are characterized by a cysteine-rich extracellular domain, a single hydrophobic trans-membrane domain, and a C-terminal cytoplasmic serine/ threonine kinase domain (Schiller *et al.*, 2004). Native TGF-β binds with high affinity (K_d~5–30 pM) to the TβRII dimer to form a signaling complex (Massagué, 1998). Upon binding to TGF-β, TβRII recruits the TβRI into an activated heterotetrameric receptor complex (Figure 1A). The regulatory GS region of TβRI is phosphorylated by the cytosolic domain of TβRII, which in turn activates the adjacent serine/ threonine kinase domain. This causes the phosphorylation of the downstream effectors, the Smad

proteins—Smad2 or Smad3, in the presence of another protein SARA (Smad Anchor for Receptor Activation). The activated Smad2/3 associates with Smad4 and translocates into the nucleus to regulate gene expression. The activation of this signaling cascade thereafter is responsible for the stimulation of further cellular activity, and any method to regulate this signaling step will provide a handle to modulate TGF-β -mediated cell responses in the wound tissue.

Ground breaking work by Kiessling and co-workers (Li *et al.*, 2010) identified peptide ligands that are capable of binding to the extracellular domain of both TβRI (TβRI-ED) and TβRII (TβRII-ED) with high affinity (K_d~ 10^{-5} M), but do not interfere with TGF-β binding. The two receptors have small extracellular domains and large surface areas buried in the heterotetrameric complex with TGF-β (Groppe *et al.*, 2008). Nonetheless, the receptors possess a novel binding site for the identified peptide ligands that is distinct from the TGF-β binding site, and therefore does not impede the activity of the growth factor. In addition, a multivalent display of these peptide ligands on a PEG-based dendrimer enhanced their functional affinities (Li *et al.*, 2010). Further work showed that preorganization of the TGF-β receptors by these peptide ligands bound to a synthetic surface, augmented avid TGF-β binding, since they were poised for activation by even small amounts of TGF-β, thus lowering the local threshold concentration for signal. Such peptide ligand-functionalized surfaces can amplify cell-signaling by endogenous TGF-β without the need to add exogenous TGF-β (K_d<< 5 pM) (Li *et al.*, 2011).

We sought to see if a similar approach can be used in an *in vivo* model to amplify TGF-β signaling, and thereby modulate the various processes of wound healing that are affected directly or indirectly by the TGF-β signaling pathway. Amongst the variety of synthetic and natural scaffolds that have been explored for delivery of biologically active moieties in the body, type I

and type II collagen can be isolated easily from animal tissues and shows high biocompatibility. TGF-β administered into full-thickness wounds in rabbits by encapsulation in a collagen-sponge scaffold led to greater inflammatory response, and to faster re-epithelialization and contraction rates (Pandit *et al.*, 1999). Similarly, the injection and topical application of TGF-β into wounds has also been studied extensively (Ammann *et al.*, 1990; Beck *et al.*, 1993; Ksander *et al.*, 1990; Ksander *et al.*, 1993; Mustoe *et al.*, 1987) for the ability to enhance healing by increasing tensile strength, promoting fibroblast proliferation and collagen matrix deposition. Still, all of these approaches required the administration of exogenous TGF-β. Our strategy involves using the damaged collagen-bed as a surface for immobilizing the peptide receptor ligand identified by Kiessling and co-workers and thereby preorganizing the TGF-β receptors (Figure 1B). We believe that our method will enhance the sensitivity of the cells displaying these receptors on their surface to the circulating endogenous TGF-β already present in the wounds (TGF-β is at a concentration of ~1 pM in human serum (Slevin *et al.*, 2000)).

This mode exploits the propensity of a collagen mimetic peptide (**CMP**) to anneal to endogenous collagen under physiological conditions and thereby act as an effective delivery system. We have successfully shown that peptides containing $(ProProGly)_7$ moieties in their sequence are capable of binding to native type I collagen *in vitro* and *ex vivo* at room temperature and physiologically relevant pH, and can anchor molecules conjugated to them in the wound tissue (Chattopadhyay *et al.*, 2012). Here, we report on the conjugation of the TGF-β receptor ligand (**Tβrl**) to CMP with the sequence $(ProProGly)_7$, and we tested the effect of this conjugate on cellular proliferation, migration, and collagen deposition mediated by TGF-β in different stages of wound healing.

4.3 Results and discussion

Work by Kiessling and co-workers identified two peptides, of which we chose to use **Tβrl** (LTGKNFPMFHRN) as our effector peptide to sensitize the cells surface receptors to TGF-β signaling. This peptide binds specifically to both TβRI-ED and TβRII-ED with moderately high affinity (K_d~ 10^{-5} M) (Li *et al.*, 2010). The binding site is distinct from that employed for binding with TGF-β, and this indicates that both receptors TβRI-ED and TβRII-ED share a novel binding spot that serves as target for modulation of TGF-β signaling. The functional affinity of the peptide ligands is increased by ~100-fold when they are displayed multivalently, and our strategy to immobilize **Tβrl** on the surface of native collagen of wounds *in vivo* holds promise for sensitizing the cell surface receptors to endogenous TGF-β released in the initial stages of wound healing.

Mouse models of wound healing play a key role in helping us understand the underlying mechanisms involved in wound healing, and have a critical part in the study and establishment of new therapeutic strategies. It has been established in earlier works by Michaels *et al.* that of the ten different diabetic murine models, *db/db* mice exhibit severe impairments of wound healing, and excisional wounds in these mice show a statistically significant delay in wound closure, decreased granulation tissue formation, decreased vascularization in the wound bed, and diminished cellular proliferation (Michaels *et al.*, 2007). Male mice (homozygous for $Lepr^{db}$ strain) become obese at three to four weeks of age and blood sugar typically elevates at four to eight weeks of age. We chose these genetically diabetic mice for our study because they exhibit characteristics similar to adult human onset type II diabetes mellitus (Coleman, 1978; Kämpfer *et al.*, 2000) and as a result showed impaired wound healing response due to the *db/db* genotype (Brem *et al.*, 2007)—an ideal model to study wound healing since ~90% of adult human patients

have type II diabetes. These mice also show delayed and reduced expression of keratinocyte growth factor (Werner *et al.*, 1994) and peripheral neuropathy similar to diabetic adult humans (Norido *et al.*, 1984). The course of wound healing in these mice closely follows the clinical observations of human diabetic patients (Greenhalgh, 2003). Previous work has shown that subcutaneous implantation of polyvinyl alcohol sponges injected with TGF-β in diabetic rats leads to an increased collagen deposition, indicating the efficacy of the growth factor in accelerating healing under conditions of defective wound repair (Broadley *et al.*, 1989).

The collagen mimetic peptide **CMP,** the peptide receptor ligand **Tβrl**, and the receptor ligand conjugated to **CMP** (**Tβrl–CMP**) were synthesized by solid-phase peptide synthesis (SPPS). We have previously reported that $(ProProGly)_7$ moieties successfully anneal to collagen type I *in vitro* and *ex vivo* (Chattopadhyay *et al.*, 2012). These peptides can be used to deliver and anchor small fluorophore molecules in *ex vivo* wound tissue at room temperature and are not toxic to the dermal fibroblast cell line. Earlier efforts to use collagen mimetic peptides as delivery vehicles for wound healing factors involved the use of $(ProHypGly)_n$ analogues and a charged template (Wang *et al.*, 2008b). These peptides preferred to maintain a triple helical form at room temperature and required pre-heating at 80 °C prior to application. Our strategy circumvents these issues and adapts the treatment to more clinically relevant conditions. In the original phage display study, the peptide LTGKNFPMFHRN was presented as a fusion to the N-terminus of the PIII coat protein (Li *et al.*, 2010). In the design of **Tβrl–CMP** we mimicked this display and chose to covalently conjugate the peptide receptor ligand to the N-terminus of **CMP**.

We chose to use an excisional wound model for our experiments. This wound model heals from the wound margins and provides the broadest assessment of the various parameters for wound healing like re-epithelialization, fibrovascular proliferation, contracture, and

angiogenesis (Greenhalgh *et al.*, 2001). This model in diabetic mice also provides for larger dorsal surfaces that are useful for the easy application of topical agents directly into the wound bed, as well as the availability of two wounds side-by-side on the same mouse.

4.3.1 Tβrl–CMP in wound healing

Two splinted wounds (8 mm o.d.) were created in the craniodorsal region of each *db/db* mouse (n = 5 mice/10 wounds) under anesthesia and topically treated with 25 μL of **Tβrl–CMP** (20 mM) solution in 5% w/v PEG/saline vehicle. Insulin (5 μL, 50 I.U. in saline) was added to each of the wounds and incubated for 30 min under anesthesia. The mice were then allowed to recover and monitored over a period of 12 days. As a control, we treated a second group of mice in a similar manner with insulin (5 μL, 50 I.U. + 25 μL of saline). Clinical evidence indicate that insulin increases vascularization, stimulates proliferation, enhances phagocytosis, and promotes contraction in the wound (Belfield *et al.*, 1970) and is therefore effective in wound healing. Insulin treatment also promoted re-epithelialization and collagen deposition in burn-wound models (Madibally *et al.*, 2003). When injected in diabetic mice wounds, insulin solutions caused a reduction in the mean hyperglycaemia levels (Weringer *et al.*, 1982), but it has been suggested that the increased rate of wound healing may also be attributed to the zinc which is used to crystallize insulin (Greenway *et al.*, 1999). Polyethylene glycol 8000 (PEG, 5% w/v in saline) (Brown *et al.*, 1994; Greenhalgh *et al.*, 1990) was used to dissolve **Tβrl–CMP** and was also tested as a control, along with saline (0.9% w/v sodium chloride). **CMP** (25 μL, 20 mM) and **Tβrl** (25 μL, 20 mM) in 5% w/v PEG/saline were applied as controls to compare against the sustained biological activity of **Tβrl–CMP**.

Fibrovascular influx and deposition of new collagen in the wounds were visualized with picosirius red and reported as a percentage of the total area. The picosirius red stain illuminated areas of new collagen deposited, as well as previously present dermal collagen. Due to more extensive cross-linking and maturation, the older collagen appears dense and brighter, compared to the fibrillar and lighter form of newly formed collagen. Upon release from the degranulating platelets, TGF-β1 chemotactically attracts fibroblasts into the wound site (Abe *et al.*, 2001; Ashcroft *et al.*, 1999; Postlethwaite *et al.*, 1987) and stimulates their proliferation (Lal *et al.*, 2003). As part of a positive feedback mechanism, fibroblasts then release more TGF-β in response to the TGF-β signaling, as well as promote collagen synthesis. On treatment of diabetic excisional wounds with our conjugated TGF-β peptide receptor ligand, we observed a significant increase in the amount of collagen deposited in the wound bed, compared to that in control wounds treated with the delivery vehicle 5% w/v PEG/saline, the anchoring peptide **CMP** and insulin (Figure 2). This corroborates with work done previously where topical application of TGF-β in animal models enhanced the fibroblast production of collagen and fibronectin significantly (Lynch *et al.*, 1989; Roberts *et al.*, 1988) and stimulated granulation tissue formation in several wound healing models (Roberts *et al.*, 1986; Roberts, 1995). Collagen production was affected negatively when TGF-β was blocked with antibodies (Roberts *et al.*, 2001). As expected, the soluble form of **Tβrl**, when introduced into the wound, did not show any significant enhancement in collagen formation or maturation over the control wounds. The normal wound healing process is associated with a transient accumulation of fibroblasts that express elevated levels of TβRI and TβRII, but the highest cellular density was observed in the deepest regions of the granulation tissue (Schmid *et al.*, 1998). **Tβrl** tethered to the wound bed via collagen mimetic peptides are poised to preorganize these receptors, and to enhance the

cellular sensitivity to TGF-β signaling. This resulted in formation of new collagen, without the need for exogenous application of soluble TGF-β. Earlier work has shown that tethering TGF-β1 to a PEG-based polymer scaffold actually causes a significant increase in matrix production and collagen deposition (Mann *et al.*, 2001). Such a treatment also counteracts the attenuation of ECM production which is otherwise observed in presence of biomaterials containing cell-adhesive ligands (Mann *et al.*, 1999). Our test peptide **Tβrl–CMP** can thus be surmised to behave in a similar manner and promote cellular adhesion, while strengthening the wound bed itself by improved collagen synthesis and consequent ECM production. The soluble form of the peptide receptor ligand, however, cannot participate in such preorganization and hence the response to its treatment is the same as that of control treatments.

A similar response was also observed when analyzing the wounds for inflammatory response. Upon cutaneous injury, endogenous TGF-β is rapidly elevated in a narrow window of time after the injury (Kane *et al.*, 1991; Wang *et al.*, 2006) and reaches a peak level three days post 6-mm full-thickness wounding in transgenic mice. This coincides with the peak of the inflammation during early stages of wound healing (Wang *et al.*, 2006). Subcutaneous injection of TGF-β results in a histological pattern of inflammatory cell recruitment (neutrophils, macrophages), fibroblast proliferation, and vascular growth, similar to the process of normal inflammation and repair in cutaneous wounds (Roberts *et al.*, 1986). In the early stages, the growth factor provides an extremely chemotactic ligand for human peripheral blood monocytes, (Wahl *et al.*, 1987) which is a key phenomenon in the initiation of an inflammatory response. Through a positive feedback mechanism, the recruited monocytes and macrophages produce more TGF-β perpetuating their activity, and also produce mitogenic and chemotactic substances that act on other cells. Our analysis of the wounds in diabetic mice after 12 days showed a

significantly enhanced inflammatory influx in the wounds treated with **TβrI–CMP** over the vehicular control, the collagen mimetic peptide, and the soluble ligand (Figure 3). It is also competitive with insulin treatment, which is shown to be effective in healing cutaneous injuries (Madibally *et al.*, 2003). The macrophages, once activated, downregulate their receptors for TGF-β and hence their sensitivity for stimulation (Wahl *et al.*, 1987). The peripheral blood monocytes also become susceptible to deactivation by TGF-β (Tsunawaki *et al.*, 1988). This self-regulates the inflammatory stage by inhibiting the proteolytic environment created by the inflammatory cells and easing the healing process into the proliferative phase (Edwards *et al.*, 1987). We observe concurrent behavior in our treatments with the conjugated peptide receptor ligand, where the inflammatory activity after day 16 is lowered and becomes comparable to control wounds.

Re-epithelialization of the wound bed is the process by which keratinocytes proliferate and migrate from wound edges to create a barrier over the wound. The role of TGF-β in this process is not completely understood. Studies *in vitro* showed that TGF-β inhibits keratinocyte proliferation and simultaneously enhances their migration (Badiavas *et al.*, 2001; Jeong *et al.*, 2004). *In vivo* studies have also given inconclusive results: transgenic mice that over-express the growth factor showed enhanced epithelialization in partial-thickness wounds, (Tredget *et al.*, 2005) whereas using anti-TGFβ antibodies in rabbits resulted in impaired epithelialization. On the other hand, mice null for Smad3 showed accelerated keratinocyte proliferation and epithelialization compared to wild-type mice (Ashcroft *et al.*, 1999; Ashcroft *et al.*, 2000). In our experiment, we noticed a trend towards increased epithelialization of the wound bed when the cells are sensitized to endogenous TGF-β by preorganizing the TβRI and TβRII on the cell surface by using receptor ligands tethered to the collagen matrix, compared to the control

treatments (Figure 4). This strategy takes advantage of the fact that additional TGF-β is not introduced into the wound — the cells simply respond more quickly to the endogenously produced growth factor, which modulated the proliferative and migratory properties of the keratinocytes, in a manner similar to TGF-β -treatment as reported previously.

We did not notice any significant difference in the rate of wound closure in the test wounds. This was partly due to scab formation on the wounds, removal of which disturbed the newly formed epidermis and made wound size measurements inconclusive (Figure 5). We have earlier demonstrated that use of a splinted-model for wound healing aids in more effective analysis of wound closure in murine models and more close resembles wound closure in humans. Mouse models, though inexpensive and easy to handle, diverge from human-skin models as the major mechanism of wound closure is contraction; in humans, re-epithelialization and granulation tissue formation are the major phases of wound healing (Davidson, 1998; Greenhalgh *et al.*, 2001). Galiano *et al.* demonstrated that the use of splints around excise wounds in *db/db* mice allows healing to occur by granulocyte formation and re-epithilialization, while minimizing the effects of contraction compared to un-splinted wound models (Galiano *et al.*, 2004).

Accordingly, we applied and sutured O-rings around the wound margins to act as splints and downregulate contracture in the diabetic mouse-model. We also increased the sample size to eight mice per group, with two wounds each, to provide for better analysis, and used saline (0.9% sodium chloride) as an additional control to compare activity of the ligand in the two vehicles: saline and 5% w/v PEG/saline. The test wounds were treated with 25 μL of **Tβrl–CMP** (20 mM in 5% w/v PEG/saline), while the controls **CMP** and soluble **Tβrl** were also applied at the same concentration (in 5% w/v PEG/saline). The mice were housed in separate cages and

monitored over the next 16 days. On histopathological analysis post euthanasia on Day 16, the wounds treated with **Tβrl–CMP** were all closed completely, except for one wound (Figure 6). The mean value for the wound size was significantly lower than the wounds treated with either saline or 5% w/v PEG/saline (Figure 7A). Surprisingly, soluble **Tβrl**-treatment also showed slightly enhanced wound closure, though it was not significantly different from any of the controls, and was comparable to the treatment with **CMP**.

On comparing the extent of re-epithelialization, we noticed a clear tendency of improved keratinocyte proliferation in the wound beds treated with **Tβrl–CMP**, over the control wounds treated with the vehicles or the collagen mimetic peptide **CMP** (Figure 7B). It has been reported that TGF-β promotes epithelial cell attachment and migration *in vivo* (Hebda, 1988; Hebda, 1989) and stimulates the expression of keratinocyte integrins during re-epithelialization (Gailit *et al.*, 1994). Keratinocyte-migration takes place across a substrate, typically the dermis. The deposition of a substantial granulation tissue layer in the longer time period of the splinted-wound experiments (16 days) provided the requisite surface for the migration of keratinocytes and increased the length of new epithelial layer formed (Figure 7B).

4.3.2 Dose response

We decided to test the potency of the TGF-β receptor ligand on ECM formation by treating the wounds with a range of doses of the conjugated **Tβrl–CMP**. Identical 6 mm o.d. wounds were created on the backs of *db/db* (5 mice/10 wounds per group), and were then incubated with 25 μL solutions of **Tβrl–CMP** using 5-fold serial dilutions of concentrations between 50 mM and 80 μM for 30 min. The mice were then recovered and the wounds analyzed after a period of 12 days. The amount of new collagen formed in the wound bed was identified

with picosirius red stain and expressed as a percentage of marked area in the wound bed (to a depth of 0.75 mm from the healed surface). The extent to which collagen was deposited appeared to be comparable in the wounds treated with 0.08, 0.4, 2.0, and 10.0 mM solutions, but increased visibly in the wounds treated with 50 mM solution (Figure 8A). Although the numbers were not statistically different from each other, the difference was noticeable on the histopathological slides (Figure 4.9). On comparing the extent of re-epithelialization in the wounds treated with different doses of **Tβrl–CMP**, we did not see a marked difference in the treatments, although a trend for higher response resulted on treatment with the higher doses (Figure 4.8B). Inflammatory response indicated the increased presence of mononuclear cells in wounds treated with higher doses, compared to lower doses of 0.04 and 0.8 mM, where there still were discernible amounts of neutrophils and polymorphonuclear cells.

4.4 Materials and methods

Commercial chemicals were of reagent grade or better, and were used without further purification. Anhydrous solvents were obtained from CYCLE-TAINER® solvent delivery systems (J. T. Baker, Phillipsburg, NJ). HPLC-grade solvents were obtained in sealed bottles (Fisher Chemical, Fairlawn, NJ). In all reactions involving anhydrous solvents, glassware was either oven- or flame-dried. Commercially available insulin (Novolin® R; rDNA origin, Novo Nordisk, Princeton, NJ) was used as a control. Polyethylene Glycol 8000 (PEG) (Fisher Bioreagents®, Fairlawn, NJ) and Bacteriostatic 0.9% Sodium Chloride (Hospira, Lake Forest, IL) were used to prepare 5% w/v PEG/saline solution as a delivery medium for the treatments. Male mice (BKS.Cg-*Dock7*^{m}+/+ *Lepr*^{db}/J, Jackson Laboratories, Bar Harbor, ME) were used as the animal model. The mice were anesthetized with Isoflurane (Abbott Laboratories, Abbott Park, IL), injected with Buprenex (buprenorphine hydrochloride, Reckitt Benckiser, Berkshire, UK)

for pain management and the wounds were cleaned with 4% chlorhexidine gluconate (Purdue Products, L. P., Stanford, CT) and saline. The O-ring splints (15 mm o.d. x 11 mm i.d., 2mm thickness, McMaster Carr® silicone O-rings, Chicago, IL) came in ready-to-use packages.

Semi-preparative HPLC was performed with a Varian Dynamax C-18 reversed phase column. Analytical HPLC was performed using a Vydac C-18 reversed phase column. Mass spectrometry was performed with an Applied Biosystems Voyager DE-Pro (matrix-assisted laser desorption/ionization) mass spectrometer from Life Technologies in the Biophysics Instrumentation Facility at University of Wisconsin–Madison.

4.4.1 Peptide synthesis and purification

Peptides were synthesized by solid-phase peptide synthesis using a 12 channel Symphony® peptide synthesizer from Protein Technologies, (Tucson, AZ) at the University of Wisconsin–Madison Biotechnology Center. The first proline residue in **Tβrl–CMP** was coupled to the resin after a swell cycle, and the next 7 residues were subjected to normal couplings (30 min). The subsequent 12 amino acids were subjected to extended couplings (60 min). Fmoc-deprotection was achieved by treatment with piperidine (20% v/v) in DMF. **CMP** was synthesized by SPPS on Fmoc-Gly-Wang Resin (0.4–0.7 mmol/g, 100–200 mesh, Novabiochem®, EMD Chemicals, Gibbstown, NJ) by the sequential coupling of FmocProOH and FmocProProGlyOH. The **Tβrl–CMP** strand was initiated by coupling the subterminal Proline residue to Fmoc-Gly-Wang Resin and subsequent segment condensation using excess (5 equiv/coupling) FmocProOH, FmocProProGlyOH trimers (synthesized as reported previously (Jenkins *et al.*, 2005)), FmocAsn(Trt)OH, FmocArg(Pbf)OH, FmocHis(Trt)OH, FmocPheOH, FmocMetOH, FmocLys(Boc)OH, FmocGlyOH, FmocThr(*t*Bu)OH, and FmocLeuOH. The soluble receptor ligand **Tβrl** was either bought from Biomatik (Wilmigton, DE) or synthesized at

the Peptide Synthesis Facility on Fmoc-Asn(Trt)-Wang Resin (0.54 mmol/g, 100-200 mesh, Novabiochem®, EMD Chemicals, Gibbstown, NJ).The residues were converted to active esters by treatment with 1-hydroxybenzotriazole (HOBt, 3 equiv), *O*-benzotriazole-*N*,*N*,*N*',*N*'-tetramethyl-uronium-hexafluoro-phosphate (HBTU, 3 equiv) and *N*-methylmorpholine (NMM, 6 equiv). **CMP** was cleaved from the Fmoc-Gly-Wang Resin by using 95:2.5:2.5 trifluoroacetic acid/triisopropylsilane/water (total volume: 2 mL) and **Tβrl–CMP** was cleaved from the Fmoc-Gly-Wang Resin using 92.5:5:2.5 trifluoroacetic acid /thioanisole/ethanedithiol (total volume: 2 mL). Both of the peptides were precipitated from *t*-butylmethylether at 0 °C, isolated by centrifugation and purified by semi-preparative HPLC using the following linear gradients: **CMP**, 5% B to 85% B over 45 min) and **Tβrl–CMP**, 10% B to 90% B over 50 min where solvent A was H_2O containing TFA (0.1% v/v) and solvent B was CH_3CN containing TFA (0.1% v/v). **CMP** was readily soluble in dH_2O but **Tβrl–CMP** required addition of CH_3CN (20% v/v) to form a clear solution for HPLC analysis. All of the peptides were judged to be >90% pure by HPLC and MALDI–TOF mass spectrometry: (*m*/*z*) $[M + H]^+$ calculated for **CMP** 1777, found 1777; (*m*/*z*) $[M + H]^+$ calculated for **Tβrl–CMP** 3221, found 3221.

4.4.2 *In vivo* mice model

Male mice (homozygous for $Lepr^{db}$, Jackson Laboratories, Bar Harbor, ME) between the ages of 8–12 weeks were used. The mice were housed in groups until the day of surgery and then housed individually post-surgery in separate cages. The experimental protocol followed was according to the guidelines issued by the Institutional Animal Care and Use Committee (IACUC) at the University of Wisconsin–Madison. The mice were provided food and water *ad libitum*, as well as enrichment, and housed in a temperature-controlled environment with 12 h light and dark cycles.

On the day of the surgery, the mice were anaesthetized with isoflurane using an induction chamber. Buprenorphine, diluted in 0.9% saline to a concentration of 0.01 mg/mL, was injected subcutaneously (0.4 mL/mouse) for pain management. Eyes were lubricated and hind nails clipped. The craniodorsal region was shaved using electric clippers and the shaved area was scrubbed with alternating cotton swabs of chlorhexidine and sterile saline in circular strokes. Residual hair was removed. For the non-splinted wound model, identical 8-mm wounds were created on each side of the body with a biopsy punch, and the wounding was completed using forceps and scissors to prevent the punch from lacerating the subcutaneous tissue. The wounds were then treated with the test compound and the controls, and then allowed to incubate for 30 min while the mouse was still under anesthesia. The wounds were photographed and the mice were then recovered in their cages. For the dose-response experiments, un-splinted wounds were created with a 6 mm biopsy punch and then treated with 25 μL of **Tβrl–CMP** in 5-fold increase of concentration, followed by incubation for 30 min under anesthesia.

For the splinted-wound model, splints were bilaterally placed in a symmetric arrangement, as per Galiano *et al.* using adhesive and then secured to the skin using 8 interrupted sutures using 5-0 nylon suture, encircling the splints with the knots. Wounds were created in the centre of the splints using the 8-mm biopsy punch, and the skin was removed using forceps and scissors. The wounds were then treated with the test compound and the controls and allowed to incubate for 30 min, while the mouse was still under anesthesia. The wounds were photographed and the mice were then recovered on a warming pad.

Mice were monitored daily for behavioral changes and body weights recorded on days 1, 3, 6, 9, 12, and 16. The splints were checked daily and any broken or untied suture was replaced according to the experimental protocol. During a 24-h period, if only one suture was

compromised, it was replaced by a new suture. If two or more sutures were compromised during a 24-h period, the wound was no longer considered splinted and was removed from the study.

Digital photos were taken on the last day of the experiment and image analysis was performed by calculating the wound area (mm^2), using ImageJ Software (NIH). Wound closure was defined as the reduction in area between wound edges over the course of the study and was reported as a percentage of the original wound size.

4.4.3 Harvesting the wounds

Histopathology cassettes were labeled for mouse and wound identification. Note cards (1 inch sq.) were fitted to the bottom of the histopathology cassettes and one edge was labeled "cranial" that would be lined up with the cranial side of the wound harvested. On the final day of the experiment, mice were euthanized using Beuthanasia®-D (0.5 mL/mouse). Using a scalpel blade and scissors, a ¾ inch × ¾ inch square area of tissue is taken from the mouse, keeping the wound centered in the tissue section. Deep dissection was performed to harvest several layers of tissue deep in the wound. The square section of tissue was affixed to the note card, with the cranial edge lined up against the labeled edge of the card. The cassettes were then closed and placed in formalin-filled jars, to be processed for histopathological processing.

4.4.4 Histopathological analyses

After euthanasia, the entire wound bed as well as the intact skin margin greater than 5 mm was excised to the retro-peritoneum. The harvested tissue was then fixed in 10% v/v formalin for at least 24 h, and then sectioned through the center of the lesion. The center was marked with India ink prior to fixation. Routine paraffin processing was performed and the tissue samples were serially sectioned at a thickness of 5 μm, ensuring that the center of the lesion was

included on the slide. The slides were then stained with hematoxylin, eosin and picosirius red. A mounted digital camera (Olympus DP72, Melville, NY) was used to photograph the sections using light microscopy. Size of the wound, length of re-epithilialization, amount of fibrovascular proliferation in the dermis, and inflammatory response were measured as parameters to study wound healing on the slides containing the centre of the lesion. Measurements were taken and analyzed using image-analysis software (CellScience Dimension 1.4, Olympus, Melville, NY). Size of the wound was defined as the area of the wound not covered by advancing epithelial layer and was calculated by measuring the distance between the opposite free edges of the wound. Length of re-epithelialization was defined by the length of the layer of proliferating keratinocytes covering the wound area and was calculated by measuring the distance between the free edge of the keratinocyte layer and the base where the cells were still associated with native dermal tissue. Both sides of the lesion were measured and the final result was the sum of the two measurements. For wounds that had undergone complete re-epithelialization, a single measurement was taken from base to base.

Fibrovascular dermal proliferation was measured by examining the picosirius red-stained sections under polarized light, which highlighted the newly deposited dermal collagen. Using the image-analysis software, the wound bed was selected, amount of new collagen in the selected area was automatically measured and the figure expressed as a percentage of the total wound area. The inflammatory response was assessed using a semi-quantitative histopathological scoring system ranging from 0 to 4, where 0 indicated no inflammation, 1 indicates 0–25% of the wound area being affected, 2 indicates 25–50% of the wound area being affected, 3 indicates 50–75% of the wound area being affected, and 4 indicates >75% of the wound area being affected. The inflammatory response was also categorized as 'acute', when more than 75% of the

cells were neutrophils; 'chronic active'– when there was a 1:1 ratio of neutrophils and mononuclear cells; and 'chronic'– when more than 75% of the inflammatory cells were mononuclear.

4.4.5 Statistical analyses

All data were analyzed using a Mann–Whitney rank sum test, and statistical significance was set to $p < 0.05$. Statistical analyses were executed using the GraphPad Prism Version 5.0 (GraphPad Software, La Jolla, CA).

4.5 Conclusions

Our results demonstrate that the **Tβrl–CMP** conjugate can be immobilized in the wound bed due to the propensity of the collagen mimetic peptide domain to anneal to damaged endogenous collagen type I. Thus immobilized, the receptor ligand peptides can amplify the TGF-β signal without the administration of any additional TGF-β. Our method upregulates collagen formation in an otherwise impaired healing model like the diabetic mice that show diminished collagen deposition under normal conditions.

The closure of severe wounds where viable tissue has been destroyed by trauma involves deposition of new collagen tissue matrix. This amount varies depending on the severity of the damage. Fibroblasts generate the forces of contraction, and collagen controls the forces of wound closure and tensile strength. Amplified TGF-β activity in the initial stages of the wound healing process will help in quickly building up the tensile strength in the wounds and close the wounds

faster, due to stimulation of fibroblast proliferation and activity, as well as keratinocyte migration over the surface of the wounds. This type of healing may involve some amount of scarring, but could prove very effective in recovering from badly damaged wounds as is observed in 3rd-or 4th-degree burn wounds and traumatic mechanical damage, which would otherwise lead to lifelong impairment in the patients. Moreover, dose response studies indicate that the amount of collagen deposition can be regulated by lowering the concentration of **Tβrl–CMP** without substantial changes in the rate of epithelialization or wound closure.

Figure 4.1: Graphical representation of the TGF-β -receptor complex formation and subsequent activation of the Smad2/3 proteins in cell cytoplasm by the kinase domain of the complex. The phosphorylated Smad2/3 then associates with the Smad4 and translocates into the nucleus to bind with DNA-binding partners and regulate gene expression. (A) In the native state, TβRI and TβRII form non-covalent homodimers on the cell surface that bind to TGF-β with high avidity (K_d ~ 5–30 pM). (B) Preorganization of the TGF-β signaling complex on the collagen matrix via conjugation with collagen mimetic peptide $(PPG)_7$ that can anneal with native collagen in the wound bed. Such preorganization of the extracellular domains of the receptors should cause avid interaction with endogenous TGF-β.

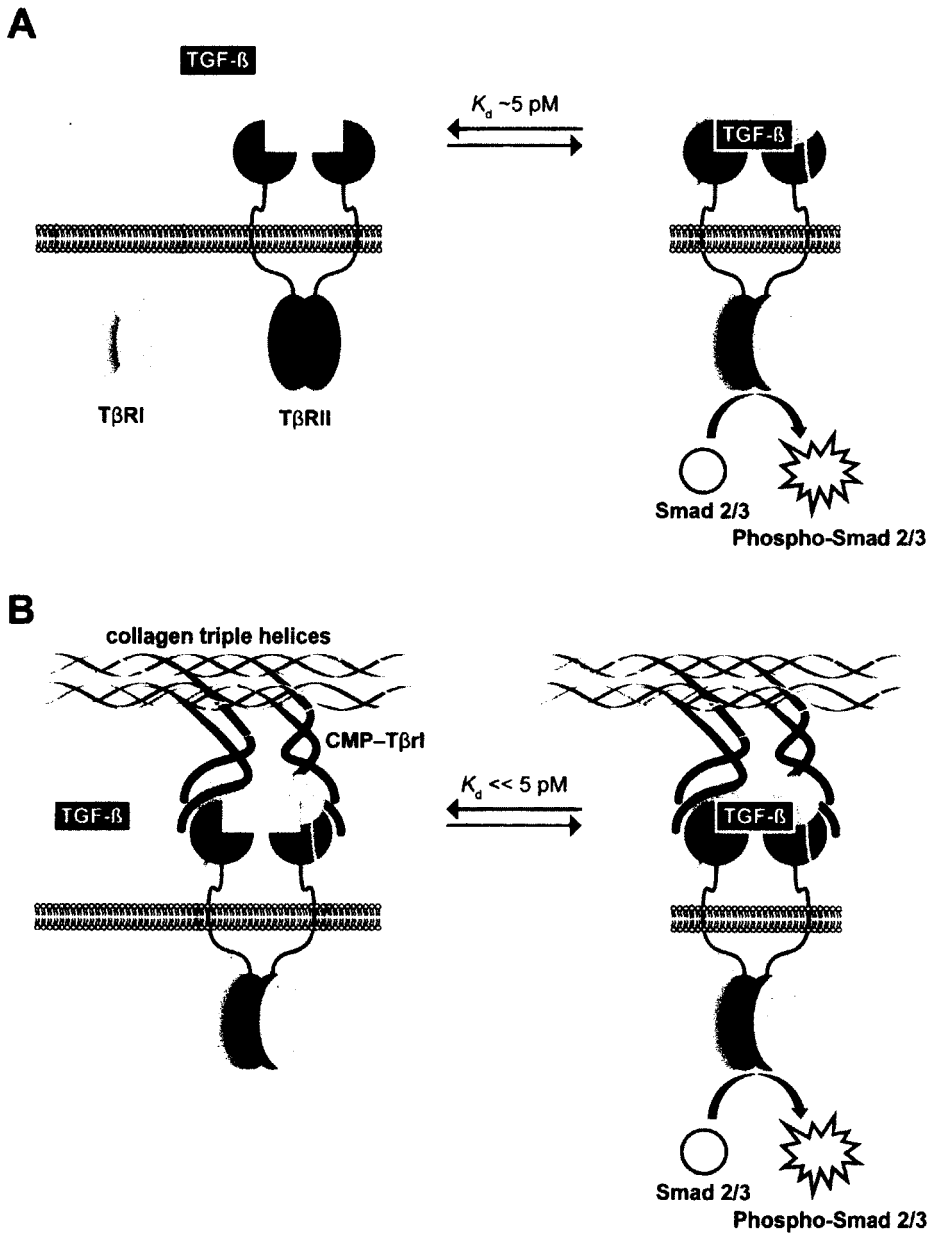

Figure 4.2. Bar graph showing the effect of **Tβrl-**immobilization (0.5 μmol in 5% w/v PEG/saline) on collagen deposition in non-splinted mouse wounds. Data are from Day 12 post-treatment. Fibrovascular influx was scored on a scale of 0–4, and was significantly higher ($p < 0.05$) in wounds treated with **Tβrl–CMP** in comparison to all the control-treated wounds (*). Values are the median ± SE ($n = 10$).

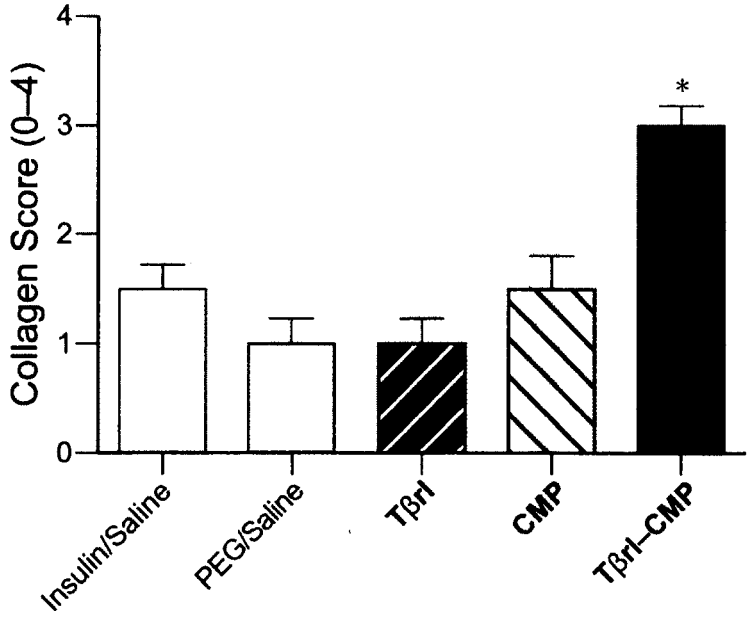

Figure 4.3. Bar graph showing the effect of **Tβrl**-immobilization (0.5 μmol in 5% w/v PEG/saline) on inflammation in non-splinted mouse wounds. Data are from Day 12 post-treatment. Inflammation was scored on a scale of 0–4, and was significantly higher ($p < 0.05$) in wounds treated with **Tβrl–CMP** in comparison to control wounds treated with the vehicle, soluble **Tβrl**, and **CMP** (*). Values are the median ± SE ($n = 10$).

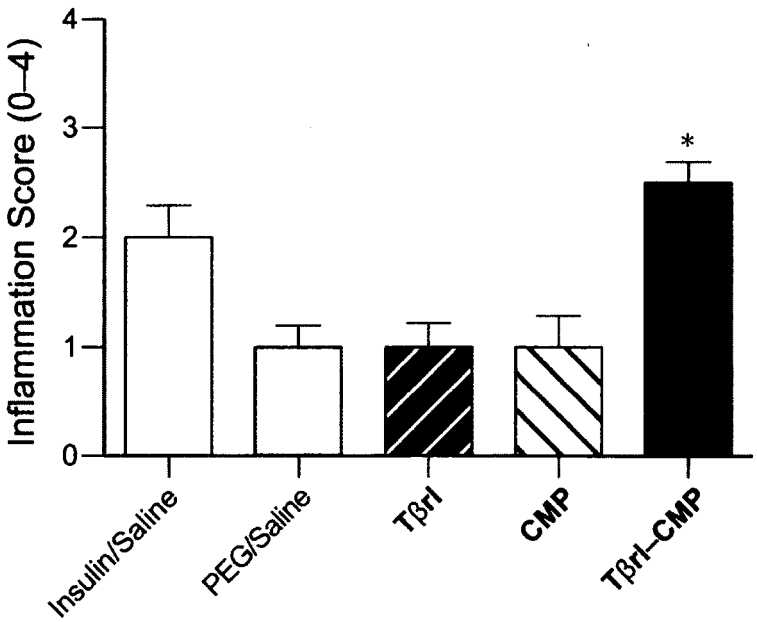

Figure 4.4. Bar graph showing the effect of **Tβrl**-immobilization (0.5 μmol in 5% w/v PEG/saline) on re-epithelialization of non-splinted mouse wounds. Data are from Day 12 post-treatment. The extent of re-epithelialization with **Tβrl–CMP** -treatment was higher than that of all the control-treatments. Values are the mean ± SE (n = 10).

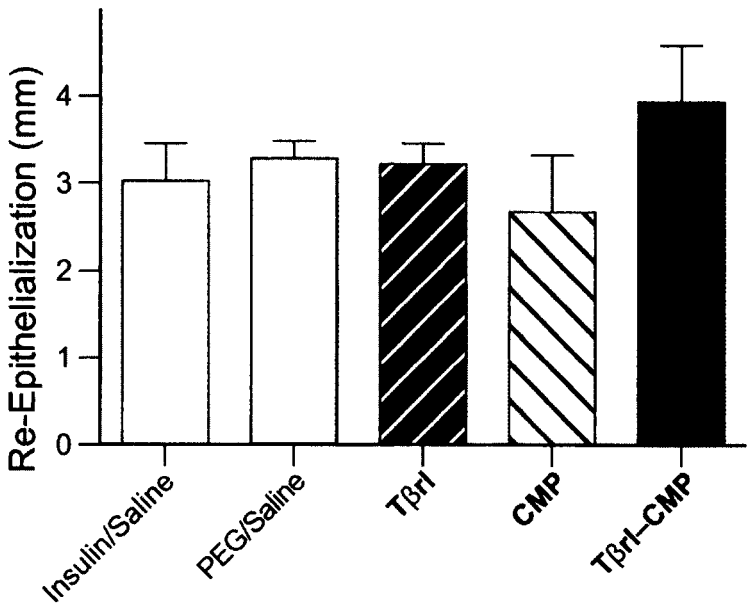

Figure 4.5. Bar graph showing the effect of **Tβrl**-immobilization (0.5 μmol in 5% w/v PEG/saline) on closure of non-splinted mouse wounds. Data are from Day 12 post-treatment. There was no significant difference between the sizes of the wounds, which was calculated as a percentage of the original wound size on Day 0. Values are the mean ± SE (n = 10).

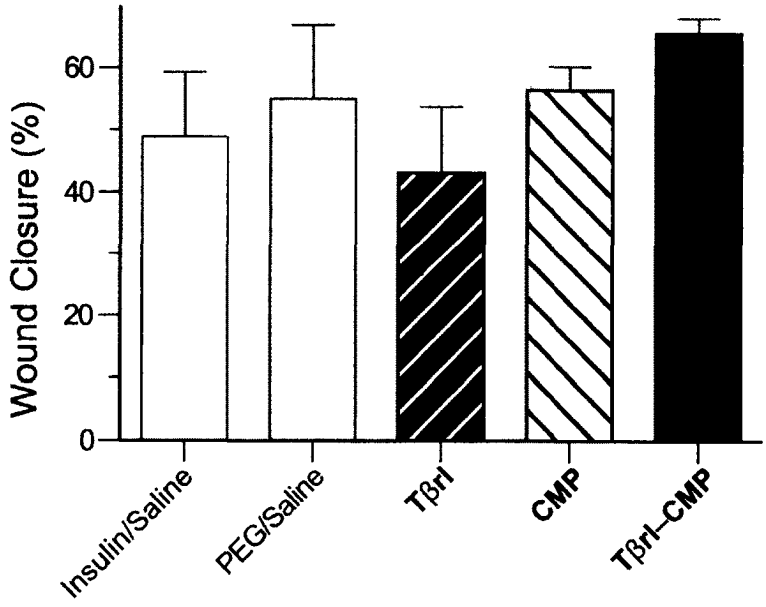

Figure 4.6. Photographs depicting the effect of **Tβrl**-immobilization on splinted mouse wounds. Images are from Day 0 (immediately post-treatment) or Day 16 after removal of the splints but before euthanasia. Wounds were treated with (A) saline; (B) PEG (5% w/v) in saline; (C) Soluble **Tβrl** (0.5 μmol) in 5% w/v PEG/saline; (D) **CMP** (0.5 μmol) in 5% w/v PEG/saline; (E) **Tβrl–CMP** (0.5 μmol) in 5% w/v PEG/saline. All wounds treated with **Tβrl–CMP** except for one showed complete closure (n = 16).

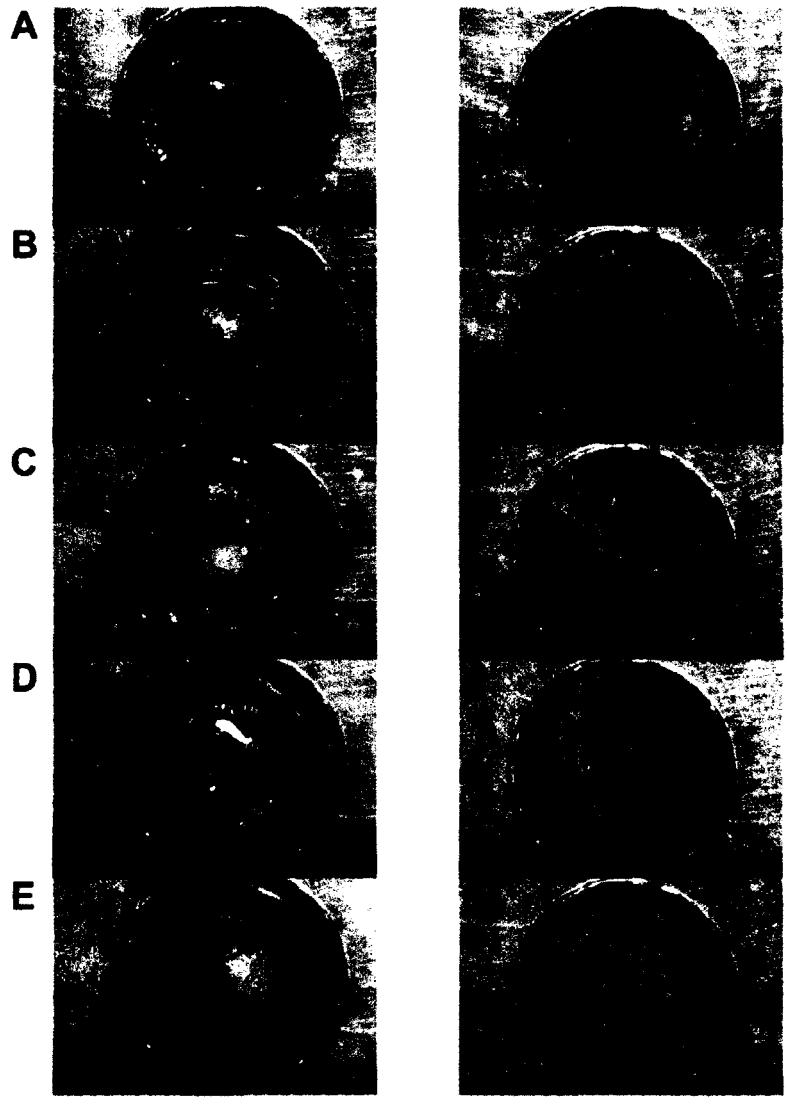

Figure 4.7. Bar graph showing the effect of **Tβrl**-immobilization (0.5 μmol in 5% w/v PEG/saline) on size and re-epithelialization of splinted mouse wounds. Data are from Day 16 post-treatment. (A) The mean size of the **Tβrl–CMP** -treated wounds was significantly different (*) from that of all the controls ($p < 0.05$). (B) **Tβrl–CMP** treatment showed significantly more extensive (*) epithelial layer formation compared to both saline and PEG/saline controls ($p < 0.05$). Values are the mean ± SE ($n = 16$).

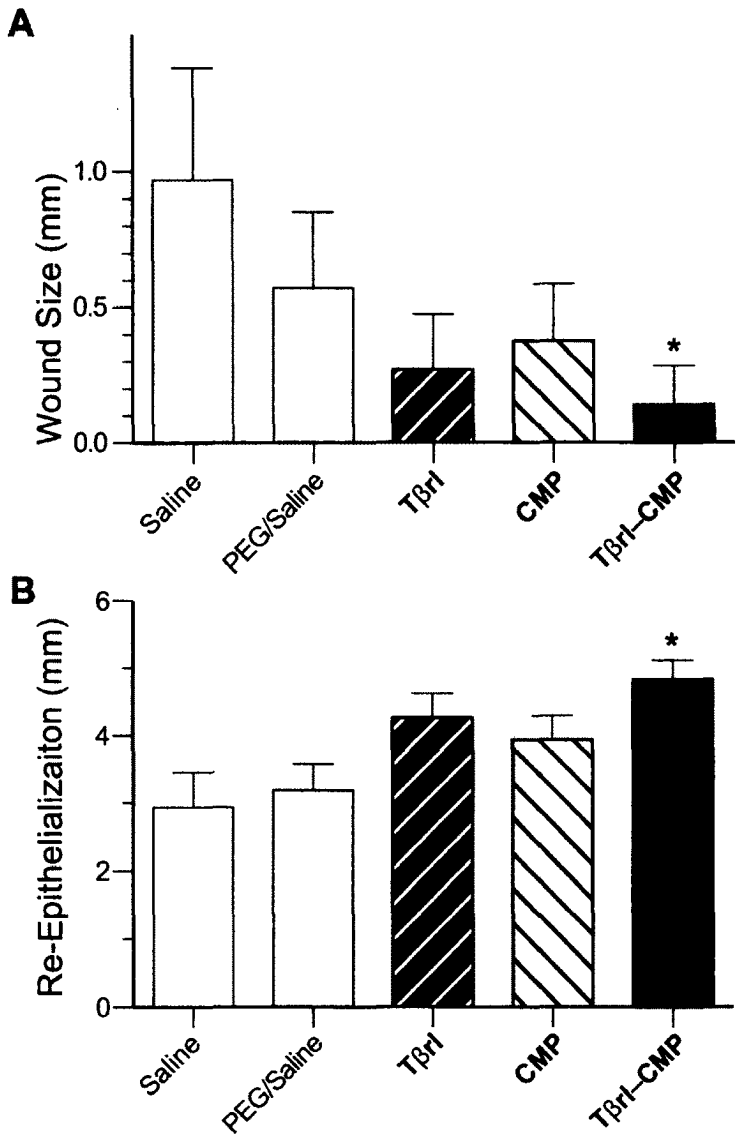

Figure 4.8. Bar graphs showing dose response to increasing concentrations of **Tβrl–CMP** solutions in saline (25 μL) in 6 mm non-splinted mouse wounds. Data are from Day 12 post-treatment. (A) New collagen deposition (calculated as percentage of a de-marked area of the wound at a depth of 0.75 μm from the healed surface). (B) Re-epithelialization. Collagen deposition was up-regulated at higher concentrations of **Tβrl–CMP**. Values are the mean ± SE (n = 10).

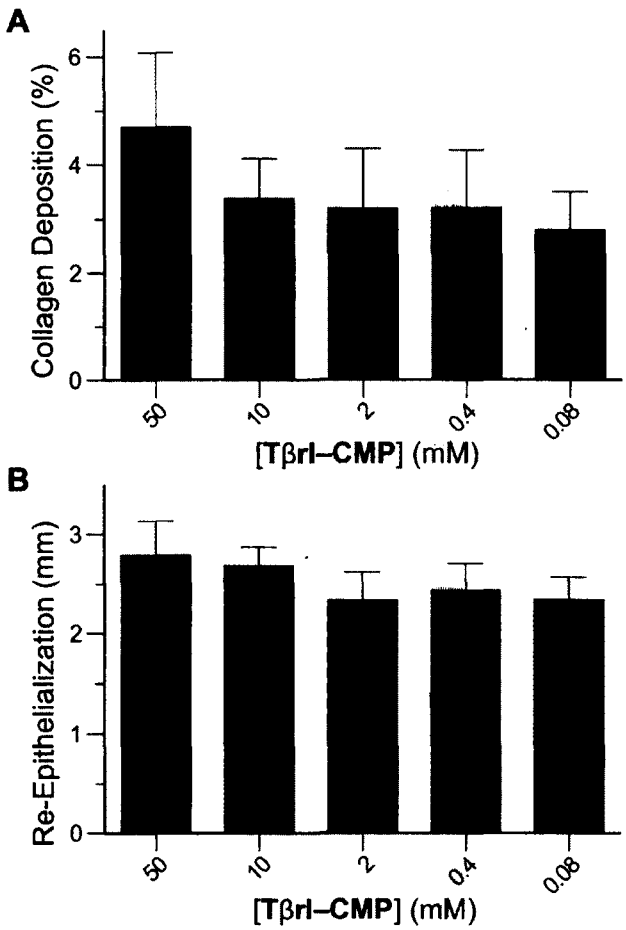

Figure 4.9. Histological images depicting the effect of **Tβrl**-immobilization in different doses on collagen deposition and size in non-splinted mouse wounds. Data are from Day 12 post-treatment. Left: Wounds stained with picosirius red and imaged under polarized light. Right: Wounds stained with hemotoxylin and eosin. Images represent wounds treated with **Tβrl–CMP** at concentrations of (A) 50 mM in saline; (B) 10 mM in saline; (C) 2 mM in saline; (D) 0.4 mM in saline; (E) 0.08 mM in saline. At this time point, lesions were still present in all the wounds, and there was more collagen deposition in the wounds treated with higher concentrations of **Tβrl–CMP**.

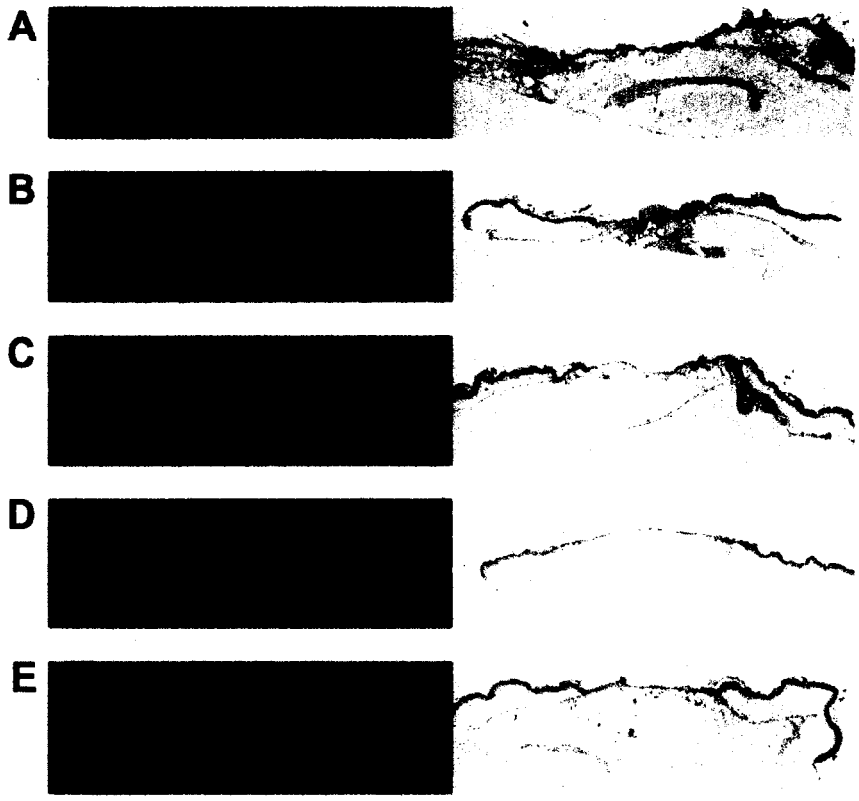

4.6 Acknowledgments

We are grateful to Patricia Kierski, Diego Calderon, Dana Tackes, Kevin Johnson, and Zachary Joseph for help with the wound surgery and animal care. We are also grateful to Dr. Lingyin Li and Prof. Nicholas Abbott for constructive discussions, and Dr. Langdon Martin, Dr. Kevin Desai, and Chelcie Eller for critical reading of the manuscript. This work was supported by grants R01 AR044276 and RC2 AR058971 (NIH). MALDI-TOF spectrometry was performed at the University of Wisconsin–Madison Biophysics Instrumentation Facility, which was established with Grants BIR-9512577 (NSF) and S10 RR13790 (NIH).

CHAPTER 5

Future Directions

5.1 To identify and design the covalent attachment of growth factors and other molecules to the collagen mimetic peptides

In Chapter 3 and Chapter 4, we demonstrated the feasibility of attaching short peptide molecules with established biological activities to a collagen mimetic peptide capable of binding to endogenous collagen and modulating the wound-healing process. Now, we can extend this strategy to larger growth factors that have been proven to influence the wound healing process as well as regulate cellular activity in a systemic manner. For example, diabetic foot ulcers, a major complication in patients with diabetes mellitus, is observed in 15–20% of the affected patients, and is the cause for ~85% of all lower leg amputations. These ulcers are a major burden on the health-care industry, and there are no effective treatment plans for such slow-healing wounds. Both vascular endothelial growth factor (VEGF) and fibroblast growth factor-2 (FGF-2) are potent stimuli for angiogenesis, a critical step of wound healing that is impaired in diabetic patients. A pharmacological promotion of angiogenesis would also promote diabetic foot ulcer-healing. The collagen mimetic peptides can be used to locally deliver VEGF or FGF with high specificity in the impaired wound tissue, and modulate the formation of new blood vessels in the area.

Since the growth factors often need to be transported across the cell membrane, this strategy would require the use of a cleavable linker molecule between the collagen mimetic peptide and the bioactive molecules. The linker should be cleavable under physiological conditions in a non-intrusive manner, and non-toxic with minimal chemical byproducts. Linkers that are affected by slight changes in pH conditions or on exposure to infrared light might prove to be useful in this regard. The linker region would also ensure the complete availability of the bioactive peptide/protein molecule to the cells and their receptors by increasing their separation

from the anchoring collagen base. Such linkers would also be useful for attaching the collagen mimetic peptides covalently to anti-microbial peptides. Many of these anti-microbial peptides have short sequences rich in hydrophobic residues and act by disrupting the bacterial cell membrane. Site-specific delivery of these peptides could increase their effectiveness and help in managing the microbial baggage of wound tissues.

The same strategy would also be valid for the delivery of small-molecule drugs that target organs and tissues rich in fibrillar collagen. The collagen mimetic peptides could be attached to bio-compatible fluorophores and be used to image badly damaged wound tissue in the deeper sections of the body as well as cancerous tissue, and thereby ensure a well-directed treatment and expedited healing. In conclusion, these collagen mimetic peptides show potential to be a safe and effective delivery system for myriad different wound-healing strategies.

5.2 Multivalent display of collagen-mimetic peptides on a peptide backbone for therapeutic purposes

In Chapter 2, we demonstrated the ability of short collagen mimetic peptides based on flpFlpGly and ProProGly units to form heterotrimeric triple helices with endogenous collagen type I. In the last decade there has been some progress in the development of interesting collagen peptide-based assemblies by including other structural components covalently linked to the collagen mimetic peptides. Stabilized collagen triple helices were composed using very short sequences of collagen mimetic peptides, that would otherwise be monomeric [$(ProProGly)_5$], via linking them to dendrimers (Kinberger *et al.*, 2002). The strategy can also help in constructing hydrogels using dendrimer-linked collagen mimetic peptides that can act as thermo-responsive

drug carriers. Various covalently knotted collagen mimetic peptides have been including a dendrimers in which terminal groups were modified with the collagen mimetic peptide (Gly-Pro-Nleu)$_n$ [Nleu: *N*-isobutylglycine] (Kinberger *et al.*, 2002; Kinberger *et al.*, 2006).

Such studies could be extended to our model collagen mimetic peptides to design peptide–polymer conjugates useful for wound-healing studies. The synthetic target would be achieved by covalently linking such peptides to linear polymers and designing a peptide–polymer "brush" that could display the biological activity of the peptides on the surface. Appropriate block co-polymers have been created by using the ring-opening metathesis polymerization (ROMP) (Pontrello *et al.*, 2005). We could use this strategy to synthesize block co-polymers that act as the backbone of a peptide–polymer "brush", and then attach covalently a large number of collagen mimetic strands (Scheme 5.2.1).

We could use the above strategy to design and synthesize peptide–polymer conjugates with (flpFlpGly)$_7$ units that are displayed multivalently on the polymer surface and are thereby available for annealing to native type I collagen in the traumatized tissue of a wound bed. The tethered (flpFlpGly)$_7$ units could then 'solder' the frayed tissue together and expedite the rate of wound closure. This strategy might be particularly useful for the treatment of large wounds, complementing extant tissue-grafting methods.

In initial studies, we could functionalize the peptide–polymer conjugates with small fluorophores and characterize their ability to bind and congeal native collagen *in vitro*. We could also use gold nanoparticles to functionalize these peptide–polymer conjugates, fix them on tissue sections and visualize their binding using transmission electron microscopy.

We could also choose to display $(ProProGly)_7$ units in the synthesis of these peptide–polymer conjugates. Work by other groups has indicated that clustering the collagen mimetic peptide on the surface of dendrimers induced the formation of collagen-like triple helices, even when the peptides were of relatively short sequences. When tethered to dendrimers, the collagen mimetic peptides exhibited more highly triple-helical structures than did the free peptides (Higashi *et al.*, 2000; Kinberger *et al.*, 2006; Kojima *et al.*, 2009). The triple-helix formation could also be controlled by modulating the length of the conjugated peptides and the temperature of the solution. Generally, triple-helix formation is promoted at lower temperatures. We could identify the melting temperature for these surface-tethered triple helices and attempt to construct a hydrogel by cooling an aqueous solution of the peptide–polymer conjugate to a temperature lower than the T_m. Such a hydrogel would resemble closely the extracellular matrix in composition, and could be used as a potential cellular matrix for controlled drug release. Previous studies have shown that conjugating ProHypGly-based collagen mimetic peptides with pre-formed PEG-based hydrogels can be used to encapsulate chondrocytes and enhance tissue production (Lee *et al.*, 2006), while triblock copolymers containing ProHypGly units are capable of assembling into spherulites (Martin *et al.*, 2003).

5.3 Design and synthesis of a collagen 'duplex'

An important off-shoot of the wound-healing aspect of this thesis work is to establish (or disavow) the idea of collagen "strand invasion" by collagen mimetic peptides in wounded tissue. Testing the theory in an *ex vivo* or *in vivo* model is difficult. We could, however, approach this

goal *in vitro* by the rational design of a collagen 'duplex' that could act as 'nest' for model collagen mimetic peptides.

The strategy could involve growing two peptide chains simultaneously from the same resin bead, and then covalently linking the chains on their free ends using a disulfide linkage (Figure 5.2.1A). Test collagen mimetic peptides could be incubated with the double-stranded template, and the thermodynamics of a spontaneous triple-helix formation could be studied *in vitro*. Our initial design of such a template involved linking one end of the 'duplex' via the formation of a thioether bond (Figure 5.3.1B). The glycine residues at either end would provide the required flexibility for spontaneous formation of a disulfide bond at the other end. Based on previous work done in our lab (Gottlieb, D. and Raines, R. T., unpublished results), the synthesis of a thioether bond on solid phase was not successful (Figure 5.3.1C).

Our efforts to modify the strategy included replacing the thioether linkage with an amine linkage (Figure 5.3.2A) using a second lysine residue (Figure 5.3.2B). This strategy was not successful in building the two strands simultaneously on a solid phase. When we used Fmoc-6-aminohexanoic acid (Fmoc-aha) to form the amine linkage (Figure 5.3.2C), and cleaved the double-stranded peptide from resin under standard cleavage conditions, the terminal cysteine residues oxidized spontaneously. The mass spectroscopy trace appears to indicate polymerization via intermolecular disulfide-bond formation (Figure 5.3.3).

Future efforts to synthesize this template could include using a low-loading resin (like NovaPEG Rink Amide Resin) and FmocProProGlyOH units, and synthesizing the double-stranded peptide template on a solid phase without using automated synthesis.The first coupling of FmocLys(Mmt)OH can be followed by selective deprotection of the ε-amino group,and

subsequent coupling of a β-alanine residue that could serve as the basis for synthesizing the second strand concomitantly. In order to prevent unwanted polymerization of the cysteine thiols, the final oxidation step should be performed in very dilute solutions using mild oxidizing agents, such as 2, 2'- dithiodipyridine, 5% DMSO, or exposure to air over a controlled time interval.

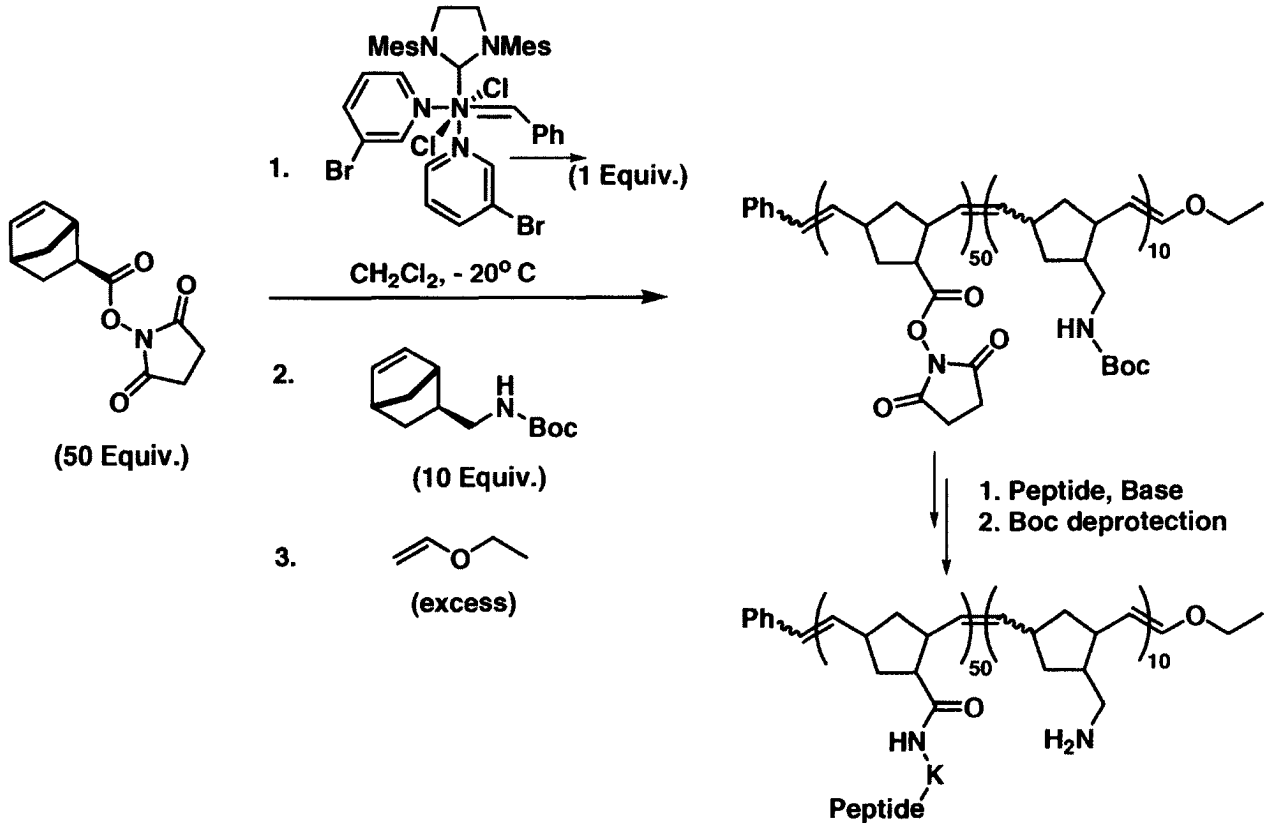

Scheme 5.2.1. Synthesis of CMP–polymer conjugate

Figure 5.3.1. Design of a collagen 'duplex' template. (A) The template could act as a scaffold to study triple helix formation in vitro. (B) Duplex strands linked by thioether and disulfide bonds at the C- and N-terminus respectively. (C) Solid-phase synthetic scheme for thioether synthesis

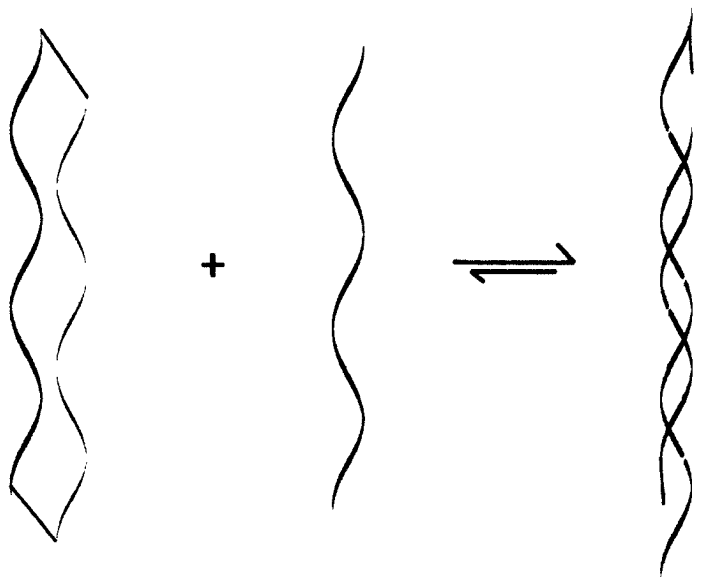

A. Collagen "duplex" Collagen Triple Helix

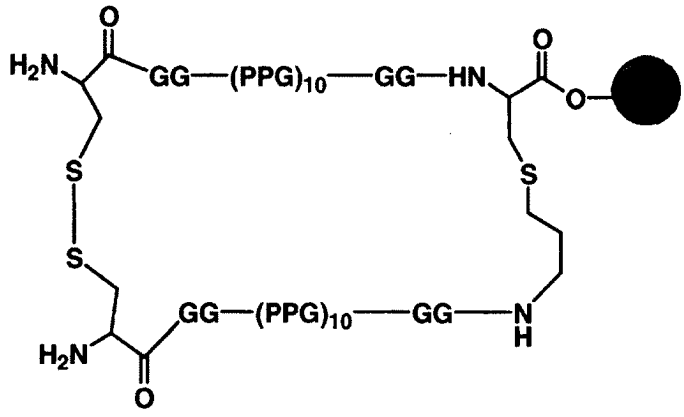

B.

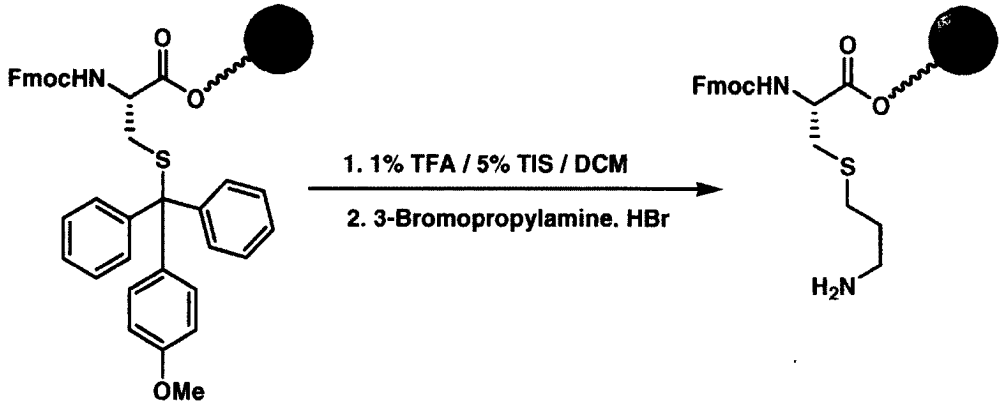

C.

Figure 5.3.2. Alternative design for a collagen 'duplex' template. (A) Duplex strands linked by amino and disulfide bonds at the C- and N-terminus respectively. (B) Solid phase synthetic scheme for di-lysine coupling. (C) Solid-phase synthetic scheme for coupling of Fmoc-6-aminohexanoic acid to lysine.

A.

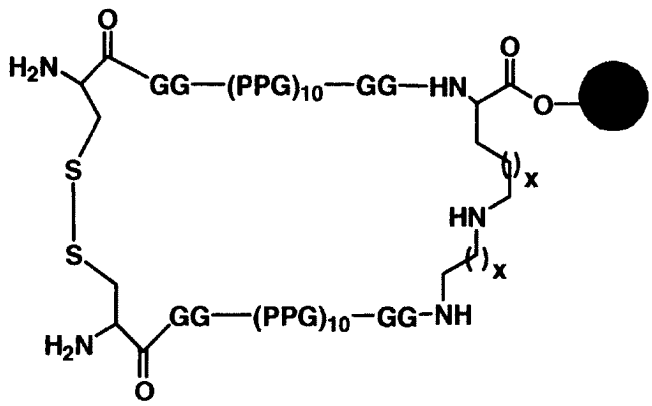

B.

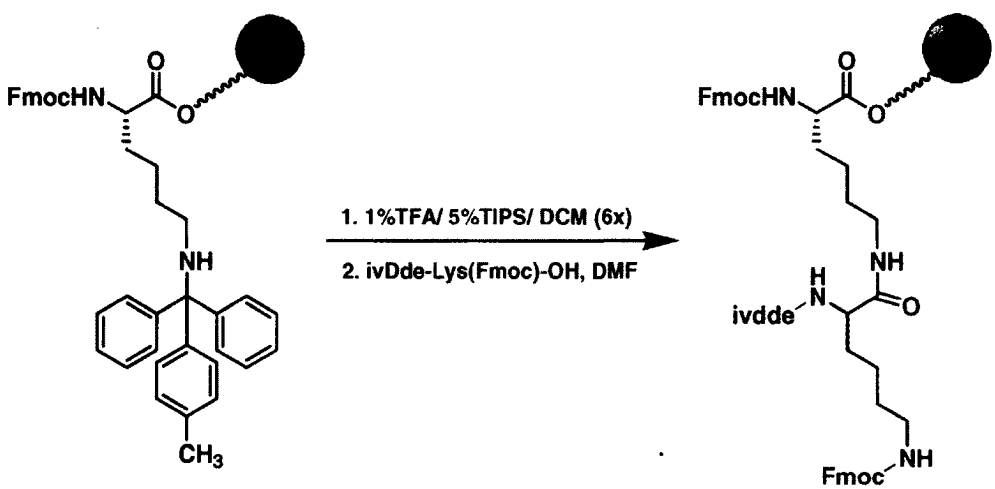

C.

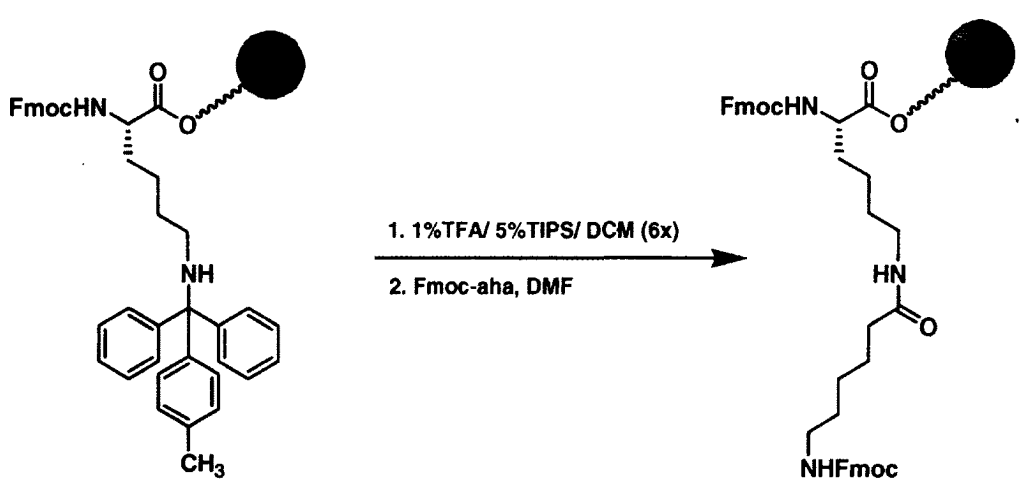

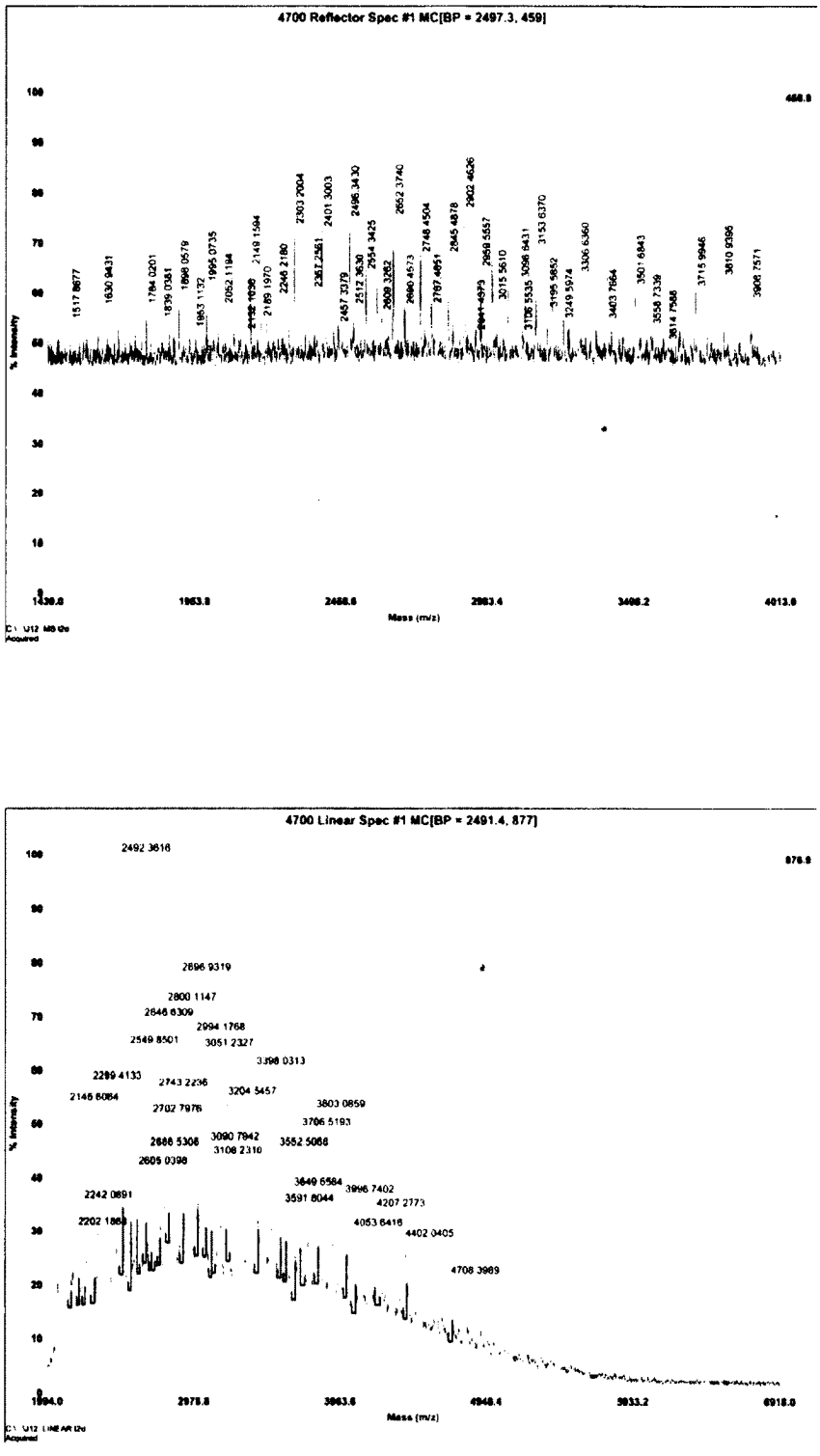

Figure 5.3.3. MALDI–TOF mass-spectra for the polymeric products of the synthetic scheme outlined in Figure 5.3.2C

APPENDIX

Appendix 1: For Chapter 2

A.1 Collagen mimetic peptides annealing to *in vivo* diabetic wounds

The *db/db* mouse exhibits clinically relevant characteristics like obesity, insulin resistance, and severe hyperglycemia of human onset diabetes, with a concomitant delay in wound healing. These mice also show typical complications associated with diabetic patients such as peripheral neuropathy, microvascular lesions, thickening of the basement membrane, and immunodeficiency. As a result the *db/db* mice are used extensively used for studies on dermal repair.

The *db/db* mouse is a well-established model of hyperphagia with an inherent predisposition to severe obesity. The levels of subcutaneous and visceral fat layers in *db/db* mice are significantly higher compared to the wild-type as seen in Figure A.1.1. In a typical skin cross-section the extensive granulation tissue layer overlays the adipose cell layer (Figure A.1.2). In *db/db* mice the adipose layer is more extensive. Earlier research by different groups has shown the feasibility of delivering stromal cells and growth factors into dorsal wounds of *db/db* mice using collagen-based biomaterials (Kondo *et al.*, 2011 [Epub ahead of print; Sept 22]; Maeda *et al.*, 2001; Nambu *et al.*, 2011). Our efforts to target wound healing using collagen mimetic peptides is based on the ability of such peptides to bind to endogenous collagen type I present in the wound bed. This criterion required us to ensure that the extensive adipose layer in *db/db* mice will not provide an impediment to our studies.

A.1.1 Experimental methods

Collagen mimetic peptide with fluoroproline units [Ac–(flpFlpFly)$_7$–(GlySer)$_3$–LysOH] (**CMP 1**) was synthesized by coupling FmocflpFlpGlyOH, FmocGlyOH, and FmocSerOH on FmocLys(Boc)-Wang resin using standard SPPS procedures as described earlier. CMP 1 was conjugated to 5-carboxyfluorescein, NHS ester as per the protocol described earlier to afford fluorescently tagged **^{F}CMP 1**.

Identical 8-mm wounds were created in the dorsal region of *db/db* mice (8–10 weeks old). The test wounds were treated with fluorophore-tagged collagen mimetic peptide (**^{F}CMP 1,** 25 μL, 20 mM), and the control wounds were treated with free fluorophore 5-carboxyfluorescein reacted with ethylamine. The wounds were incubated for 30 min while the mice were under the influence of anesthesia, and then washed with 1x PBS. The mice were euthanized and the wounds were harvested following the specified protocols described earlier. The wounds were imaged using a dissecting fluorescent microscope.

A.1.2 Results and discussion

^{F}CMP 1 annealed to cutaneous wounds in *db/db* mice post washing, and the fluorescence was limited to the wound bed (Figure A.1.3). The wounds treated with the free dye did not show any fluorescence. The collagen mimetic peptides designed can thus be used effectively for wound healing studies.

Figure A.1.1. Comparison of 10-week-old *db/db* and normal mice. (A) Exposure of subcutaneous and visceral fat showing more fat in the *db/db* mouse compared to the wild-type mouse. (B) Sections of epididymal fat of *db/db* and wild-type mice, showing large size of *db/db* adipocytes compared with wild-type despite identical food intake. [Adapted from (Wang *et al.*, 2008c)]

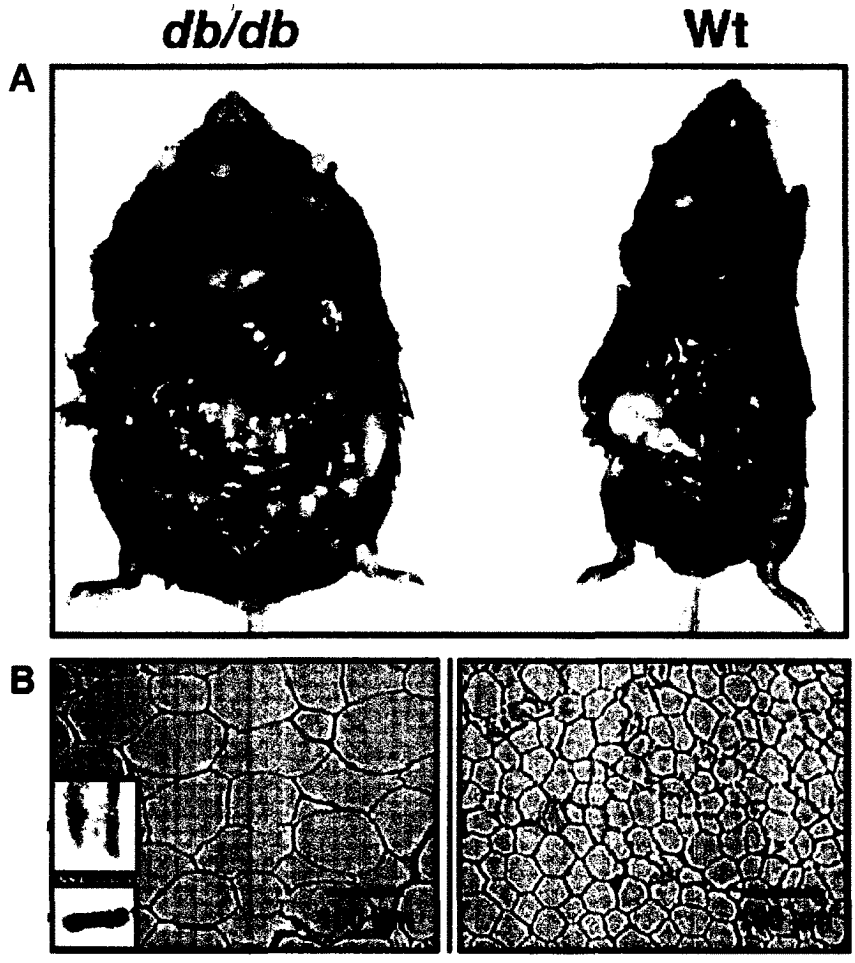

Figure A.1.2. Graphical representation of the cross-section of a wound bed in skin

[Adapted from Wounds © 2004 Health Management Publications]

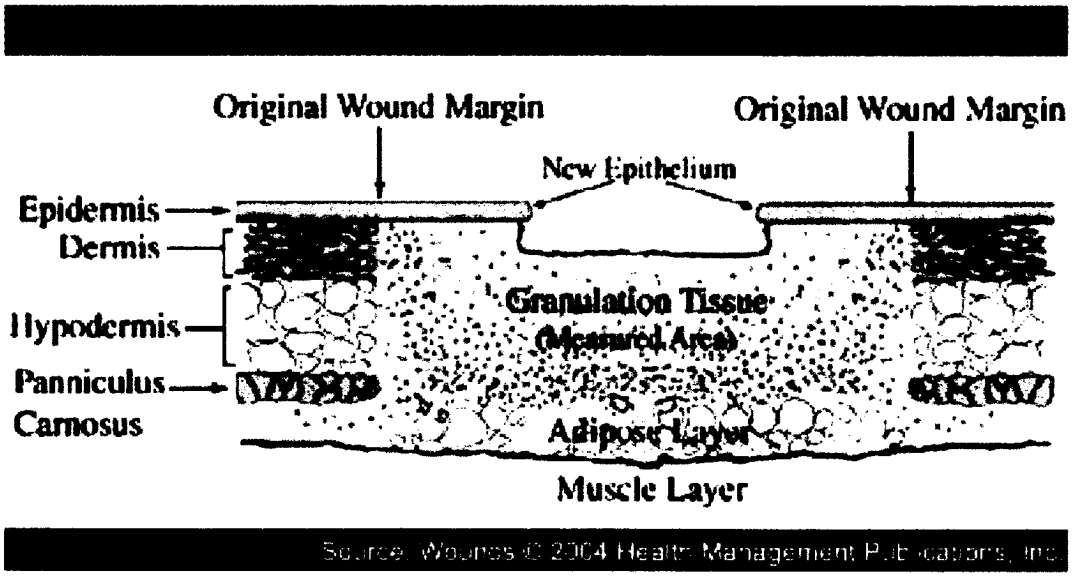

Figure A.1.3. Photographs of the annealing of ^{F}**CMP 1** to *db/db* mouse collagen *in vivo*. Fluorescently labeled CMP 1 and 5-FAM were applied to 8-mm cutaneous dorsal wounds on mice, washed, and imaged. A. Wound treated 5-FAM. B. Wound treated with ^{F}**CMP 1**. The outline of the wound-edge is shown in (A) and (B).

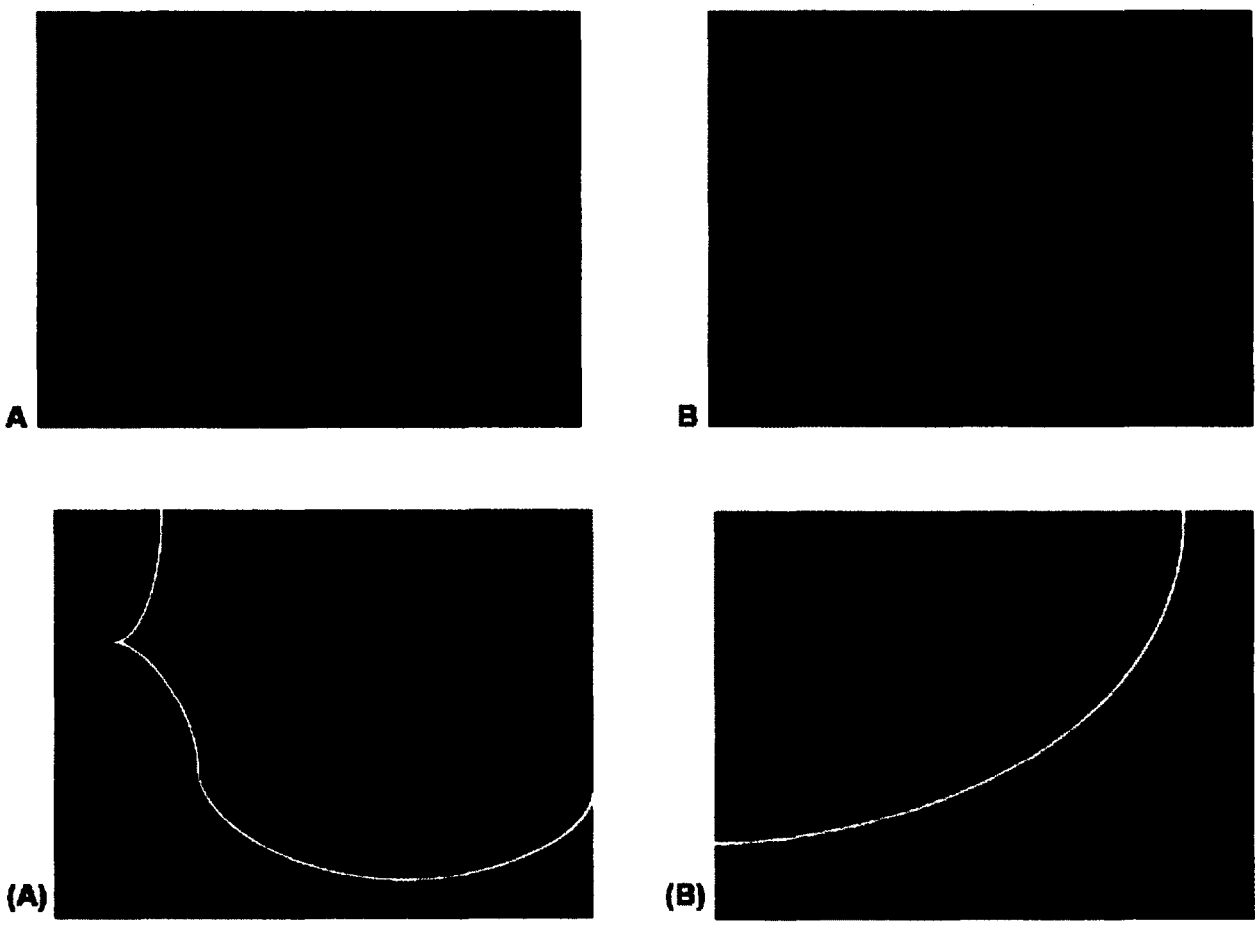

Appendix 2: For Chapter 3

A.2 Dose response of CMP–SubP

We tested the potency of Substance P conjugated to collagen mimetic peptides in wound healing by treating the wounds with increasing doses of the conjugated **CMP–SubP**. Identical wounds with an outer diameter of 6 mm were created on the backs of *db/db* mice (5 mice/ 10 wounds per group), and incubated with 25 μL solutions of **CMP–SubP** in 5-fold increase in concentrations between 80 μM to 50 mM for 30 min. The mice were then recovered and the wounds analyzed after a period of 12 days.

A.2.1 Results and discussion

Length of re-epithelialization was defined by the length of the layer of proliferating keratinocytes covering the wound area and was calculated by measuring the distance between the free edge of the keratinocyte layer and the base where the cells were still associated with native dermal tissue. Both sides of the lesion were measured and the final result was the sum of the two measurements. The extent of re-epithelialization in wounds treated with 0.08, 0.4 and 2 mM of **CMP–SubP** solution were comparable and did not show any notable differences (Figure A.2.1). However there was a marked decrease in epithelial cover in wounds treated with high doses of **CMP–SubP**, and the wounds remained open longer when a high concentration of the conjugate was used.

The amount of new collagen formed in the wound bed was identified with picosirius red stain and expressed as a percentage of total area of the wound bed. The extent to which collagen was deposited appeared to be comparable in the wounds treated with 50 and 10 mM solutions, and peaked on administration of a 2 mM solution of the conjugate (Figure A.2.2). The response

was affected with solutions of lower concentrations. A similar trend was observed in the inflammatory response which indicated that concentrations of ~2 mM elicited the maximum influx of polymorphonuclear and mononuclear cells into the wound tissue in 12 days (Figure A.2.3).

Based on the results obtained we decided to use an optimized concentration of 1 mM **CMP–SubP** for our experiments involving a splinted-wound model in *db/db* mice. At this concentration, wound closure and epithelialization is substantial without compromising on the extent of collagen deposition and inflammatory response.

Figure A.2.1. Bar graph representing extent of re-epithelialization in response to increasing concentrations of **CMP–SubP** solutions in 6 mm non-splinted wounds. Wounds were treated with 0.08, 0.4, 2, 10, and 50 mM solutions (25 μL) in 5% w/v PEG/saline. Data are from Day 12 post-treatment. There were no significant differences in the mean length of the new epithelial layer formed in wounds treated with 0.08, 0.4, and 2 mM **CMP–SubP**. Values are the mean ± SE (n = 10).

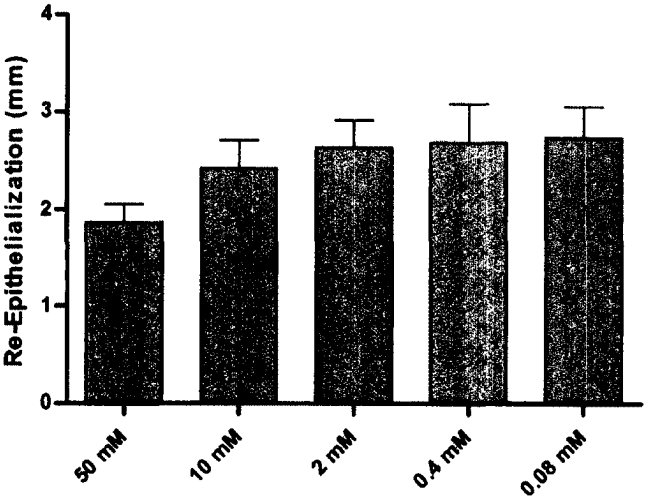

Figure A.2.2. Bar graph representing collagen deposition in response to increasing concentrations of **CMP–SubP** solutions in 6 mm non-splinted wounds. Wounds were treated with 0.08, 0.4, 2, 10, and 50 mM solutions (25 μL) in 5% w/v PEG/saline. Data are from Day 12 post-treatment. New collagen deposition was maximal at 2 mM concentration of **CMP–SubP**. Values are the mean ± SE (n = 10).

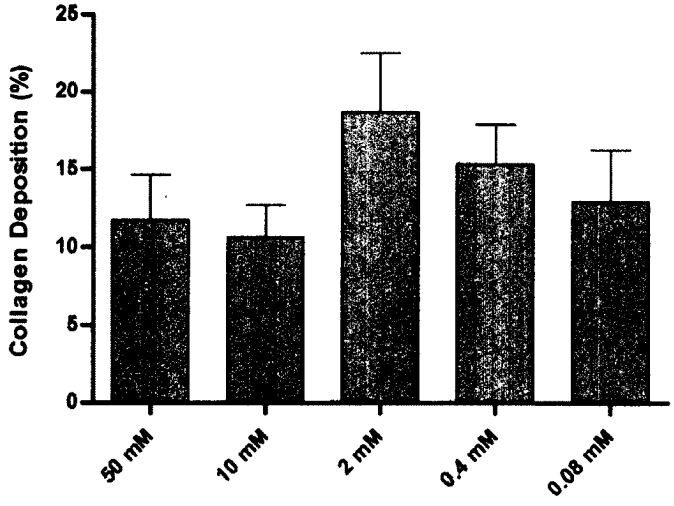

Figure A.2.3. Bar graph representing inflammatory influx in response to increasing concentrations of **CMP–SubP** solutions in 6 mm non-splinted wounds. Wounds were treated with 0.08, 0.4, 2, 10, and 50 mM solutions (25 μL) in 5% w/v PEG/saline. Data are from Day 12 post-treatment. The influx of inflammatory cells peaked on treatment with 2 mM **CMP–SubP** solution. Data represents median ± SE (n = 10).

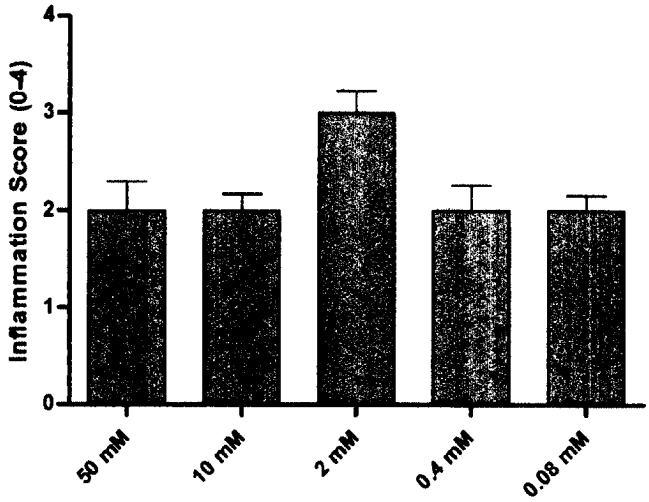

Appendix 3: For Chapter 4

A.3.1 The effects of topical insulin administration in wounds treated with Tβrl–CMP

Un-splinted wounds in the craniodorsal region of diabetic mice (3 mice/ group) were treated them with 15 μL of **Tβrl–CMP** (20 mM in saline). One of these groups was also treated with 5 μL insulin (50 I.U in saline). The wounds were monitored over a period of 12 days and then visualized under a camera as well by histopathological analysis.

A.3.1.1 Results and discussion

On inspecting the wounds visually, there was no significant difference in the extent of closure of wounds treated with **Tβrl–CMP**, with or without the presence of insulin (Figure A.3.1A). This was supported by histopathological scoring, which indicated a reduced wound-size in absence of insulin (Figure A.3.1B). The mean length of new epithelial layer formed (Figure A.3.1C) and collagen synthesized (Figure A.3.1D) are comparable in both the groups. A combination of **Tβrl–CMP** and insulin also led to a depression in inflammatory response in the wounds (Figure A.3.1E).

Based on the analyzed results, we decided to cease the use of topical insulin in studies involving the splinted-wound model.

Figure A.3.1. Bar graph showing the additive effect of insulin (50 I.U) during **Tβrl–CMP**-immobilization on non-splinted mouse wounds. Data are from Day 12 post-treatment. (A) Wound closure, which refers to reduction in area between wound edges as a percentage of the original area. (B) Wound size, which refers to histopathological measurement of wound of the largest diameter. (C) Length of new epithelial layer, measured as the length of advancing keratinocyte layers on either edges of the wound bed. (D) Collagen deposition measured as a percentage of a de-marked area of the wound. (E) Inflammation score. Data represents mean ± SE ($n = 6$).

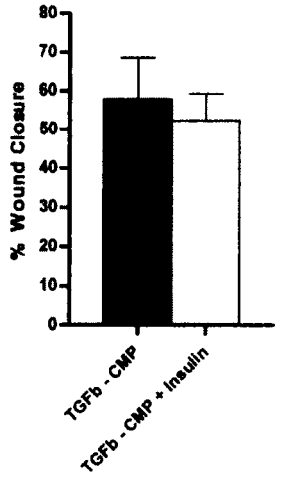

A

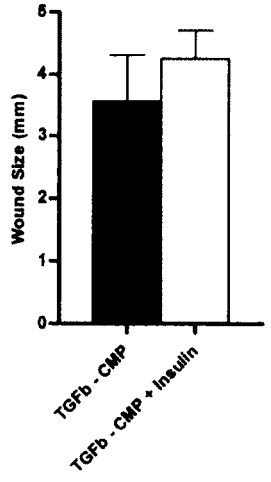

B

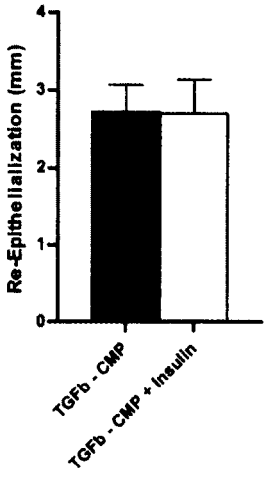

C

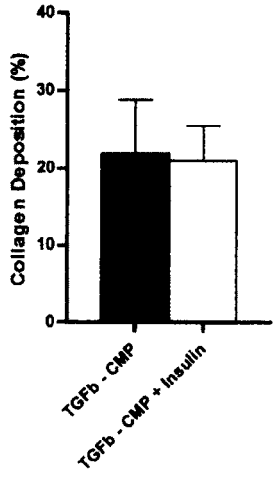

D

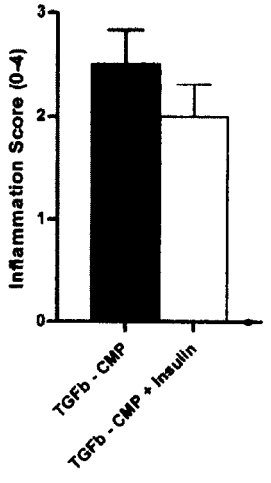

E

A.3.2 Extent of collagen deposition in wounds treated with Tβrl–CMP 16 days post-treatment

In experiments similar to the ones described previously, we made an attempt to analyze wounds treated with **Tβrl–CMP** and observed over a longer period of time i.e. 16 days. **Tβrl–CMP** (25 μL, 20 mM) was topically applied to identical 8 mm-diameter wounds created on either side of the cranio-dorsal region in five *db/db* mice (10 wounds). Insulin (5 μL, 50 I.U) was added to each of the wounds. Control wounds were treated with the delivery vehicle 5% PEG/saline, insulin, soluble unconjugated peptide **Tβrl** (25 μL, 20 mM), and the collagen mimetic peptide **CMP** [$(ProProGly)_7$; 25 μL, 20 mM]. The wounds were incubated for 30 min while the mice were under anesthesia, and then the mice were recovered and observed over the next 16 days.

An identical experiment using *splinted* wounds in *db/db* mice was also carried out over a period of 16 days. The test wounds (8 mice/ 16 wounds) were treated with **Tβrl–CMP** (25 μL, 20 mM), while the control wounds were treated with saline, 5% PEG/saline, unconjugated **Tβrl** (25 μL, 20 mM), and the collagen mimetic peptide **CMP** [$(ProProGly)_7$; 25 μL, 20 mM].

A.3.2.1 Results and discussions

In the un-splinted model, the levels of new collagen deposition in the wounds treated with the test conjugate and the control solutions were comparable (Figure A.3.2.1). In our previous study we had observed a significantly higher deposition of fresh collagen after 12 days when wounds were treated with **Tβrl–CMP** at the same concentration. On analysis of the *splinted* wounds after 16 days, we observed a similar trend of comparable levels of collagen

deposition in a de-marked area of all the wounds (to the depth of 0.75 μm depth from the healed surface) (Figure A.3.2.2).

In light of our current results from wounds analyzed after 16 days, it appears that a single topical administration of **Tβrl–CMP** on day 0 promotes enhanced levels of collagen synthesis and deposition in the wound bed at an earlier time point of the healing process. This elevated response is however tempered in the later period of the healing period, such that the total amount of collagen in the wounds by the time of complete closure is comparable to that in wounds treated with control solutions. Such a response pattern has the potential to impart mechanical strength to the wound matrix via early collagen deposition and formation of the extracellular matrix, while tempering the collagen deposition in subsequent periods, and thereby avoid the possibility of extensive scarring.

Figure A.3.2.1. Bar graph showing the effect of **Tβrl–CMP** –immobilization on collagen deposition of non-splinted mouse wounds. Data are from Day 16 post-treatment. Collagen deposition was comparable in all the wounds. Values are the median ± SE (n = 10).

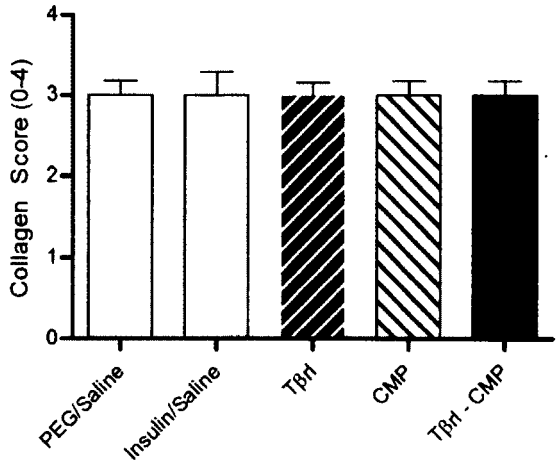

Figure A.3.2.2. Bar graph showing the effect of **Tβrl–CMP** –immobilization on collagen deposition of splinted mouse wounds. Data are from Day 16 post-treatment. Collagen deposition was comparable in all the wounds. Values are the mean ± SE (n = 16).

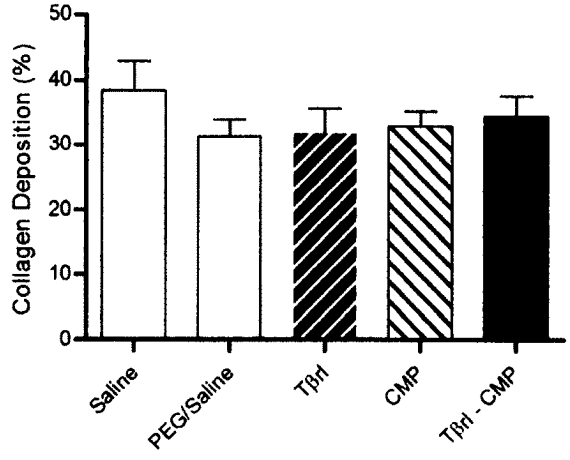

A.3.3 Inflammatory response in wounds treated with Tβrl–CMP 16 days post-treatment

The inflammatory response in wounds treated with **Tβrl–CMP** (25 μL, 20 mM) at an advanced time point in the wound healing process was also analyzed. After 16 days post-surgery both *non-splinted* and *splinted*-wound models as described above were scored for the levels of inflammatory cell influx into the affected tissue.

A.3.3.1 Results and discussion

Analysis of non-splinted wounds 12 days post-treatment had indicated that **Tβrl–CMP** elicited a significantly ($p < 0.05$) increased level of inflammatory response in the wound bed compared to treatment with 5% PEG/saline, unconjugated **Tβrl**, and **CMP** solutions. After 16 days the inflammatory activity in the tissues was reduced and was comparable to the vehicular control as well as the control peptides (Figure A.3.3.1).

The pattern observed in the splinted-wound model, the inflammatory response-pattern observed was identical and all the treated wounds had comparable levels of polymorphonuclear and mononuclear cells (Figure A.3.3.2)

Figure A.3.3.1. Bar graph showing the effect of **Tβrl–CMP** –immobilization on inflammatory influx of non-splinted mouse wounds. Data are from Day 16 post-treatment. Values are the median ± SE (n = 10).

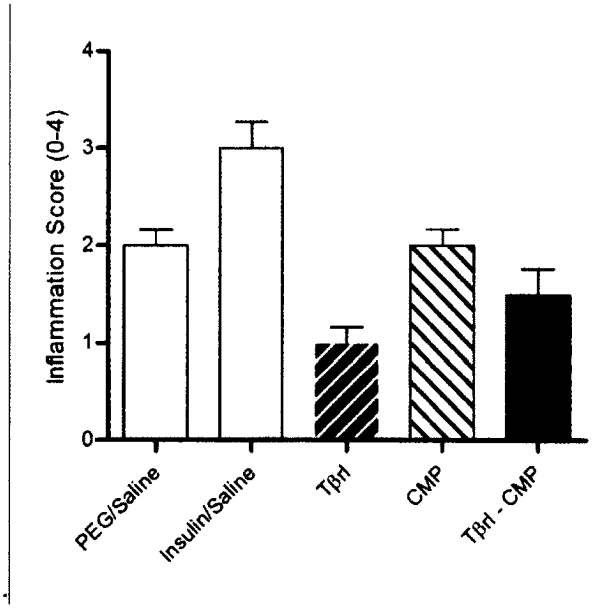

Figure A.3.3.2. Bar graph showing the effect of **Tβrl–CMP** –immobilization on inflammatory influx of splinted mouse wounds. Data are from Day 16 post-treatment. Values are the median ± SE (n = 16).

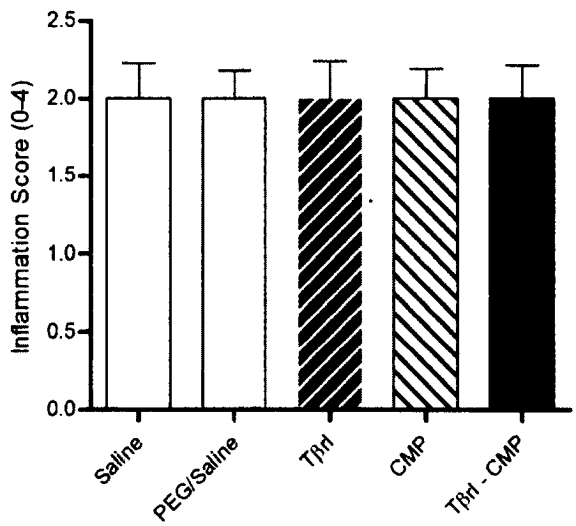

A.3.4 Inflammatory reaction and wound size in response to increasing concentrations of Tβrl–CMP

We analyzed the potency of TGF-β receptor ligand conjugated to collagen mimetic peptides in wound healing by treating the wounds with increasing doses (five-fold) of conjugated **Tβrl–CMP**. Identical wounds with an outer diameter of 6 mm were created on the backs of *db/db* mice (5 mice/ 10 wounds per group), and incubated with 25 μL solutions of **Tβrl–CMP** in five-fold increase in concentrations between 80 μM to 50 mM for 30 min. The mice were then recovered and the wounds analyzed for inflammatory response and wound size after a period of 12 days.

A.3.4.1 Results and discussion

The inflammatory response was assessed using a semi-quantitative histopathological scoring system ranging from 0 to 4, where 0 indicated no inflammation, 1 indicates 0–25% of the wound area being affected, 2 indicates 25–50% of the wound area being affected, 3 indicates 50–75% of the wound area being affected, and 4 indicates >75% of the wound area being affected. The inflammatory response was also categorized as 'acute', when more than 75% of the cells were neutrophils; 'chronic active'– when there was a 1:1 ratio of neutrophils and mononuclear cells; and 'chronic'– when more than 75% of the inflammatory cells were mononuclear.

On analyzing the data the overall inflammatory score for the different treatments did not show a specific trend. However on classifying the wounds as 'acute', 'chronic active' and 'chronic' based on the criteria delineated, there was clear trend of increasing percentage of 'chronic active' wounds when treated with a higher concentration of **Tβrl–CMP** (Figure

A.3.4.1). This indicates that at higher concentrations, **Tβrl–CMP** promotes the advancement of the inflammatory phase from the 'acute' to the 'chronic active' stage, with an influx of monocytes, macrophages and fibroblasts. This would lead to an earlier resolution of the inflammatory phase, overlapping with the initial proliferative phase of wound healing.

The wound size was measured as the largest separation between the wound edges 12 days post-treatment. On analysis, there was no observable difference in the size of the wounds subjected to varying concentrations of **Tβrl–CMP** (Figure A.3.4.2).

Figure A.3.4.1. Bar graph representing inflammatory reaction in the wounds in response to increasing concentrations of **Tβrl–CMP** in non-splinted 6 mm mouse wounds. Wounds were treated with 0.08, 0.4, 2, 10, and 50 mM solutions (25 μL) in 5% w/v PEG/saline. Data are from Day 12 post-treatment. Values are the median ± SE (n = 10). The number of 'chronic active' wounds was measured as a percentage of the total number of wounds receiving treatment [▲]. The inflammatory score for a wound treated with 20 mM **Tβrl–CMP** in a separate experiment is also indicated in the same graph [▲].

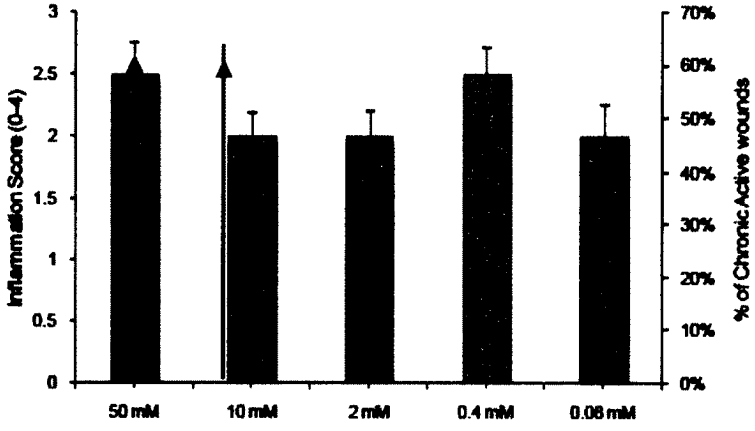

Figure A.3.4.2. Bar graph representing wound size in response to increasing concentrations of **Tβrl–CMP** in non-splinted 6 mm mouse wounds. Wounds were treated with 0.08, 0.4, 2, 10, and 50 mM solutions (25 μL) in 5% w/v PEG/saline. Data are from Day 12 post-treatment. Values are the mean ± SE (n = 10).

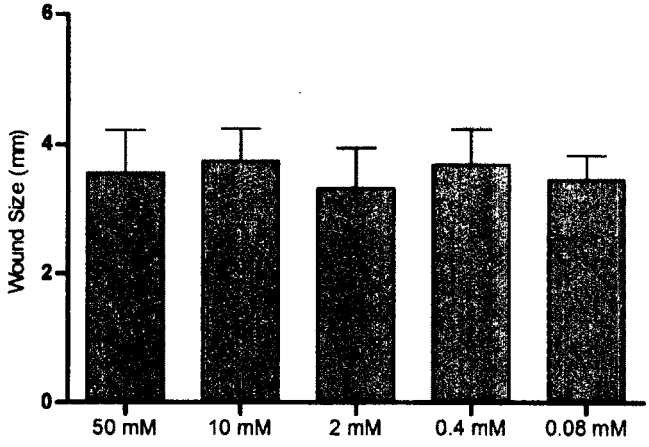

REFERENCES

Abe, R.; Donnelly, S. C.; Peng, T.; Bucala, R.; Metz, C. N. Peripheral Blood Fibrocytes: Differentiation Pathway and Migration to Wound Sites; *J. Immunol.* **2001**, *166*, 7556-7562.

Aimes, R. T.; Quigley, J. P. Matrix Metalloproteinase-2 Is an Interstitial Collagenase; *J. Biol. Chem.* **1995**, *270*, 5872-5876.

Allan, J. A.; Hembry, R. M.; Angal, S.; Reynolds, J. J.; Murphy, G. Binding of latent and high Mr active forms of stromelysin to collagen is mediated by the C-terminal domain; *J. Cell Sci.* **1991**, *99*, 789-795.

Allan, J. A.; Docherty, A. J.; Barker, P. J.; Huskisson, N. S.; Reynolds, J. J.; Murphy, G. Binding of gelatinases A and B to type-I collagen and other matrix components; *Biochem. J* **1995**, *309*, 299-306.

Altman, A. M.; Matthias, N.; Yan, Y.; Song, Y.-H.; Bai, X.; Chiu, E. S.; Slakey, D. P.; Alt, E. U. Dermal matrix as a carrier for in vivo delivery of human adipose-derived stem cells; *Biomaterials* **2008**, *29*, 1431-1442.

Ammann, A. J.; Beck, L. S.; DeGuzman, L. E. O.; Hirabayashi, S. E.; Pun Lee, W.; McFatridge, L.; Nguyen, T. U. E.; Xu, Y.; Mustoe, T. A. Transforming growth factor-β effect on soft tissue repair; *Ann. N. Y. Acad. Sci.* **1990**, *593*, 124-134.

Ananthanarayanan, V. S.; Orlicky, S. Interaction of substance P and its N- and C-terminal fragments with Ca^{2+}: Implications for hormone action; *Biopolymers* **1992**, *32*, 1765-1773.

Ashcroft, G. S.; Yang, X.; Glick, A. B.; Weinstein, M.; Letterio, J. J.; Mizel, D. E.; Anzano, M.; Greenwell-Wild, T.; Wahl, S. M.; Deng, C.; Roberts, A. B. Mice lacking Smad3 show accelerated wound healing and an impaired local inflammatory response; *Nat. Cell Biol.* **1999**, *1*, 260-266.

Ashcroft, G. S.; Roberts, A. B. Loss of Smad3 modulates wound healing; *Cyto. Gro. Fac. Rev.* **2000**, *11*, 125-131.

Assoian, R. K.; Komoriya, A.; Meyers, C. A.; Miller, D. M.; Sporn, M. B. Transforming growth factor-beta in human platelets. Identification of a major storage site, purification, and characterization; *J. Biol. Chem.* **1983**, *258*, 7155-7160.

Aszódi, A.; Legate, K. R.; Nakchbandi, I.; Fässler, R. What Mouse Mutants Teach Us About Extracellular Matrix Function; *Annu. Rev. Cell Dev. Biol.* **2006**, *22*, 591-621.

Badiavas, E. V.; Zhou, L.; Falanga, V. Growth inhibition of primary keratinocytes following transduction with a novel TGFβ-1 containing retrovirus; *J. Dermatol. Sci.* **2001**, *27*, 1-6.

Badylak, S. F. Xenogeneic extracellular matrix as a scaffold for tissue reconstruction; *Transpl. Immunol.* **2004**, *12*, 367-377.

Bar-Shavit, Z.; Goldman, R.; Stabinsky, Y.; Gottlieb, P.; Fridkin, M.; Teichberg, V. I.; Blumberg, S. Enhancement of phagocytosis — A newly found activity of Substance P residing in its N-terminal tetrapeptide sequence; *Biochem. Biophys. Res. Commun.* **1980**, *94*, 1445-1451.

Barnes, P. J.; Brown, M. J.; Dollery, C. T.; Fuller, R. W.; Heavey, D. J.; Ind, P. W. Histamine is released from skin by substance P but does not act as the final vasodilator in the axon reflex; *Br. J. Pharmacol.* **1986**, *88*, 741-745.

Baum, C. L.; Arpey, C. J. Normal cutaneous wound healing: clinical correlation with cellular and molecular events; *Dermatol. Surg.* **2005**, *31*, 674-686.

Bechetoille, N.; Dezutter-Dambuyant, C.; Damour, O.; André, V.; Orly, I.; Perrier, E. Effects of solar ultraviolet radiation on engineered human skin equivalent containing both Langerhans cells and dermal dendritic cells; *Tissue Eng.* **2007**, *13*, 2667-2679.

Beck, L. S.; DeGuzman, L.; Lee, W. P.; Xu, Y.; Siegel, M. W.; Amento, E. P. One systemic administration of transforming growth factor-beta 1 reverses age- or glucocorticoid-impaired wound healing; *J. Clin. Invest.* **1993**, *92*, 2841-2849.

Belfield, W. O.; Golinsky, S.; Compton, M. D. The use of insulin in open wound healing; *Vet. Med./ Small Animal Clinician* **1970**, *65*, 455-470.

Bella, J.; Brodsky, B.; Berman, H. M. Hydration structure of a collagen peptide; *Structure* **1995**, *3*, 893-906.

Berisio, R.; Granata, V.; Vitagliano, L.; Zagari, A. Imino acids and collagen triple helix stability: characterization of collagen-like polypeptides containing Hyp-Hyp-Gly sequence repeats; *J. Am. Chem. Soc.* **2004**, *126*, 11402-11403.

Boyce, S. Skin substitutes from cultured cells and collagen-GAG polymers; *Med. Biol. Eng. Comput.* **1998**, *36*, 791-800.

Boyce, S. T.; Christianson, D. J.; Hansbrough, J. F. Structure of a collagen-GAG dermal skin substitute optimized for cultured human epidermal keratinocytes; *J. Biomed. Mat. Res.* **1988**, *22*, 939-957.

Boyce, S. T.; Stompro, B. E.; Hansbrough, J. F. Biotinylation of implantable collagen for drug delivery; *J. Biomed. Mat. Res.* **1992**, *26*, 547-553.

Boyce, S. T.; Supp, A. P.; Warden, G. D.; Holder, I. A. Attachment of an aminoglycoside, amikacin, to implantable collagen for local delivery in wounds; *Antimicrob. Agents Chemotherapy* **1993**, *37*, 1890-1895.

Boyce, S. T.; Goretsky, M. J.; Greenhalgh, D. G.; Kagan, R. J.; Rieman, M. T.; Warden, G. D. Comparative assessment of cultured skin substitutes and native skin autograft for treatment of full-thickness burns; *Ann. Surg.* **1995**, *222*, 743-752.

Brem, H.; Tomic-Canic, M.; Entero, H.; Hanflik, A. M.; Wang, V. M.; Fallon, J. T.; Ehrlich, H. P. The synergism of age and db/db genotype impairs wound healing; *Exp. Gerontol.* **2007**, *42*, 523-531.

Bretscher, L. E.; Jenkins, C. L.; Taylor, K. M.; DeRider, M. L.; Raines, R. T. Conformational stability of collagen relies on a stereoelectronic effect; *J. Am. Chem. Soc.* **2001**, *123*, 777-778.

Broadley, K. N.; Aquino, A. M.; Hicks, B.; Ditesheim, J. A.; McGee, G. S.; Demetriou, A. A.; Woodward, S. C.; Davidson, J. M. The diabetic rat as an impaired wound healing model: stimulatory effects of transforming growth factor-beta and basic fibroblast growth factor; *Biotechnol. Ther.* **1989**, *1*, 55-68.

Brown, R. L.; Breeden, M. P.; Greenhalgh, D. G. PDGF and TGF-α Act Synergistically to improve wound healing in the genetically diabetic mouse; *J. Surg. Res.* **1994**, *56*, 562-570.

Buijtenhuijs, P.; Buttafoco, L.; Poot, A. A.; Daamen, W. F.; van Kuppevelt, T. H.; Dijkstra, P. J.; de Vos, R. A. I.; Sterk, L. M.; Geelkerken, B. R. H.; Feijen, J.; Vermes, I. Tissue engineering of blood vessels: characterization of smooth-muscle cells for culturing on collagen-and-elastin-based scaffolds; *Biotechnol. Appl. Biochem.* **2004**, *39*, 141-149.

Bury, R. W.; Mashford, M. L. Biological activity of carbon-terminal partial sequences of substance P; *J. Med. Chem.* **1976**, *19*, 854-856.

Buttow, N. C.; Zucoloto, S.; Espreafico, E. M.; Gama, P.; Alvares, E. P. Substance P enhances neuronal area and epithelial cell proliferation after colon denervation in rats; *Diges. Dis. Sci.* **2003**, *48*, 2069-2076.

Carlson, M. A.; Longaker, M. T. The fibroblast-populated collagen matrix as a model of wound healing: a review of the evidence; *Wound Rep. Regen.* **2004**, *12*, 134-147.

Carrier, P.; Deschambeault, A.; Talbot, M.; Giasson, C. J.; Auger, F. A.; Guérin, S. L.; Germain, L. Characterization of wound reepithelialization using a new human tissue-engineered corneal wound healing model; *Invest. Ophthalmol. Vis. Sci.* **2008**, *49*, 1376-1385.

Cascone, M. G.; Sim, B.; Sandra, D. Blends of synthetic and natural polymers as drug delivery systems for growth hormone; *Biomaterials* **1995**, *16*, 569-574.

Cass, D. L.; Sylvester, K. G.; Yang, E. Y.; Crombleholme, T. M.; Adzick, N. S. Myofibroblast persistence in fetal sheep wounds is associated with scar formation; *J. Pediatr. Surg.* **1997**, *32*, 1017-1022.

Cejas, M. A.; Chen, C.; Kinney, W. A.; Maryanoff, B. E. Nanoparticles that display short collagen-related peptides. Potent stimulation of human platelet aggregation by triple helical motifs; *Bioconjug. Chem.* **2007**, *18*, 1025-1027.

Chattopadhyay, S.; Murphy, C. J.; McAnulty, J. F.; Raines, R. T. Peptides that anneal to natural collagen *in vitro* and *ex vivo*; *Org. Biomol. Chem.* **2012**, *10*, xxx-xxx.

Chen, Y.-S.; Chen, C.-C.; Horng, J.-C. Thermodynamic and kinetic consequences of substituting glycine at different positions in a Pro-Hyp-Gly repeat collagen model peptide; *Peptide Sci.* **2011**, *96*, 60-68.

Chorghade, M. S.; Mohapatra, D. K.; Sahoo, G.; Gurjar, M. K.; Mandlecha, M. V.; Bhoite, N.; Moghe, S.; Raines, R. T. Practical syntheses of 4-fluoroprolines; *Journal of Fluorine Chemistry* **2008**, *129*, 781-784.

Chvapil, M.; Chvapil, T. A.; Owen, J. A. Reaction of various skin wounds in the rat to collagen sponge dressing; *J. Surg. Res.* **1986**, *41*, 410-418.

Coleman, D. Obese and diabetes: Two mutant genes causing diabetes-obesity syndromes in mice; *Diabetologia* **1978**, *14*, 141-148.

Cross, V. L.; Zheng, Y.; Won Choi, N.; Verbridge, S. S.; Sutermaster, B. A.; Bonassar, L. J.; Fischbach, C.; Stroock, A. D. Dense type I collagen matrices that support cellular remodeling and microfabrication for studies of tumor angiogenesis and vasculogenesis in vitro; *Biomaterials* **2010**, *31*, 8596-8607.

Davidson, J. M. Animal models for wound repair; *Arch. Dermatol. Res.* **1998**, *290*, (Suppl.): S1-S11.

Delgado, A. V.; McManus, A. T.; Chambers, J. P. Production of tumor necrosis factor-alpha, interleukin 1-beta, interleukin 2, and interleukin 6 by rat leukocyte subpopulations after exposure to Substance P; *Neuropeptides* **2003**, *37*, 355-361.

Delgado, A. V.; McManus, A. T.; Chambers, J. P. Exogenous administration of Substance P enhances wound healing in a novel skin-injury model; *Exp. Biol. Med.* **2005**, *230*, 271-280.

Demling, R. H.; DeSanti, L. R. N.; Orgill, D. P.; Structure, properties and evidence based clinical experience in burns; *www.burnsurgery.org*.

DeRider, M. L.; Wilkens, S. J.; Waddell, M. J.; Bretscher, L. E.; Weinhold, F.; Raines, R. T.; Markley, J. L. Collagen Stability: Insights from NMR spectroscopic and hybrid density functional computational investigations of the effect of electronegative substituents on prolyl ring conformations; *J. Am. Chem. Soc.* **2002**, *124*, 2497-2505.

Derynck, R.; Jarrett, J. A.; Chen, E. Y.; Eaton, D. H.; Bell, J. R.; Assoian, R. K.; Roberts, A. B.; Sporn, M. B.; Goeddel, D. V. Human transforming growth factor-[beta] complementary DNA sequence and expression in normal and transformed cells; *Nature* **1985**, *316*, 701-705.

Docherty, R.; Forrester, J. V.; Lackie, J. M.; Gregory, D. W. Glycosaminoglycans facilitate the movement of fibroblasts through three-dimensional collagen matrices; *J. Cell Sci.* **1989**, *92*, 263-270.

Doi, M.; Nishi, Y.; Uchiyama, S.; Nishiuchi, Y.; Nishio, H.; Nakazawa, T.; Ohkubo, T.; Kobayashi, Y. Collagen-like triple helix formation of synthetic (Pro-Pro-Gly)10 analogues: (4(S)-hydroxyprolyl-4(R)-hydroxyprolyl-Gly)10, (4(R)-hydroxyprolyl-4(R)-hydroxyprolyl-Gly)10 and (4(S)-fluoroprolyl-4(R)-fluoroprolyl-Gly)10; *J. of Pept. Sci.* **2005**, *11*, 609-616.

Doi, M. N., Y.; Uchlyama, S.; Nishluchi, Y.; Nakazawa, T.; Ohkubo, T.; Kobayashi, Y. Characterization of collagen model peptides containing 4-fluoroproline; (4(s)-fluoroproline-pro-gly)$_{10}$ forms a triple helix, but (4(r)-fluoroproline-pro-gly)$_{10}$ does not; *J. Am. Chem. Soc.* **2003**, *125*, 9922-9923.

Doillon, C. J.; Silver, F. H. Collagen-based wound dressing: Effects of hyaluronic acid and firponectin on wound healing; *Biomaterials* **1986**, *7*, 3-8.

Dunnick, C. A.; Gibran, N. S.; Heimbach, D. M. Substance P has a role in neurogenic mediation of human burn wound healing; *J. Burn Care Rehab.* **1996**, *17*, 390-396.

Edwards, D. R.; Murphy, G.; Reynolds, J. J.; Whitham, S. E.; Docherty, A. J.; Angel, P.; Heath, J. K. Transforming growth factor beta modulates the expression of collagenase and metalloproteinase inhibitor; *EMBO J.* **1987**, *6*, 1899-1904.

Ellis, D. L.; Yannas, I. V. Recent advances in tissue synthesis in vivo by use of collagen-glycosaminoglycan copolymers; *Biomaterials* **1996**, *17*, 291-299.

Engel, J.; Prockop, D. J. Does bound water contribute to the stability of collagen?; *Matrix Biol.* **1998**, *17*, 679-680.

Fallas, J. A.; O'Leary, L. E. R.; Hartgerink, J. D. Synthetic collagen mimics: self-assembly of homotrimers, heterotrimers and higher order structures; *Chem. Soc. Rev.* **2010**, *39*, 3510-3527.

Fiedler, L. R.; Schönherr, E.; Waddington, R.; Niland, S.; Seidler, D. G.; Aeschlimann, D.; Eble, J. A. Decorin regulates endothelial cell motility on collagen I through activation of insulin-like growth factor I receptor and modulation of α2β1 integrin activity; *J. Biol. Chem.* **2008**, *283*, 17406-17415.

Fielding, A. M. Preparation of neutral salt soluble collagen In: *The Methodology of Connective Tissue Research*; Hall, D. A., Ed.; Joynson-Bruvvers: Oxford, **1976**, 9-12.

Fields, G. B. A model for interstitial collagen catabolism by mammalian collagenases; *J. Theor. Biol.* **1991**, *153*, 585-602.

Fields, G. B. Synthesis and biological applications of collagen-model triple-helical peptides; *Organic & Biomolecular Chemistry* **2010**, *8*, 1237-1258.

Fonseca, J. M.; Alsina, A. M.; Francesca, R. Coating liposomes with collagen (M_r 50000) increases uptake into liver; *Biochim. Biophys. Acta - Biomembranes* **1996**, *1279*, 259-265.

Fujisato, T.; Sajiki, T.; Liu, Q.; Ikada, Y. Effect of basic fibroblast growth factor on cartilage regeneration in chondrocyte-seeded collagen sponge scaffold; *Biomaterials* **1996**, *17*, 155-162.

Gailit, J.; Welch, M. P.; Clark, R. A. F. TGF-[beta]1 Stimulates expression of keratinocyte integrins during re-epithelialization of cutaneous wounds; *J. Invest. Dermatol.* **1994**, *103*, 221-227.

Galiano, R. D.; Michaels, V. J.; Dobryansky, M.; Levine, J. P.; Gurtner, G. C. Quantitative and reproducible murine model of excisional wound healing; *Wound Rep. Regen.* **2004**, *12*, 485-492.

Geesin, J. C.; Brown, L. J.; Liu, Z.; Berg, R. A. Development of a skin model based on insoluble fibrillar collagen; *J. Biomed. Mat. Res.* **1996**, *33*, 1-8.

Gibran, N. S.; Boyce, S.; Greenhalgh, D. G. Cutaneous wound healing; *J. Burn Care Res.* **2007**, *28*, 577-579.

Gilbert, T. W.; Sellaro, T. L.; Badylak, S. F. Decellularization of tissues and organs; *Biomaterials* **2006**, *27*, 3675-3683.

Gorham, S. D.; Light, N. D.; Diamond, A. M.; Willins, M. J.; Bailey, A. J.; Wess, T. J.; Leslie, N. J. Effect of chemical modifications on the susceptibility of collagen to proteolysis. II. Dehydrothermal crosslinking; *Int. J. Biol. Macromol.* **1992**, *14*, 129-138.

Greenhalgh, D. G.; Sprugel, K. H.; Murray, M. J.; Ross, R. PDGF and FGF stimulate wound healing in the genetically diabetic mouse; *Am. J. Pathol.* **1990**, *136*, 1235-1246.

Greenhalgh, D. G.; Warden, G. D. Wound care models; *"Surgical research", London: Academic Press* **2001**, 379-391.

Greenhalgh, D. G. Wound healing and diabetes mellitus; *Clin. Plas. Surg.* **2003**, *30*, 37-45.

Greenway, S. E.; Filler, L. E.; Greenway, F. L. Topical insulin in wound healing: a randomised, double-blind, placebocontrolled trial; *J. Wound Care* **1999**, *8*, 526-528.

Griffith, M.; Jackson, W. B.; Lagali, N.; Merrett, K.; Li, F.; Fagerholm, P. Artificial corneas: a regenerative medicine approach; *Eye* **2009**, *23*, 1985-1989.

Groppe, J.; Hinck, C. S.; Samavarchi-Tehrani, P.; Zubieta, C.; Schuermann, J. P.; Taylor, A. B.; Schwarz, P. M.; Wrana, J. L.; Hinck, A. P. Cooperative assembly of TGF-beta superfamily signaling complexes is mediated by two disparate mechanisms and distinct modes of receptor binding; *Mol. Cell* **2008**, *29*, 157-168.

Gurtner, G. C.; Werner, S.; Barrandon, Y.; Longaker, M. T. Wound repair and regeneration; *Nature* **2008**, *453*, 314-321.

Harriger, M. D.; Supp, A. P.; Warden, G. D.; Boyce, S. T. Glutaraldehyde crosslinking of collagen substrates inhibits degradation in skin substitutes grafted to athymic mice; *J. Biomed. Mat. Res.* **1997**, *35*, 137-145.

Hart, P. J.; Deep, S.; Taylor, A. B.; Shu, Z.; Hinck, C. S.; Hinck, A. P. Crystal structure of the human TβR2 ectodomain-TGF-β3 complex; *Nat. Struct. Mol. Biol.* **2002**, *9*, 203-208.

Hartgerink, J. D.; Beniash, E.; Stupp, S. I. Self-Assembly and mineralization of peptide-amphiphile nanofibers; *Science* **2001**, *294*, 1684-1688.

Hartgerink, J. D.; Beniash, E.; Stupp, S. I. Peptide-amphiphile nanofibers: A versatile scaffold for the preparation of self-assembling materials; *Proc. Natl. Acad. Sci. U.S.A* **2002**, *99*, 5133-5138.

Hebda, P. A. Stimulatory effects of transforming growth factor-beta and epidermal growth factor on epidermal cell outgrowth from porcine skin explant cultures; *J. Invest. Dermatol.* **1988**, *91*, 440-445.

Hebda, P. A. The acceleration of epidermal wound healing in partial thickness burns by transforming growth factor-beta; *J. Invest. Dermatol. (Abstract of the ESDR-JSID-SID Tricontinental Meeting)* **1989**, *92*, 442.

Hennessy, K. M.; Pollot, B. E.; Clem, W. C.; Phipps, M. C.; Sawyer, A. A.; Culpepper, B. K.; Bellis, S. L. The effect of collagen I mimetic peptides on mesenchymal stem cell adhesion and differentiation, and on bone formation at hydroxyapatite surfaces; *Biomaterials* **2009**, *30*, 1898-1909.

Higashi, N.; Koga, T.; Niwa, M. Dendrimers with attached helical peptides; *Adv. Mat.* **2000**, *12*, 1373-1375.

Hodges, J. A.; Raines, R. T. Stereoelectronic effects on collagen stability: The dichotomy of 4-fluoroproline diastereomers; *J. Am. Chem. Soc.* **2003**, *125*, 9262-9263.

Hodges, J. A.; Raines, R. T. Stereoelectronic and steric effects in the collagen triple helix: Toward a code for strand association; *J. Am. Chem. Soc.* **2005**, *127*, 15923-15932.

Holmgren, S. K.; Taylor, K. M.; Bretscher, L. E.; Raines, R. T. Code for collagen's stability deciphered; *Nature* **1998**, *392*, 666-667.

Holmgren, S. K.; Bretscher, L. E.; Taylor, K. M.; Raines, R. T. A hyperstable collagen mimic; *Chem. Biol.* **1999**, *6*, 63-70.

Holzer, P. Local effector functions of capsaicin-sensitive sensory nerve endings: Involvement of tachykinins, calcitonin gene-related peptide and other neuropeptides; *Neuroscience* **1988**, *24*, 739-768.

Holzer, P. Neurogenic vasodilatation and plasma leakage in the skin; *Gen. Pharmacol.: Vas. Sys.* **1998**, *30*, 5-11.

Inoue, O.; Suzuki-Inoue, K.; Shinoda, D.; Umeda, Y.; Uchino, M.; Takasaki, S.-i.; Ozaki, Y. Novel synthetic collagen fibers, poly(PHG), stimulate platelet aggregation through glycoprotein VI; *FEBS Letters* **2009**, *583*, 81-87.

Inouye, K.; Sakakibara, S.; Prockop, D. J. Effects of the stereo-configuration of the hydroxyl group in 4-hydroxyproline on the triple-helical structures formed by homogeneous peptides resembling collagen; *Biochim. Biophys. Acta. Prot. Struc.* **1976**, *420*, 133-141.

Iwamoto, I.; Ueki, I. F.; Borson, D. B.; Nadel, J. A. Neutral endopeptidase modulates Tachykinin-induced increase in vascular permeability in Guinea pig skin; *Int. Arch. Allergy Immunol.* **1989**, *88*, 288-293.

Iwamoto, I.; Yamazaki, H.; Nakagawa, N.; Kimura, A.; Tomioka, H.; Yoshida, S. Differential effects of two C-terminal peptides of substance P on human neutrophils; *Neuropeptides* **1990**, *16*, 103-107.

Jenkins, C. L.; Raines, R. T. Insights on the conformational stability of collagen; *Nat. Prod. Rep.* **2002**, *19*, 49-59.

Jenkins, C. L.; Vasbinder, M. M.; Miller, S. J.; Raines, R. T. Peptide bond isosteres: Ester or (E)-alkene in the backbone of the collagen triple helix; *Org. Lett.* **2005**, *7*, 2619-2622.

Jeong, H.-W.; Kim, I.-S. TGF-β1 enhances βig-h3-mediated keratinocyte cell migration through the α3β1 integrin and PI3K; *J. Cell. Biochem.* **2004**, *92*, 770-780.

Johnson, G.; Jenkins, M.; McLean, K. M.; Griesser, H. J.; Kwak, J.; Goodman, M.; Steele, J. G. Peptoid-containing collagen mimetics with cell binding activity; *J. Biomed. Mat. Res.* **2000**, *51*, 612-624.

Joosten, E. A. J.; Bär, P. R.; Gispen, W. H. Collagen implants and cortico-spinal axonal growth after mid-thoracic spinal cord lesion in the adult rat; *J. Neurosci. Res.* **1995**, *41*, 481-490.

Kähler, C. M.; Herold, M.; Wiedermann, C. J. Substance P: A competence factor for human fibroblast proliferation that induces the release of growth-regulatory arachidonic acid metabolites; *J. Cell. Physiol.* **1993a**, *156*, 579-587.

Kähler, C. M.; Sitte, B. A.; Reinisch, N.; Wiedermann, C. J. Stimulation of the chemotactic migration of human fibroblasts by substance P; *Eur. J. Pharmacol.* **1993b**, *249*, 281-286.

Kähler, C. M.; Herold, M.; Reinisch, N.; Wiedermann, C. J. Interaction of substance P with epidermal growth factor and fibroblast growth factor in cyclooxygenase-dependent proliferation of human skin fibroblasts; *J. Cell. Physiol.* **1996**, *166*, 601-608.

Kämpfer, H.; Paulukat, J.; Mühl, K.; Wetzler, C.; Pfeilschifter, J.; Frank, S. Lack of interferon-γ production despite the presence of interleukin-18 during cutaneous wound healing; *Mol. Med.* **2000**, *6*, 1016-1027.

Kane, C. J. M.; Hebda, P. A.; Mansbridge, J. N.; Hanawalt, P. C. Direct evidence for spatial and temporal regulation of transforming growth factor β1 expression during cutaneous wound healing; *J. Cell. Physiol.* **1991**, *148*, 157-173.

Kasamatsu, H.; Robberson, D. L.; Vinograd, J. A novel closed-circular mitochondrial DNA with properties of a replicating intermediate; *Proc. Natl. Acad. Sci. U.S.A* **1971**, *68*, 2252-2257.

Khalil, Z.; Helme, R. Sensory peptides as neuromodulators of wound healing in aged rats; *J. Gerontol. Series A: Biol. Sci. Med. Sci.* **1996**, *51A*, B354-B361.

Khew, S. T.; Yang, Q. J.; Tong, Y. W. Enzymatically crosslinked collagen-mimetic dendrimers that promote integrin-targeted cell adhesion; *Biomaterials* **2008**, *29*, 3034-3045.

Kinberger, G. A.; Cai, W.; Goodman, M. Collagen mimetic dendrimers; *J. Am. Chem. Soc.* **2002**, *124*, 15162-15163.

Kinberger, G. A.; Taulane, J. P.; Goodman, M. The design, synthesis, and characterization of a PAMAM-based triple helical collagen mimetic dendrimer; *Tetrahedron* **2006**, *62*, 5280-5286.

Kisiday, J.; Jin, M.; Kurz, B.; Hung, H.; Semino, C.; Zhang, S.; Grodzinsky, A. J. Self-assembling peptide hydrogel fosters chondrocyte extracellular matrix production and cell division: Implications for cartilage tissue repair; *Proc. Natl. Acad. Sci. U.S.A* **2002**, *99*, 9996-10001.

Klug, W. S.; Cummings, M. R.; Shotwell, M.; Spencer, C. *Concepts of Genetics*; 5 ed.; Prentice Hall: N. J., **1997**.

Koide, M.; Osaki, K.; Konishi, J.; Oyamada, K.; Katakura, T.; Takahashi, A.; Yoshizato, K. A new type of biomaterial for artificial skin: Dehydrothermally cross-linked composites of fibrillar and denatured collagens; *J. Biomed. Mat. Res.* **1993**, *27*, 79-87.

Koide, T.; Homma, D. L.; Asada, S.; Kitagawa, K. Self-complementary peptides for the formation of collagen-like triple helical supramolecules; *Bioorg. Med. Chem. Lett.* **2005**, *15*, 5230-5233.

Koide, T. Designed triple-helical peptides as tools for collagen biochemistry and matrix engineering; *Philosoph. Trans. Royal Soc. B: Biol Sci.* **2007**, *362*, 1281-1291.

Kojima, C.; Tsumura, S.; Harada, A.; Kono, K. A Collagen-mimic dendrimer capable of controlled release; *J. Am. Chem. Soc.* **2009**, *131*, 6052-6053.

Kondo, S.; Niiyama, H.; Yu, A.; Kuroyanagi, Y. Evaluation of a wound dressing composed of Hyaluronic acid and collagen sponge containing epidermal growth factor in diabetic mice; *J. Biomat. Sci. Polymer Ed.* **2011 [Epub ahead of print; Sept 22]**.

Kotch, F. W.; Raines, R. T. Self-assembly of synthetic collagen triple helices; *Proc. Natl. Acad. Sci. U.S.A* **2006**, *103*, 3028-3033.

Kotch, F. W.; Guzei, I. A.; Raines, R. T. Stabilization of the collagen triple helix by O-methylation of hydroxyproline residues; *J. Am. Chem. Soc.* **2008**, *130*, 2952-2953.

Ksander, G. A.; Chu, G. H.; McMullin, H.; Ogawa, Y.; Pratt, B. M.; Rosenblatt, J. S.; McPherson, J. M. Transforming growth factors-β1 and β2 enhance connective tissue formation in animal models of dermal wound healing by secondary intent; *Ann. N. Y. Acad. Sci.* **1990**, *593*, 135-147.

Ksander, G. A.; Gerhardt, C. O.; Olsen, D. R. Exogenous transforming growth factor-β2 enhances connective tissue formation in transforming growth factor-β1—deficient, healing-impaired dermal wounds in mice; *Wound Rep. Regen.* **1993**, *1*, 137-148.

Lal, B. K.; Saito, S.; Pappas, P. J.; Padberg, F. T.; Cerveira, J. J.; Hobson, R. W.; Durán, W. N. Altered proliferative responses of dermal fibroblasts to TGF-β1 may contribute to chronic venous stasis ulcer1 1 Competition of interest: none; *J. Vasc. Surg.* **2003**, *37*, 1285-1293.

Lal, S.; Barrow, R. E.; Wolf, S. E.; Chinkes, D. L.; Hart, D. W.; Heggers, J. P.; Herndon, D. N. Biobrane$^{(R)}$ improves wound healing in burned children without increased risk of infection; *Shock* **2000**, *14*, 314-319.

Lam, P. K.; Chan, E. S. Y.; Liew, C. T.; Lau, C. H.; Yen, S. C.; King, W. W. K. The efficacy of collagen dermis membrane and fibrin on cultured epidermal graft using an athymic mouse model; *Ann. Plast. Surg.* **1999**, *43*, 523-528.

Langenhan, J. M.; Peters, N. R.; Guzei, I. A.; Hoffmann, F. M.; Thorson, J. S. Enhancing the anticancer properties of cardiac glycosides by neoglycorandomization; *Proc. Natl. Acad. Sci., U.S.A* **2005**, *102*, 12305-12310.

Laskin, D. L.; Soltys, R. A.; Berg, R. A.; Riley, D. J. Activation of neutrophils by factors released from alveolar macrophages stimulated with collagen-like polypeptides; *Am. J. Respir. Cell Mol. Biol.* **1990**, *2*, 463-470.

Laskin, D. L.; Soltys, R. A.; Berg, R. A.; Riley, D. J. Activation of alveolar macrophages by native and synthetic collagen-like polypeptides; *Am. J. Respir. Cell Mol. Biol.* **1994**, *10*, 58-64.

Lee, C. H.; Singla, A.; Lee, Y. Biomedical applications of collagen; *Int. J. Pharm.* **2001**, *221*, 1-22.

Lee, C. H.; Whiteman, A. L.; Murphy, C. J.; Barney, N. P.; Taylor, P. B.; Reid, T. W. Substance P, insulinlike growth factor 1, and surface healing; *Arch. Ophthalmol.* **2002**, *120*, 215-217.

Lee, H. J.; Lee, J.-S.; Chansakul, T.; Yu, C.; Elisseeff, J. H.; Yu, S. M. Collagen mimetic peptide-conjugated photopolymerizable PEG hydrogel; *Biomaterials* **2006**, *27*, 5268-5276.

Lee, H. J.; Yu, C.; Chansakul, T.; Hwang, N. S.; Varghese, S.; Yu, S. M.; Elisseeff, J. H. Enhanced chondrogenesis of mesenchymal stem cells in collagen mimetic peptide-mediated microenvironment; *Tissue Eng. Part A* **2008**, *14*, 1843-1851.

Lefebvre, F.; Gorecki, S.; Bareille, R.; Amedee, J.; Bordenave, L.; Rabaud, M. New artificial connective matrix-like structure made of elastin solubilized peptides and collagens: elaboration, biochemical and structural properties; *Biomaterials* **1992**, *13*, 28-33.

Leikina, E.; Mertts, M. V.; Kuznetsova, N.; Leikin, S. Type I collagen is thermally unstable at body temperature; *Proc. Natl. Acad. Sci., U.S.A* **2002**, *99*, 1314-1318.

Leipziger, L. S.; Glushko, V.; DiBernardo, B.; Shafaie, F.; Noble, J.; Nichols, J.; Alvarez, O. M. Dermal wound repair: role of collagen matrix implants and synthetic polymer dressings; *J Am Acad Dermatol* **1985**, *12*, 409-419.

Lepistö, J.; Kujari, H.; Niinikoski, J.; Laato, M. Effects of heterodimeric isoform of platelet-derived growth factor PDGF-AB on wound healing in the rat; *Eur. Surg. Res.* **1994**, *26*, 267-272.

Li, L.; Orner, B. P.; Huang, T.; Hinck, A. P.; Kiessling, L. L. Peptide ligands that use a novel binding site to target both TGF-[small beta] receptors; *Mol. BioSys.* **2010**, *6*, 2392-2402.

Li, L.; Klim, J. R.; Derda, R.; Courtney, A. H.; Kiessling, L. L. Spatial control of cell fate using synthetic surfaces to potentiate TGF-β signaling; *Proc. Natl. Acad. Sci. U.S.A.* **2011**, *108*, 11745-11750.

Liu, M.; Warn, J. D.; Fan, Q.; Smith, P. G.; Smith, R. L. Relationships between nerves and myofibroblasts during cutaneous wound healing in the developing rat; *Cell Tissue Res.* **1999**, *297*, 423-433.

Long, C. G.; Thomas, M.; Brodsky, B. Atypical Gly-X-Y sequences surround interruptions in the repeating tripeptide pattern of basement membrane collagen; *Biopolymers* **1995**, *35*, 621-628.

Lynch, S. E.; Colvin, R. B.; Antoniades, H. N. Growth factors in wound healing. Single and synergistic effects on partial thickness porcine skin wounds; *J. Clin. Invest.* **1989**, *84*, 640-646.

Madibally, S. V.; Solomon, V.; Mitchell, R. N.; Van De Water, L.; Yarmush, M. L.; Toner, M. Influence of insulin therapy on burn wound healing in rats; *J. Surg. Res.* **2003**, *109*, 92-100.

Maeda, M.; Tani, S.; Sano, A.; Fujioka, K. Microstructure and release characteristics of the minipellet, a collagen-based drug delivery system for controlled release of protein drugs; *J. Controlled Rel.* **1999**, *62*, 313-324.

Maeda, M.; Kadota, K.; Kajihara, M.; Sano, A.; Fujioka, K. Sustained release of human growth hormone (hGH) from collagen film and evaluation of effect on wound healing in db/db mice; *J. Controlled Rel.* **2001**, *77*, 261-272.

Malkar, N. B.; Lauer-Fields, J. L.; Borgia, J. A.; Fields, G. B. Modulation of triple-helical stability and subsequent melanoma cellular responses by single-site substitution of fluoroproline derivatives; *Biochemistry* **2002**, *41*, 6054-6064.

Mann, B. K.; Tsai, A. T.; Scott-Burden, T.; West, J. L. Modification of surfaces with cell adhesion peptides alters extracellular matrix deposition; *Biomaterials* **1999**, *20*, 2281-2286.

Mann, B. K.; Schmedlen, R. H.; West, J. L. Tethered-TGF-β increases extracellular matrix production of vascular smooth muscle cells; *Biomaterials* **2001**, *22*, 439-444.

Marchand, R.; Woerly, S.; Bertrand, L.; Valdes, N. Evaluation of two cross-linked collagen gels implanted in the transected spinal cord; *Brain Res. Bull.* **1993**, *30*, 415-422.

Marini, D. M.; Hwang, W.; Lauffenburger, D. A.; Zhang, S.; Kamm, R. D. Left-handed helical ribbon intermediates in the self-assembly of a β-sheet peptide; *Nano Lett.* **2002**, *2*, 295-299.

Marks, M. G.; Doillon, C.; Silvert, F. H. Effects of fibroblasts and basic fibroblast growth factor on facilitation of dermal wound healing by type I collagen matrices; *J. Biomed. Mat. Res.* **1991**, *25*, 683-696.

Martin, R.; Waldmann, L.; Kaplan, D. L. Supramolecular assembly of collagen triblock peptides; *Biopolymers* **2003**, *70*, 435-444.

Massagué, J. TGF-β signal transduction; *Ann. Rev. Biochem.* **1998**, *67*, 753-791.

McGovern, U. B.; Jones, K. T.; Shiarpe, G. R. Intracellular calcium as a second messenger following growth stimulation of human keratinocytes; *Br. J. Dermatol.* **1995**, *132*, 892-896.

McPherson, J. M.; Ledger, P. W.; Sawamura, S.; Conti, A.; Wade, S.; Reihanian, H.; Wallace, D. G. The preparation and physicochemical characterization of an injectable form of reconstituted, glutaraldehyde cross-linked, bovine corium collagen; *J. Biomed. Mat. Res.* **1986a**, *20*, 79-92.

McPherson, J. M.; Sawamura, S.; Armstrong, R. An examination of the biologic response to injectable, glutaraldehyde cross-linked collagen implants; *J. Biomed. Mat. Res.* **1986b**, *20*, 93-107.

Michaels, J.; Churgin, S. S.; Blechman, K. M.; Greives, M. R.; Aarabi, S.; Galiano, R. D.; Gurtner, G. C. db/db mice exhibit severe wound-healing impairments compared with other murine diabetic strains in a silicone-splinted excisional wound model; *Wound Rep. Regen.* **2007**, *15*, 665-670.

Miles, C. A.; Bailey, A. J. Thermally labile domains in the collagen molecule; *Micron* **2001**, *32*, 325-332.

Mo, X.; An, Y.; Yun, C.-S.; Yu, S. M. Nanoparticle-assisted visualization of binding interactions between collagen mimetic peptide and collagen fibers; *Angew. Chem. Int. Ed.* **2006**, *45*, 2267-2270.

Mustoe, T.; Pierce, G.; Thomason, A.; Gramates, P.; Sporn, M.; Deuel, T. Accelerated healing of incisional wounds in rats induced by transforming growth factor-beta; *Science* **1987**, *237*, 1333-1336.

Nakamura, M.; Ofuji, K.; Chikama, T.-i.; Nishida, T. Combined effects of substance P and insulin-like growth factor-1 on corneal epithelial wound closure of rabbit in vivo; *Curr. Eye Res.* **1997**, *16*, 275-278.

Nambu, M.; Ishihara, M.; Kishimoto, S.; Yanagibayashi, S.; Yamamoto, N.; Azuma, R.; Kanatani, Y.; Kiyosawa, T.; Mizuno, H. Stimulatory effect of autologous adipose tissue-derived stromal cells in an atelocollagen matrix on wound healing in diabetic db/db mice; *J. Tissue Eng.* **2011**.

Nielsen, P. E. Peptide nucleic acid. A molecule with two identities; *Acc. Chem. Res.* **1999**, *32*, 624-630.

Nilsson, J.; von Euler, A. M.; Dalsgaard, C.-J. Stimulation of connective tissue cell growth by substance P and substance K; *Nature* **1985**, *315*, 61-63.

Nishi, Y.; Uchiyama, S.; Doi, M.; Nishiuchi, Y.; Nakazawa, T.; Ohkubo, T.; Kobayashi, Y. Different Effects of 4-Hydroxyproline and 4-Fluoroproline on the stability of collagen triple helix; *Biochemistry* **2005**, *44*, 6034-6042.

Nishida, T.; Nakamura, M.; Ofuji, K.; Reid, T. W.; Mannis, M. J.; Murphy, C. J. Synergistic effects of substance P with insulin-like growth factor-1 on epithelial migration of the cornea; *J. Cell. Physiol.* **1996**, *169*, 159-166.

Norido, F.; Canella, R.; Zanoni, R.; Gorio, A. Development of diabetic neuropathy in the C57BL/Ks (db/db) mouse and its treatment with gangliosides; *Exp. Neurol.* **1984**, *83*, 221-232.

Ohuchi, E.; Imai, K.; Fujii, Y.; Sato, H.; Seiki, M.; Okada, Y. Membrane type 1 matrix metalloproteinase digests interstitial collagens and other extracellular matrix macromolecules; *J. Biol. Chem.* **1997**, *272*, 2446-2451.

Olsen, D.; Yang, C.; Bodo, M.; Chang, R.; Leigh, S.; Baez, J.; Carmichael, D.; Perälä, M.; Hämäläinen, E.-R.; Jarvinen, M.; Polarek, J. Recombinant collagen and gelatin for drug delivery; *Adv. Drug Deliv. Rev.* **2003**, *55*, 1547-1567.

Orwin, E. J.; Hubel, A. In vitro culture characteristics of corneal epithelial, endothelial, and keratocyte cells in a native collagen matrix *Tissue Eng.* **2000**, *6*, 304-319.

Paíno, C. L.; Fernandez-Valle, C.; Bates, M. L.; Bunge, M. B. Regrowth of axons in lesioned adult rat spinal cord: promotion by implants of cultured Schwann cells; *J. Neurocytol.* **1994**, *23*, 433-452.

Pajean, M.; Herbage, D. Effect of collagen on liposome permeability; *Int. J. Pharmaceut.* **1993**, *91*, 209-216.

Pandit, A.; Ashar, A.; Feldman, D. The effect of TGF-beta delivered through a collagen scaffold on wound healing; *J. Invest. Surg.* **1999**, *12*, 89-100.

Paramonov, S. E.; Gauba, V.; Hartgerink, J. D. Synthesis of collagen-like peptide polymers by native chemical ligation; *Macromolecules* **2005**, *38*, 7555-7561.

Parenti, A.; Amerini, S.; Ledda, F.; Maggi, C. A.; Ziche, M. The tachykinin NK1 receptor mediates the migration-promoting effect of substance P on human skin fibroblasts in culture; *Naunyn-Schmiedeberg's Arch. Pharmacol.* **1996**, *353*, 475-481.

Park, J.-C.; Hwang, Y.-S.; Lee, J.-E.; Park, K. D.; Matsumura, K.; Hyon, S.-H.; Suh, H. Type I atelocollagen grafting onto ozone-treated polyurethane films: Cell attachment, proliferation, and collagen synthesis; *J. Biomed. Mat. Res.* **2000**, *52*, 669-677.

Parkhurst, M. R.; Saltzman, W. M. Quantification of human neutrophil motility in three-dimensional collagen gels. Effect of collagen concentration; *Biophys. J.* **1992**, *61*, 306-315.

Parkhurst, M. R.; Saltzman, W. M. Leukocytes migrate through three-dimensional gels of midcycle cervical mucus; *Cell. Immunol.* **1994**, *156*, 77-94.

Paterlini, M. G.; Nemethy, G.; Scheraga, H. A. The energy of formation of internal loops in triple helical collagen polypeptides; *Biopolymers* **1995**, *35*, 607-619.

Payan, D.; Brewster, D.; Goetzl, E. Stereospecific receptors for substance P on cultured human IM-9 lymphoblasts; *J. Immunol.* **1984**, *133*, 3260-3265.

Peters, W. J. Biological dressings in burns-A review; *Ann. Plast. Surg.* **1980**, *4*, 133-137.

Petite, H.; Rault, I.; Huc, A.; Menasche, P.; Herbage, D. Use of the acyl azide method for cross-linking collagen-rich tissues such as pericardium; *J. Biomed. Mat. Res.* **1990**, *24*, 179-187.

Piez, K. A. Molecular and aggregate structures of the collagens In: *Extracellular Matrix Biochemistry*; Piez, K. A., Reddi, A. H., (Eds.); Elsevier: New York, **1984**, 1-40.

Piez, K. A. Collagen In: *Encyclopedia of polymer science and engineering*; Wiley: New York, **1985**, 699-727.

Pinkas, D. M.; Ding, S.; Raines, R. T.; Barron, A. E. Tunable; Post-translational Hydroxylation of Collagen Domains in Escherichia coli; *ACS Chem. Bio.* **2011**, *6*, 320-324.

Ponticiello, M. S.; Schinagl, R. M.; Kadiyala, S.; Barry, F. P. Gelatin-based resorbable sponge as a carrier matrix for human mesenchymal stem cells in cartilage regeneration therapy; *J. Biomed. Mat. Res.* **2000**, *52*, 246-255.

Pontrello, J. K.; Allen, M. J.; Underbakke, E. S.; Kiessling, L. L. Solid-phase synthesis of polymers using the ring-opening metathesis polymerization; *J. Am. Chem. Soc.* **2005**, *127*, 14536-14537.

Postlethwaite, A. E.; Seyer, J. M.; Kang, A. H. Chemotactic attraction of human fibroblasts to type I, II, and III collagens and collagen-derived peptides; *Proc. Natl. Acad. Sci. U.S.A* **1978**, *75*, 871-875.

Postlethwaite, A. E.; Keski-Oja, J.; Moses, H. L.; Kang, A. H. Stimulation of the chemotactic migration of human fibroblasts by transforming growth factor beta; *J. Exp. Med.* **1987**, *165*, 251-256.

Powell, H. M.; Boyce, S. T. EDC cross-linking improves skin substitute strength and stability; *Biomaterials* **2006**, *27*, 5821-5827.

Powell, H. M.; Boyce, S. T. Wound closure with EDC cross-linked cultured skin substitutes grafted to athymic mice; *Biomaterials* **2007**, *28*, 1084-1092.

Przybyla, D. E.; Chmielewski, J. Higher-order assembly of collagen peptides into nano- and microscale materials; *Biochemistry* **2010**, *49*, 4411-4419.

Ramos, C.; Montano, M.; Cisneros, J.; Sommer, B.; Delgado, J.; Gonzalez-Avila, G. Substance P up-regulates matrix metalloproteinase-1 and down-regulates collagen in human lung fibroblast; *Exp. Lung Res.* **2007**, *33*, 151-167.

Ramshaw, J. A. M.; Shah, N. K.; Brodsky, B. Gly-X-Y tripeptide frequencies in collagen: A context for host–guest triple-helical peptides; *J. Struct. Biol.* **1998**, *122*, 86-91.

Rao, K. P. Recent developments of collagen-based materials for medical applications and drug delivery systems *J. Biomater. Sci.* **1996**, *7*, 623-645.

Régnier, M.; Staquet, M.-J.; Schmitt, D.; Schimdt, R. Integration of Langerhans cells into a pigmented reconstructed human epidermis; *J. Invest. Dermatol.* **1997**, *109*, 510-512.

Reid, T. W.; Murphy, C. J.; Iwahashi, C. K.; Foster, B. A.; Mannis, M. J. Stimulation of epithelial cell growth by the neuropeptide substance P; *J. Cell. Biochem.* **1993**, *52*, 476-485.

Renner, C.; Alefelder, S.; Bae, J. H.; Budisa, N.; Huber, R.; Moroder, L. Fluoroprolines as tools for protein design and engineering; *Angew. Chem. Int. Ed.* **2001**, *40*, 923-925.

Roberts, A. B.; Sporn, M. B.; Assoian, R. K.; Smith, J. M.; Roche, N. S.; Wakefield, L. M.; Heine, U. I.; Liotta, L. A.; Falanga, V.; Kehrl, J. H. Transforming growth factor type beta: rapid induction of fibrosis and angiogenesis in vivo and stimulation of collagen formation in vitro; *Proc. Natl. Acad. Sci. U.S.A.* **1986**, *83*, 4167-4171.

Roberts, A. B. Transforming growth factor-β: activity and efficacy in animal models of wound healing; *Wound Rep. Regen.* **1995**, *3*, 408-418.

Roberts, A. B.; Piek, E.; Böttinger, E. P.; Ashcroft, G.; Mitchell, J. B.; Flanders, K. C. Is Smad3 a major player in signal transduction pathways leading to fibrogenesis?; *Chest* **2001**, *120*, S43-S47.

Roberts, C. J.; Birkenmeier, T. M.; McQuillan, J. J.; Akiyama, S. K.; Yamada, S. S.; Chen, W. T.; Yamada, K. M.; McDonald, J. A. Transforming growth factor beta stimulates the expression of fibronectin and of both subunits of the human fibronectin receptor by cultured human lung fibroblasts; *J. Biol. Chem.* **1988**, *263*, 4586-4592.

Rosell, S.; Bjorkroth, U.; Chang, D.; Yamaguchi, I.; Wan, Y.-P.; Rackur, G.; Fisher, G.; Folkers, K.; *"Substance P" (edited by von Euler, U. S.; Pernow, B.), Raven Press, N.Y* **1977**, 83-88.

Rosenblatt, J.; Rhee, W.; Wallace, D. The effect of collagen fiber size distribution on the release rate of proteins from collagen matrices by diffusion; *J. Controlled Rel.* **1989**, *9*, 195-203.

Rosenthal, F. M.; Kohler, G. Collagen as matrix for neo-organ formation by gene-transfected fibroblasts; *Anticancer Res.* **1997**, *17*, 1179-1186.

Rubin, A. L.; Stenzel, K. H.; Miyata, T.; White, M. J.; Dunn, M. Collagen as a vehicle for drug delivery; *J. Clin. Pharmacol.* **1973**, *13*, 309-312.

Ruderman, R. J.; Wade, C. W. R.; Shepard, W. D.; Leonard, F. Prolonged resorption of collagen sponges: Vapor-phase treatment with formaldehyde; *J. Biomed. Mat. Res.* **1973**, *7*, 263-265.

Ruff, M. R.; Wahl, S. M.; Pert, C. B. Substance P receptor-mediated chemotaxis of human monocytes; *Peptides* **1985**, *6*, 107-111.

Saltzman, W. M.; Parkhurst, M. R.; Parsons-Wingerter, P.; Zhu, W. H. Three-dimensional cell cultures mimic tissues; *Ann. N. Y. Acad. Sci.* **1992**, *665*, 259-273.

Samuel, C.; Coghlan, J.; Bateman, J. Effects of relaxin, pregnancy and parturition on collagen metabolism in the rat pubic symphysis; *J. Endocrinol.* **1998**, *159*, 117-125.

Schiller, M.; Javelaud, D.; Mauviel, A. TGF-β-induced SMAD signaling and gene regulation: consequences for extracellular matrix remodeling and wound healing; *J. Dermatol. Sci.* **2004**, *35*, 83-92.

Schmid, P.; Itin, P.; Cherry, G.; Bi, C.; Cox, D. A. Enhanced expression of transforming growth factor-beta type I and type II receptors in wound granulation tissue and hypertrophic scar; *Am. J. Pathol.* **1998**, *152*, 485-493.

Schultz, G. S.; Wysocki, A. Interactions between extracellular matrix and growth factors in wound healing; *Wound Rep. Reg.* **2009**, *17*, 153-162.

Scott, J. R.; Tamura, R. N.; Muangman, P.; Isik, F. F.; Xie, C.; Gibran, N. S. Topical substance P increases inflammatory cell density in genetically diabetic murine wounds; *Wound Rep. Regen.* **2008**, *16*, 529-533.

Seegers, H. C.; Hood, V. C.; Kidd, B. L.; Cruwys, S. C.; Walsh, D. A. Enhancement of angiogenesis by endogenous Substance P release and Neurokinin-1 receptors during neurogenic inflammation; *J. Pharmacol. Exp. Ther.* **2003**, *306*, 8-12.

Shoulders, M. D.; Guzei, I. A.; Raines, R. T. 4-Chloroprolines: Synthesis, conformational analysis, and effect on the collagen triple helix; *Biopolymers* **2008**, *89*, 443-454.

Shoulders, M. D.; Kamer, K. J.; Raines, R. T. Origin of the stability conferred upon collagen by fluorination; *Bioorg. & Med. Chem. Lett.* **2009a**, *19*, 3859-3862.

Shoulders, M. D.; Raines, R. T. Collagen structure and stability; *Ann. Rev. Biochem.* **2009b**, *78*, 929-958.

Shoulders, M. D.; Satyshur, K. A.; Forest, K. T.; Raines, R. T. Stereoelectronic and steric effects in side chains preorganize a protein main chain; *Proc. Natl. Acad. Sci. U.S.A* **2010**, *107*, 559-564.

Singer, A. J.; Clark, R. A. F. Cutaneous wound healing; *N. Engl. J. Med.* **1999**, *341*, 738-746.

Slavin, J.; Nash, J. R.; Kingsnorth, A. N. Effect of transforming growth factor beta and basic fibroblast growth factor on steroid-impaired healing intestinal wounds; *Br. J. Surg.* **1992**, *79*, 69-72.

Slevin, M.; Krupinski, J.; Slowik, A.; Kumar, P.; Szczudlik, A.; Gaffney, J. Serial measurement of vascular endothelial growth factor and transforming growth factor-ß1 in serum of patients with acute ischemic stroke; *Stroke* **2000**, *31*, 1863-1870.

Smethurst, P. A.; Onley, D. J.; Jarvis, G. E.; O'Connor, M. N.; Knight, C. G.; Herr, A. B.; Ouwehand, W. H.; Farndale, R. W. Structural basis for the platelet-collagen interaction; *J. Biol. Chem.* **2007**, *282*, 1296-1304.

Smith, D. J. J. Use of biobrane in wound management; *J. Burn Care Res.* **1995**, *16*, 317-320.

Smith, P.; Liu, M. Impaired cutaneous wound healing after sensory denervation in developing rats: effects on cell proliferation and apoptosis; *Cell Tissue Res.* **2002**, *307*, 281-291.

Söderhäll, C.; Marenholz, I.; Kerscher, T.; Rüschendorf, F.; Esparza-Gordillo, J.; Worm, M.; Gruber, C.; Mayr, G.; Albrecht, M.; Rohde, K.; Schulz, H.; Wahn, U.; Hubner, N.; Lee, Y.-A. Variants in a novel epidermal collagen gene (COL29A1) are associated with atopic dermatitis; *PLoS Biol.* **2007**, *5*, 1952-1961.

Song, S.-Z.; Morawiecki, A.; Pierce, G. F.; Pitt, C. G.; Collagen film for sustained delivery of proteins; **1992**, Eur. Patent 92305467.3.

Speer, D. P.; Chvapil, M.; Eskelson, C. D.; Ulreich, J. Biological effects of residual glutaraldehyde in glutaraldehyde-tanned collagen biomaterials; *J. Biomed. Mat. Res.* **1980**, *14*, 753-764.

Sporn, M. B.; Roberts, A. B.; Shull, J. H.; Smith, J. M.; Ward, J. M.; Sodek, J. Polypeptide transforming growth factors isolated from bovine sources and used for wound healing in vivo; *Science* **1983**, *219*, 1329-1331.

Stemberger, A.; Grimm, H.; Bader, F.; Rahn, H. D.; Ascherl, R. Local treatment of bone and soft tissue infections with the collagen gentamicin sponge; *Eur. J. Surg.* **1997**, *578*, 17–26.

Stompro, B. E.; Hansbrough, J. F.; Boyce, S. T. Attachment of peptide growth factors to implantable collagen; *J. Surg. Res.* **1989**, *46*, 413-421.

Sung, K. E.; Su, G.; Pehlke, C.; Trier, S. M.; Eliceiri, K. W.; Keely, P. J.; Friedl, A.; Beebe, D. J. Control of 3-dimensional collagen matrix polymerization for reproducible human mammary fibroblast cell culture in microfluidic devices; *Biomaterials* **2009**, *30*, 4833-4841.

Supp, A. P.; Wickett, R. R.; Swope, V. B.; Harriger, M. D.; Hoath, S. B.; Boyce, S. T. Incubation of cultured skin substitutes in reduced humidity promotes cornification in vitro and stable engraftment in athymic mice; *Wound Rep. Regen.* **1999**, *7*, 226-237.

Suzuki, S.; Kawai, K.; Ashoori, F.; Morimoto, N.; Nishimura, Y.; Ikada, Y. Long-term follow-up study of artificial dermis composed of outer silicone layerand inner collagen sponge; *Br. J. Plast. Surg.* **2000**, *53*, 659-666.

Tanaka, T.; Danno, K.; Ikai, K.; Imamura, S. Effects of Substance P and Substance K on the growth of cultured keratinocytes; *J. Invest. Dermatol.* **1988**, *90*, 399-401.

Tiller, J. C.; Bonner, G.; Pan, L.-C.; Klibanov, A. M. Improving biomaterial properties of collagen films by chemical modification; *Biotechnol. Bioeng.* **2001**, *73*, 246-252.

Timpl, R. Immunology of the Collagens In: *Extracellular Matrix Biochemistry*; Piez, K. A., Reddi, A. H., (Eds.); Elsevier: New York, **1984**, 159-190.

Toolan, B. C.; Frenkel, S. R.; Pachence, J. M.; Yalowitz, L.; Alexander, H. Effects of growth-factor-enhanced culture on a chondrocyte-collagen implant for cartilage repair; *J. Biomed. Mat. Res.* **1996**, *31*, 273-280.

Tredget, E. B.; Demare, J.; Chandran, G.; Tredget, E. E.; Yang, L.; Ghahary, A. Transforming growth factor-β and its effect on reepithelialization of partial-thickness ear wounds in transgenic mice; *Wound Rep. Regen.* **2005**, *13*, 61-67.

Trottier, V.; Marceau-Fortier, G.; Germain, L.; Vincent, C.; Fradette, J. Using human adipose-derived stem/stromal cells for the production of new skin substitutes; *Stem Cells* **2008**, *26*, 2713-2723.

Tsunawaki, S.; Sporn, M.; Ding, A.; Nathan, C. Deactivation of macrophages by transforming growth factor-[beta]; *Nature* **1988**, *334*, 260-262.

Tu, R.; Lu, C. L.; Thyagarajan, K.; Wang, E.; Nguyen, H.; Shen, S.; Hata, C.; Quijano, R. C. Kinetic study of collagen fixation with polyepoxy fixatives; *J. Biomed. Mat. Res.* **1993**, *27*, 3-9.

Uchio, Y.; Ochi, M.; Matsusaki, M.; Kurioka, H.; Katsube, K. Human chondrocyte proliferation and matrix synthesis cultured in Atelocollagen® gel; *J. Biomed. Mat. Res.* **2000**, *50*, 138-143.

Underwood, R. A.; Gibran, N. S.; Muffley, L. A.; Usui, M. L.; Olerud, J. E. Color Subtractive–Computer-assisted image analysis for quantification of cutaneous nerves in a diabetic mouse model; *J. Histochem. Cytochem.* **2001**, *49*, 1285-1291.

Van ,der Laan, J. S.; Lopez, G. P.; van Wachem, P. B.; Nieuwenhuis, P.; Ratner, B. D.; Bleichrodt, R. P.; Schakenraad, J. M. Tee-plasma polymerized dermal sheep collagen for the repair of abdominal wall defects; *Int. J. Artif. Organs* **1991**, *14*, 661–666.

van Luyn, M. J. A.; van Wachem, P. B.; Damink, L. H. H. O.; Dijkstra, P. J.; Feijen, J.; Nieuwenhuis, P. Secondary cytotoxicity of cross-linked dermal sheep collagens during repeated exposure to human fibroblasts; *Biomaterials* **1992**, *13*, 1017-1024.

van Wachem, P. B.; van Luyn, M. J. A.; Ponte da Costa, M. L. Myoblast seeding in a collagen matrix evaluated in vitro; *J. Biomed. Mat. Res.* **1996**, *30*, 353-360.

Vaneerdeweg, W.; Bresseleers, T.; Du Jardin, P.; Lauwers, P.; Pauli, S.; Thyssens, K.; Van Marck, E.; Elseviers, M.; Eyskens, E. Comparison between plain and gentamicin containing collagen sponges in infected peritoneal cavity in rats; *Eur. J. Surg.* **1998**, *164*, 617-621.

Vitagliano, L.; Berisio, R.; Mazzarella, L.; Zagari, A. Structural bases of collagen stabilization induced by proline hydroxylation; *Biopolymers* **2001**, *58*, 459-464.

Wachol-Drewek, Z.; Pfeiffer, M.; Scholl, E. Comparative investigation of drug delivery of collagen implants saturated in antibiotic solutions and a sponge containing gentamicin; *Biomaterials* **1996**, *17*, 1733-1738.

Wahl, S. M.; Hunt, D. A.; Wakefield, L. M.; McCartney-Francis, N.; Wahl, L. M.; Roberts, A. B.; Sporn, M. B. Transforming growth factor type beta induces monocyte chemotaxis and growth factor production; *Proc. Natl. Acad. Sci. U.S.A.* **1987**, *84*, 5788-5792.

Wallace, D. G.; Rhee, W.; Reihanian, H.; Ksander, G.; Lee, R.; Braun, W. B.; Weiss, B. A.; Pharriss, B. B. Injectable cross-linked collagen with improved flow properties; *J. Biomed. Mat. Res.* **1989**, *23*, 931-945.

Wang, A. Y.; Mo, X.; Chen, C. S.; Yu, S. M. Facile modification of collagen directed by collagen mimetic peptides; *J. Am. Chem. Soc.* **2005**, *127*, 4130-4131.

Wang, A. Y.; Foss, C. A.; Leong, S.; Mo, X.; Pomper, M. G.; Yu, S. M. Spatio-temporal modification of collagen scaffolds mediated by triple helical propensity; *Biomacromolecules* **2008a**, *9*, 1755-1763.

Wang, A. Y.; Leong, S.; Liang, Y.-C.; Huang, R. C. C.; Chen, C. S.; Yu, S. M. Immobilization of growth factors on collagen scaffolds mediated by polyanionic collagen mimetic peptides and its effect on endothelial cell morphogenesis; *Biomacromolecules* **2008b**, *9*, 2929-2936.

Wang, M.-Y.; Grayburn, P.; Chen, S.; Ravazzola, M.; Orci, L.; Unger, R. H. Adipogenic capacity and the susceptibility to type 2 diabetes and metabolic syndrome; *Proc. Natl. Acad. Sci. U.S.A.* **2008c**, *105*, 6139-6144.

Wang, X.-J.; Han, G.; Owens, P.; Siddiqui, Y.; Li, A. G. Role of TGF[beta]-mediated inflammation in cutaneous wound healing; *J. Invest. Dermatol. Symp. Proc.* **2006**, *11*, 112-117.

Weadock, K. S.; Miller, E. J.; Bellincampi, L. D.; Zawadsky, J. P.; Dunn, M. G. Physical crosslinking of collagen fibers: Comparison of ultraviolet irradiation and dehydrothermal treatment; *J. Biomed. Mat. Res.* **1995**, *29*, 1373-1379.

Weadock, K. S.; Miller, E. J.; Keuffel, E. L.; Dunn, M. G. Effect of physical crosslinking methods on collagen-fiber durability in proteolytic solutions; *J. Biomed. Mat. Res.* **1996**, *32*, 221-226.

Weidner, C.; Klede, M.; Rukwied, R.; Lischetzki, G.; Neisius, U.; Skov, P. S.; Petersen, L. J.; Schmelz, M. Acute effects of Substance P and calcitonin gene-related peptide in human skin - A microdialysis study; *J. Invest. Dermatol.* **2000**, *115*, 1015-1020.

Weiner, A. L.; Carpenter-Green, S. S.; Soehngen, E. C.; Lenk, R. P.; Popescu, M. C. Liposome–collagen gel matrix: A novel sustained drug delivery system; *J. Pharma. Sci.* **1985**, *74*, 922-925.

Weringer, E. J.; Kelso, J. M.; Tamai, I. Y.; Arquilla, E. R. Effects of insulin on wound healing in diabetic mice; *Acta Endocrinol.* **1982**, *99*, 101-108.

Werner, S.; Breeden, M.; Hubner, G.; Greenhalgh, D. G.; Longaker, M. T. Induction of keratinocyte growth factor expression is reduced and delayed during wound healing in the genetically diabetic mouse; *J. Invest. Dermatol.* **1994**, *103*, 469-473.

Whitaker, K.; Barrow, P.; Feree, K. A case study using chronicure to treat a stage IV chronic wound; *Ostomy Wound Manage.* **1992**, *38*, 36-44.

Wiedermann, C. J.; Wiedermann, F. J.; Apperl, A.; Kieselbach, G.; Konwalinka, G.; Braunsteiner, H. In vitro human polymorphonuclear leukocyte chemokinesis and human monocyte chemotaxis are different activities of aminoterminal and carboxyterminal substance P; *Naunyn-Schmiedeberg's Arch. Pharmacol.* **1989**, *340*, 185-190.

Wiedermann, F. J.; Kähler, C. M.; Reinisch, N.; Wiedermann, C. J. Induction of normal human eosinophil migration in vitro by Substance P; *Acta Haematol.* **1993**, *89*, 213-215.

Woolfson, D. N. Building fibrous biomaterials from α-helical and collagen-like coiled-coil peptides; *Peptide Sci.* **2010**, *94*, 118-127.

Wrana, J. L.; Attisano, L.; Cárcamo, J.; Zentella, A.; Doody, J.; Laiho, M.; Wang, X.-F.; Massague, J. TGF-beta signals through a heteromeric protein kinase receptor complex; *Cell* **1992**, *71*, 1003-1014.

Wu, X.; Black, L.; Santacana-Laffitte, G.; Patrick, C. W. Preparation and assessment of glutaraldehyde-crosslinked collagen–chitosan hydrogels for adipose tissue engineering; *J. Biomed. Mat. Res. Part A* **2007**, *81A*, 59-65.

Yamada, N.; Yanai, R.; Nakamura, M.; Inui, M.; Nishida, T. Role of the C Domain of IGFs in Synergistic promotion, with a Substance P–derived peptide, of rabbit corneal epithelial wound healing; *Invest. Ophthalmol. Vis. Sci.* **2004**, *45*, 1125-1131.

Yanaihara, N.; Yanaihara, C.; Hirohashi, M.; Sato, H.; Lizuka, Y.; Hashimoto, T.; Sakagami, M.; *"Substance P" (edited by von Euler. U. S.; Pernow. B.), Raven Press, N.Y* **1977**, 27-33.

Yannas, I.; Burke, J.; Orgill, D.; Skrabut, E. Wound tissue can utilize a polymeric template to synthesize a functional extension of skin; *Science* **1982**, *215*, 174-176.

Yannas, I. V.; Lee, E.; Orgill, D. P.; Skrabut, E. M.; Murphy, G. F. Synthesis and characterization of a model extracellular matrix that induces partial regeneration of adult mammalian skin; *Proc. Natl. Acad. Sci. U.S.A* **1989**, *86*, 933-937.

Yannas, I. V. Biologically active analogues of the extracellular matrix: artificial skin and nerves; *Angew. Chem. Int. Ed.* **1990**, *29*, 20-35.

Zeugolis, D. I.; Paul, G. R.; Attenburrow, G. Cross-linking of extruded collagen fibers—A biomimetic three-dimensional scaffold for tissue engineering applications; *J. Biomed. Mat. Res. Part A* **2009**, *89A*, 895-908.

Zhang, S. Fabrication of novel biomaterials through molecular self-assembly; *Nat. Biotechnol.* **2003**, *21*, 1171-1178.

Ziche, M.; Morbidelli, L.; Pacini, M.; Geppetti, P.; Alessandri, G.; Maggi, C. A. Substance P stimulates neovascularization in vivo and proliferation of cultured endothelial cells; *Microvascular Res.* **1990**, *40*, 264-278.

Zitelli, J. A. Wound healing for the clinician; *Adv. Dermatol.* **1987**, *2*, 243.